THE BOREHOLE INFILTRATION METHOD FOR DETERMINING SATURATED HYDRAULIC CONDUCTIVITY IN THE VADOSE ZONE: A DEEP WATER-TABLE CASE IN LOW PERMEABLE SOIL

by

Ward E. Herst

Submitted in Partial Fulfillment of
the Requirements for the Degree of
Master of Science in Hydrology

New Mexico Institute of Mining and Technology
Socorro, New Mexico

July 1986

Abstract

A borehole infiltration test was conducted in a silty-loam to a loamy soil under deep water table conditions. Saturated hydraulic conductivity (Ks) from the insitu test underestimated Ks obtained in the laboratory from vertically oriented shelby-tube permeameter samples. Soil heterogeneity is inferred to have significantly influenced Ks values obtained from the borehole infiltration test. Empirical equations which account for unsaturated flow yielded values of Ks which were not significantly different than the value of Ks obtained from the U.S. Bureau of Reclamation (USBR) equation, which does not account for unsaturated flow. Steady state was not reliably predicted by the USBR equations. Concluding the test according to USBR guidelines would have overestimated saturated hydraulic conductivity.

Infiltration rate was proportional to hydraulic conductivity but inversely proportional to hydraulic gradient. Alternate wetting and drying cycles of the soil were observed, which corresponds for the most part to changes in height of water in the borehole. Other cycles may have been caused by the influence of entrapped air.

A flow net method for computing relative hydraulic conductivity along stream tubes provided very good fit to changes in soil stratigraphy observed in shelby tube permeameter samples. A graphical procedure for estimating

steady infiltration rate from early time data overestimated the observed value of steady infiltration rate by 6%.

The instrumentation and borehole geometry for the test, S9T1, were similar to those for tests at sandy sites S5T4 through S5T8. A reduction of approximately 67 times in saturated hydraulic conductivity between the sandy and loamy sites was coupled with an increase of only 1.4 times in the volume of water needed and 35 times in the time needed to reach steady infiltration rate.

LIST OF FIGURES

LIST OF FIGURES (cont.)

LIST OF FIGURES (cont.)

LIST OF FIGURES (cont.)

LIST OF FIGURES (cont.)

LIST OF TABLES

TABLE OF CONTENTS

TABLE OF CONTENTS (cont.)

TABLE OF CONTENTS (cont.)

1. INTRODUCTION

The vadose zone (unsaturated zone) properties have recently been receiving increased attention, due in part to the proliferation of groundwater contamination problems including leakage from above-ground and below- ground waste storage sites, contaminant spills, and storage of radioactive waste. An important parameter needed for studying the effects of a contamination event, for estimating recharge rates, or for predicting seepage from dams and canals is the saturated hydraulic conductivity (Ks) of the vadose zone.

Various laboratory methods are often used to define Ks. Among these are the retrieval of 100 cubic centimeter of "undisturbed" soil samples from the field, which are then brought back to the laboratory, where testing includes placing the samples in a constant-head or falling-head permeameter. Shelby-tube samples may also be retrieved. These have the advantage of sampling a much larger volume of soil per sample than the 100 cubic centimeter samples. However, a drilling rig is often needed to push the samples into the soil.

Field techniques for estimating saturated hydraulic conductivity include the borehole infiltration test (Stephens and Neuman, 1982a), also called the shallow well pump-in method, the reverse auger hole method, and the

constant head well permeameter method (Reynolds and Elrick, 1983). A major advantage of the borehole infiltration test (as it will hereafter be referred to) is that it can be used at any depth. The basic requirements for conducting a borehole infiltration test are few. They include drilling or augering a well bore and having a supply of water. The well bore can be left standing open, or a well screen can be put into it.

1.1 Previous research

When conducting a borehole infiltration test, water is allowed to flow into the borehole at a rate which maintains a constant head of water in the borehole. The flow rate out of the borehole is monitored, and the value of steady infiltration rate into the surrounding soil is recorded. Various formulas are available which yield the value of saturated hydraulic conductivity (Ks) by inputing the steady flow rate, radius of the borehole, and height of water in the borehole (Stephens and Neuman, 1982b).

The United States Bureau of Reclamation (USBR) has designated three different criteria for determining the appropriate formula to be used to find Ks (USBR, 1974). These three conditions are based upon the height of water in the borehole and the vertical distance to the water table or to an impeding layer (figure 1). Condition I exists when the distance from the water level in the well to the water

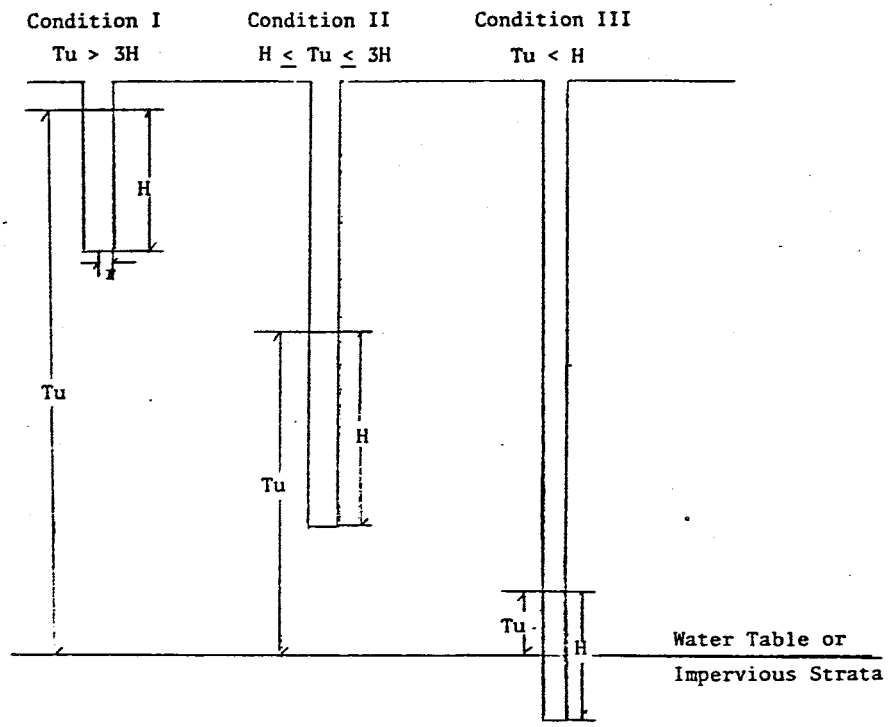

Condition I: $$K_{20} = \frac{0.159\ Q\left[\sinh^{-1}(HD) - 1\right]}{H^2}\left(\frac{\mu}{\mu_{T_{20}}}\right)$$

Condition II: $$K_{20} = \frac{0.159\ Q\ \ln\ (HD)}{H^2\left[\frac{1}{6} + \frac{1}{3}\left(\frac{H}{Tu}\right)^{-1}\right]}\left(\frac{\mu_T}{\mu_{20}}\right)$$

Condition III: $$K_{20} = \frac{0.159\ Q\ \ln\ (HD)}{H^2\left[\left(\frac{H}{Tu}\right)^{-1} - \frac{1}{2}\left(\frac{H}{Tu}\right)^{-2}\right]}\left(\frac{\mu_T}{\mu_{20}}\right)$$

Tu = distance from water level in borehole to water table or impervious strata

H = height of water in borehole

K_{20} = saturated hydraulic conductivity corrected to 20° C

Q = infiltration rate

HD = H/r, with r = radius of borehole

Figure 1. Description of shallow and deep water table table conditions for borehole infiltration tests (USBR, 1974)

table or impeding layer (Tu) exceeds three times the height of water in the borehole (H). Condition II exists when Tu is greater than H, but is less than three times H. If Tu is less than H, which occurs when the borehole extends below the water table or into the impeding layer, then condition III exists. The USBR (1974) equation which applies to each condition is presented in figure 1. Stephens and Neuman (1982a) point out that the deep and shallow water table equations do not match at the interface of these two conditions.

The conceptual model for the USBR assumes that a free surface exists, across which no flow takes place. Inside the free surface the soil is assumed to be saturated, and outside the free surface the soil is assumed to be unsaturated. Figure 2 shows the free surface concept as it pertains to condition I of the USBR. Stephens and Neuman (1982b), Stephens, et al (1983), and Rabold (1984) have offered evidence that flow is not restricted to the zone inside the free surface, but rather that flow crosses this boundary, thereby moving from a saturated to an unsaturated region. To incorporate the influence of unsaturated flow on saturated hydraulic conductivity, Stephens and Neuman (1982b) and Stephens, et al (1983) offer their own formulas for finding saturated hydraulic conductivity from borehole infiltration tests.

Lambert (1983) and Stephens, et al (1983) have found that flooding the soil surrounding the borehole with carbon

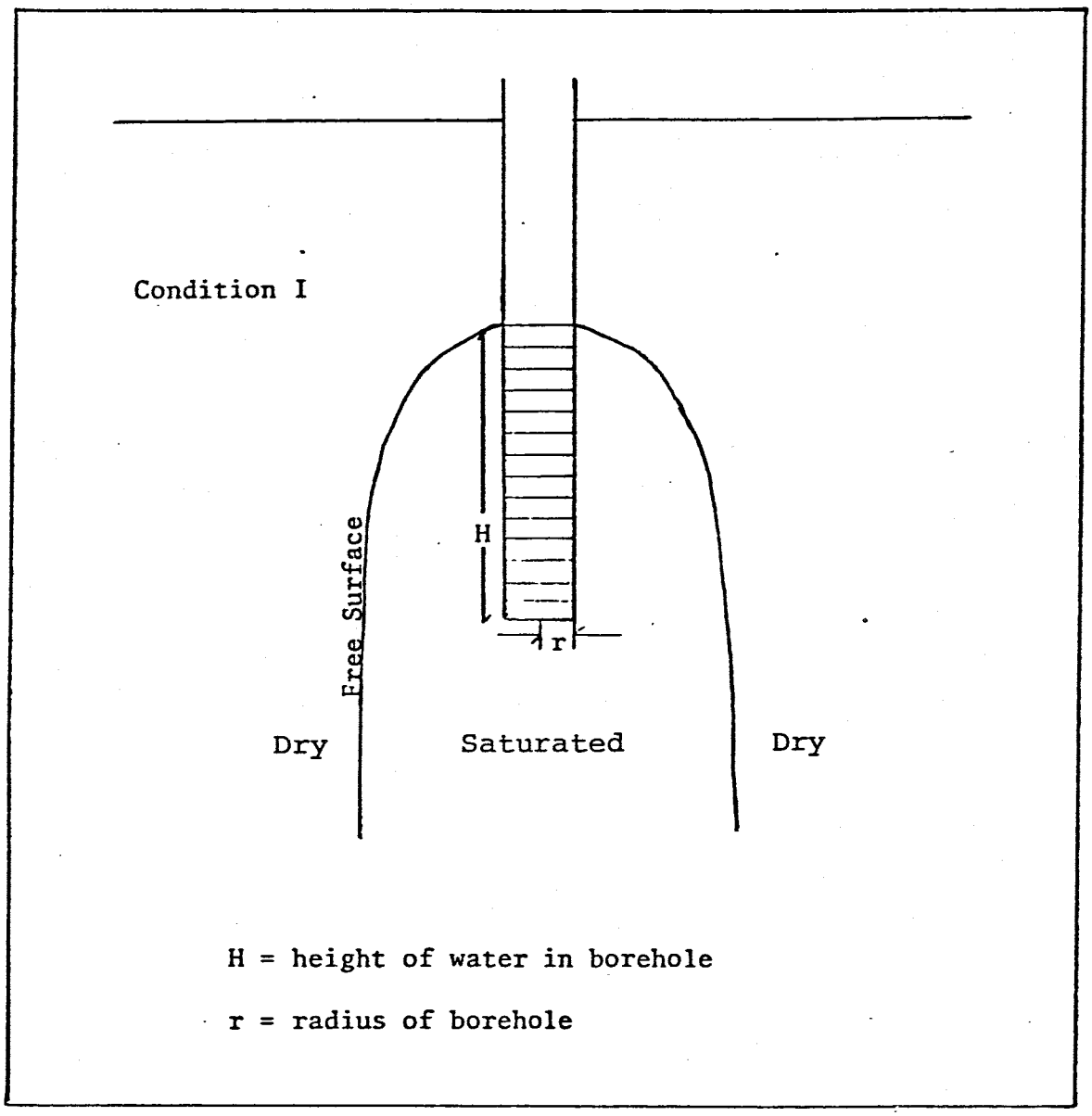

Figure 2. Infiltration from a borehole with a free surface

dioxide prior to starting infiltration results in an increase in saturated hydraulic conductivity and a decrease in the time and volume of water needed to reach steady infiltration rates, presumably because of reducing entrapped air. At 20 degrees celsius, carbon dioxide is 28 times more soluble in water than is oxygen (Hillel, 1980). It is assumed that the carbon dioxide displaces much of the oxygen in the soil and is then dissolved by the infiltrating water (Lambert, 1983).

Stephens and Neuman (1982c) and Watson (1983) studied the effect of changes in water level in the borehole on infiltration rates. They found that the flow rate out of the borehole is proportional to the square of the head of water in the borehole. Bouwer (1978) estimates the volume of soil sampled to be proportional to the head of the borehole raised to the third power. Stephens and Neuman (1982b) found that the flow rate out of borehole varies approximately linearly with depth.

Stephens, et al (1983) and Rabold (1984) found that soil water temperatures varied due to changes in the temperature of the water supply. These temperature variations affected infiltration rates even after correcting for changes in viscosity. Rabold (1984) varied the chemistry of the water supply, which was observed to affect the value of infiltration rate.

1.2 Objectives

Previous research at New Mexico Institute of Mining and Technology has concentrated on soils composed of fine sands. To date, detailed soil experiments on borehole infiltration tests under deep water-table conditions have not been conducted in loamy soils. The objectives of this paper are:

1) To conduct a borehole infiltration test (designated S9T1) under deep water table conditions (condition I) of the USBR in a loamy soil.

2) To obtain an estimate of the time and water volume needed to reach steady infiltration rate in a relatively fine-grained soil.

3) To test the empirical equations of Stephens, et al (1983) which account for capillarity, and compare the resulting values of saturated hydraulic conductivitty (Ks) to the values of Ks obtained from the USBR (1974) equation for condition I.

4) To compare the results of tests in a sandy soil to the results obtained in a loamy soil. Specific comparisons include; time needed to reach steady infiltration rate, water volume needed to reach steady state, flow out of the borehole at steady state, and saturated hydraulic conductivity for each test.

2. SITE DESCRIPTION

Field work for borehole test S9T1 was conducted on M-Mountain, which is located approximately 5.6 km (3.5 mi) west of Socorro, New Mexico, on the campus of New Mexico Institute of Mining and Technology. M-Mountain is within the Blue Canyon Field Laboratory of the Terminal Effects Research and Analysis (TERA) group, a component of the Research and Development Division of New Mexico Tech. Access to the mountain is controlled by TERA, and a permit must be issued to each person before the area can be entered.

Site S9T1 was located on a playa in the N.W. quarter of Section 17, Township 3 South, Range 1 West. The playa was called the M-Mountain waste storage site by Boyle (1984). Figures 3 and 4 show the location of the storage site, as well as the local topography. The soil in the playa grades from a sandy loam with cobbles and pebbles near the northern end of the playa to a silty clay loam with few pebbles at the southern end. In the center of the playa, the alluvial fill is approximately 14 m (45 ft) in thickness (Boyle, 1984). Below the alluvial fill are the clays of the Popatosa Formation.

The vegetation in the area is sparse and includes mostly wild grasses and a few cacti. The water table is at a depth of approximately 300 m (1000 ft) below land surface

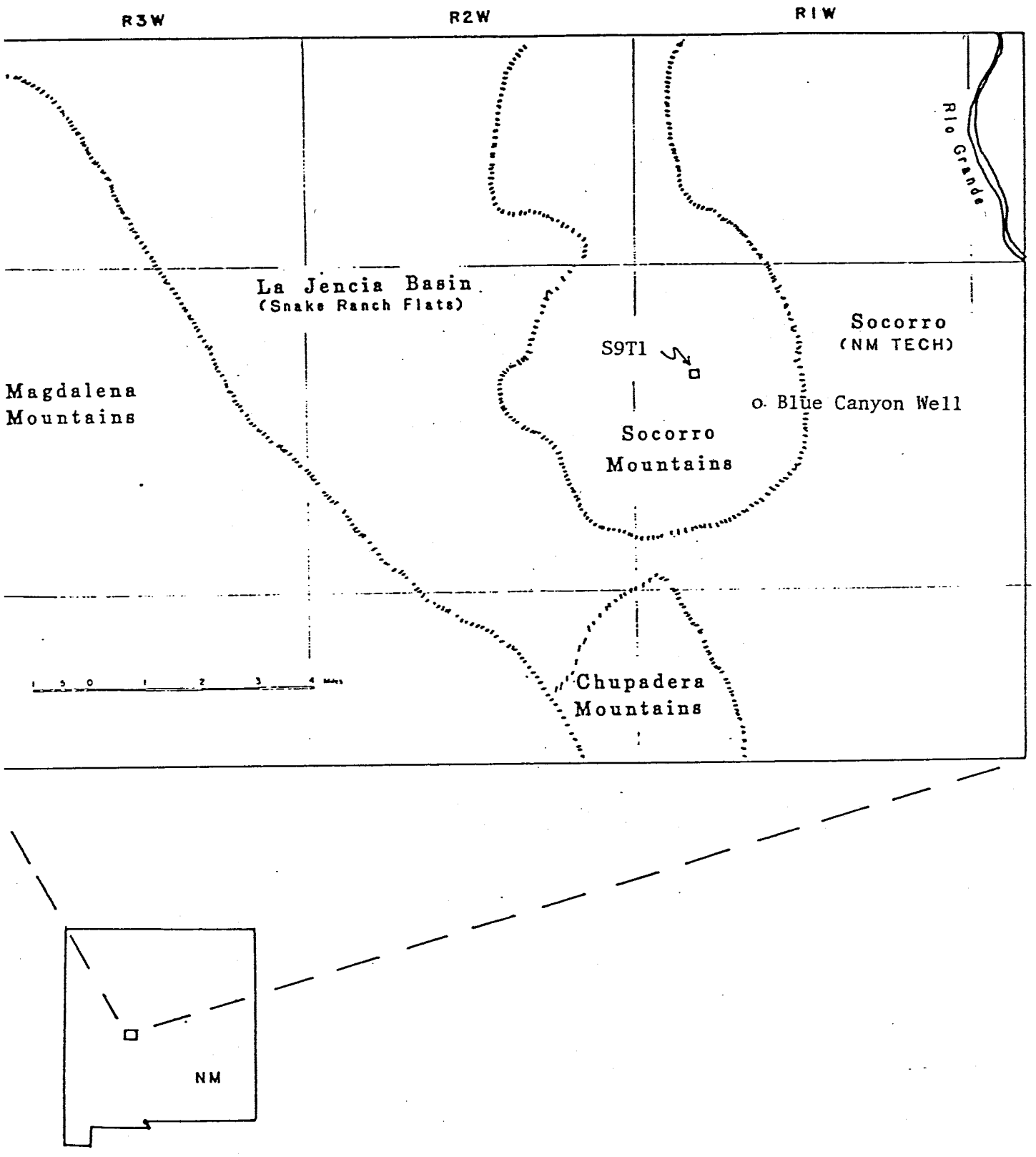

Figure 3. Geographic location of S9T1 (after Boyle, 1984)

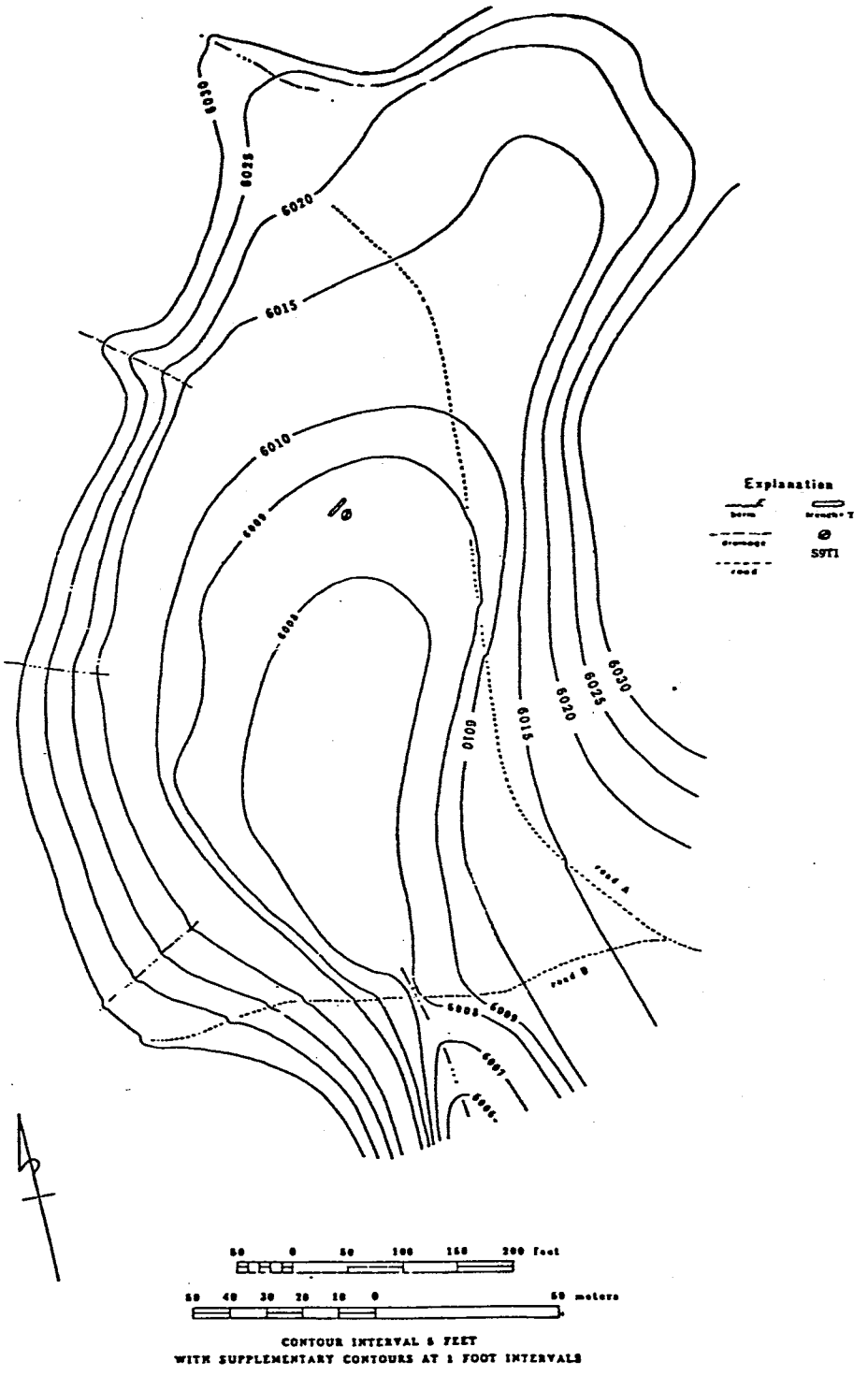

Figure 4. Local topography of S9T1 (after Boyle, 1984)

(Boyle, 1984). The borehole for S9T1 was located approximately 3 m (10 ft) south of trench T-3 as designated by Boyle (1984), who found that the soil in the vicinity of trench T-3 graded from a silty loam near the land surface to a loam at an elevation of -1.25 m (-4.1 ft) from land surface datum and a silt at an elevation of -2.5 m (-8.2 ft) (All references to elevation are relative to land surface datum).

Boyle (1984) also analyzed the clay content of the soil in the playa. From the samples he collected in trench T-3, he found that the clays were composed of approximately 40% kaolinite, 50% illite, and 10% calcium-smectite, but he cautions that these percentages were semi-quantitative. According to Hillel (1980), kaolinite does not tend to swell as much as most other clay minerals, but montmorillonite (smectite) exhibits pronounced shrink-swell behavior and illite has intermediate properties between kaolinite and montmorillonite.

For a more detailed geological description of the playa and the surrounding area, please refer to Boyle (1984).

3. HYDRAULIC PROPERTIES

Hydraulic properties examined in the laboratory include particle size distribution, soil moisture characteristic curves, and saturated hydraulic conductivity. These data suggest soil anisotropy and heterogeneity significantly influenced the results of S9T1.

3.1 Particle Size Distribution

Soil samples were collected at a radius of approximately 200 cm from the borehole at various depths as indicated on Table 1 to determine variations in grain size with depth. The soil samples were first sieved to determine the larger grain size distribution and then a hydrometer analysis was performed to determine the smaller grain size distribution. Dry sieving was performed using U.S. standard sieve sizes of 20, 30, 60, 100, and 200 mesh. Soil particles smaller the 200 mesh were collected and used in hydrometer analyses. The hydrometer samples were treated with hydrogen peroxide, and all of the samples showed a slight reaction, indicating the presence of organics. One hundred milliliters of sodium pyro-phosphate was used as a dispersing agent. The samples were placed in constant temperature bath and particle size in microns was estimated as outlined in Black (1965).

Table 1. Particle Size Analysis at Field Site S9T1

Elevation with respect to land surface (cm)	d_{10} (microns)	d_{50} (microns)	Cu
-26 to -35	0.88	17.0	31.8
-42 to -51	0.45	18.0	64.4
-58 to -65	0.61	19.5	45.9
-82 to -91	0.60	18.0	45.0
-134 to -138	0.55	11.5	41.8
-150 to -158	0.40	15.0	62.0
-168 to -179	0.40	15.0	57.0
-194 to -208	1.10	18.0	20.9
-208 to -219	1.90	20.0	15.0
-233 to -249	2.00	20.0	14.0
-264 to -275	1.70	19.0	15.0
-292 to -308	3.40	21.0	9.0
-342 to -355	1.40	18.0	17.1
-373 to -389	0.99	7.0	11.1

Table 1 indicates that the uniformity coefficient (Cu) decreases significantly below an elevation of -179 cm, implying that the soil below -179 cm is more uniform in grain size. Also, Table 1 indicates the soil below -179 cm is coarser in grain size than the soil above -179 cm.

Figure 5 illustrates the relationship between grain size and initial moisture content for S9T1. The ln d10 versus elevation plot indicates the soil is relatively finer grained above -175 cm and below -375 cm. The moisture content plot shows relatively higher moisture content in the finer grained portions of the soil profile.

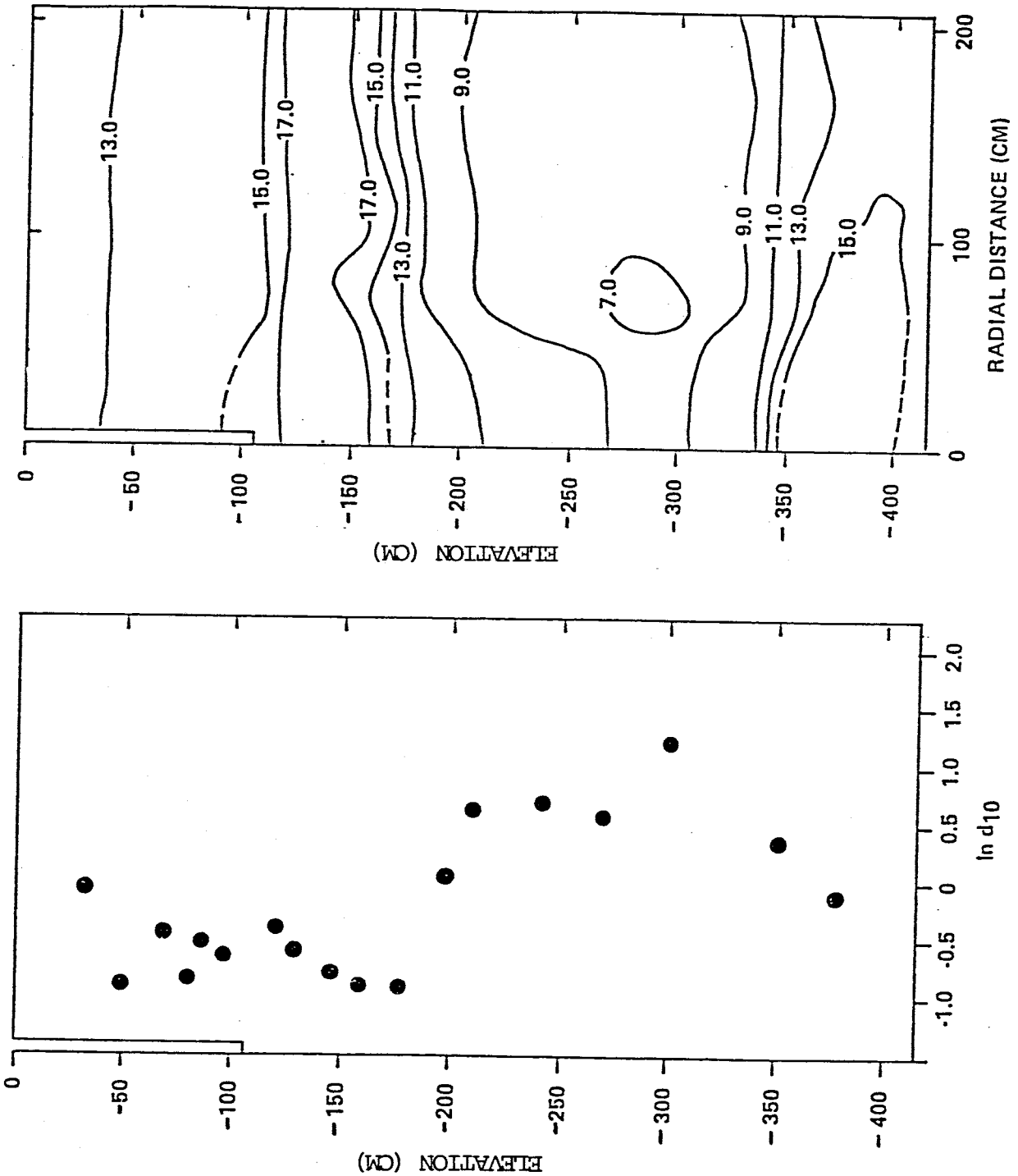

Figure 5. Ten Percent Finer Particle Size and Initial Moisture Content

3.2 Soil Moisture Characteristic Curve

The pressure head versus moisture content data were obtained from 100 cubic centimeter samples taken at a radius of 40 cm from the borehole center at elevations of -30.5, -50, -75, and -100 cm, one sample from each elevation. These elevations were chosen in order to define the soil hydraulic properties along the length of the borehole, which was screened from elevations of -30.5 cm to -106.7 cm.

The samples were taken from the side of a shallow pit approximately 100 cm deep, which was dug for the purpose of taking the samples. For each sample, a ledge was excavated on the side of the pit at the desired depth, from which the vertically oriented samples were retrieved. After a sample was pushed into the soil, the surrounding soil was excavated away with a shovel, leaving the sample undisturbed. The shovel was then gently pushed into the soil underneath the sample, and the soil and sample were picked up with the shovel. A removable plastic cap was placed over the top of the sample, and the sample was turned over. The soil was leveled flush with the bottom of the sample by shaving off any excess soil with a knife. A removable plastic cap was placed over the bottom of the sample, and the sample was returned to its original vertical orientation. After a sample was retrieved at a particular depth, the ledge was excavated to the next depth and the process repeated.

We hoped that by digging the pit and gently pushing the

samples into the soil, a more undisturbed sample would result than if a sampling device such as a slide hammer was used. The samples retrieved with a slide hammer often have undergone quite a beating before they can be taken from the soil. We realize that in many instances it is not possible to dig pits or trenches to retrieve samples. However, in this case it was possible, so the extra care was taken.

In order to saturate the samples in the laboratory, the samples were fitted with a retainer used in a laboratory permeameter (Eijkelkamp-Giesbeek, the Netherlands), and then they were placed in 500 milliliter beakers, where they were saturated from below with distilled, de-aired water. The bottom of each sample was elevated above the bottom of the beaker by the sample holding devices. A slightly higher head of water was maintained in the annular space between the samples and the beakers, which allowed water to flow from the annular spaces into the samples through screens on the bottom of each sample. Seventy- two hours were allowed for the samples to reach saturation, after which they were placed on hanging column devices. Larson (1984) describes the method used to find the pressure head-moisture content pairs using hanging columns.

At least twenty-four hours elapsed between measurements from the hanging columns in order to allow for equilibration of the samples. All readings were made between the hours of 1100 and 1230 (military time) in order to minimize temperature effects. Larson (1984) recommended that

readings be taken between the hours of 1600 and 1900. However, with the occassional afternoon thunderstorms present in the summer months, which is when these data were obtained, we thought constant temperature could be obtained during the morning hours.

The hanging columns were used to define the drainage curves to pressure heads as low as approximately -200 cm, after which the pressure heads were gradually increased to define the sorption curves. When these two curves were defined, the pressure heads were again lowered to approximately -200 cm and the samples given seventy-two hours to equilibrate. The samples were then weighed and placed in two 2-bar ceramic pressure plate extractors (two samples in each pressure plate), where a pressure of 1/2 bar (514.8 cm of water) was exerted on the samples. After allowing seventy-two hours for the samples to equilibrate, the samples were taken out of the pressure plate extractors and weighed. The difference in weights from when the samples were first placed in the pressure plate extractors and after undergoing a pressure of 1/2 bar was assumed to be caused by a loss of water from the samples and was used to calculate moisture contents at 1/2 bar pressure. The samples were then placed under 2 bars of pressure (2059 cm of water) for seventy-two hours and weighed again.

The samples were then placed in a 15 bar ceramic pressure plate extractor (Soilmoisture, Inc., Santa Barbara, Ca.), where a pressure of 5 bars (5147.5 cm of water) was

exerted on them. After seventy-two hours, the samples were again weighed. It was feared that at pressures higher than 5 bars the clays in the samples might cause the samples to pull away from the ceramic plate by shrinkage, resulting in the soil having a poor contact with the plate and thus giving poor results. Consequently, the use of the pressure plate extractor was discontinued after 5 bars, and the samples were oven dried for twenty-four hours.

Shrinkage of each sample from saturated to oven dried states ranged from 3% volume to 12% volume. These smaller volumes were used to compute the dry bulk density for each sample, after which porosities were found using equation (1):

$$n = 1 - (pb/ps) \qquad (1)$$

where 'n' is porosity, 'pb' is dry bulk density, and 'ps' is particle density (assumed to be equal 2.65 gm/cc). The results are presented in Table 2. Dry bulk densities were found to range between 1.27 gm/cc and 1.41 gm/cc, resulting in porosities of 0.47 to 0.52.

Sorption data from the hanging columns and from the pressure plates were input for the SOHYP computer model of van Genuchten (1978) in order to obtain pressure head-moisture content curves for each sample using the equations of Mualem (1976). Model 1 of SOHYP, in which the computer program is allowed to estimate residual saturation, was used to generate the curves. Sorption data were used

Table 2. Dry Bulk Density and Porosity from Laboratory Soil Moisture Characteristic Curves

Elevation (cm)	Vd	pb	n
-30.5	97	1.33	0.50
-50	93	1.34	0.49
-75	93	1.27	0.52
-100	88	1.41	0.47

Vd = dry soil volume (cm^3)
pb = dry bulk density (gm/cm^3)
n = porosity (dimensionless)
= 1 - pb/ps
ps = particle density
= 2.65 gm/cm^3

whenever possible to accurately simulate conditions as they occur in a borehole infiltration test. Figures 6 through 9 are the output from the computer program. Important parameters, such as residual moisture content (θr), alpha, and N are included in the figures.

The sample taken at an elevation of -100 cm exhibited the most pronounced shrink-swell behavior of any of the samples. This suggests that the material at an elevation of -100 cm had a comparitively large percentage of montmorillonite, a clay which exhibits strong shrink-swell behavior (Hillel, 1980).

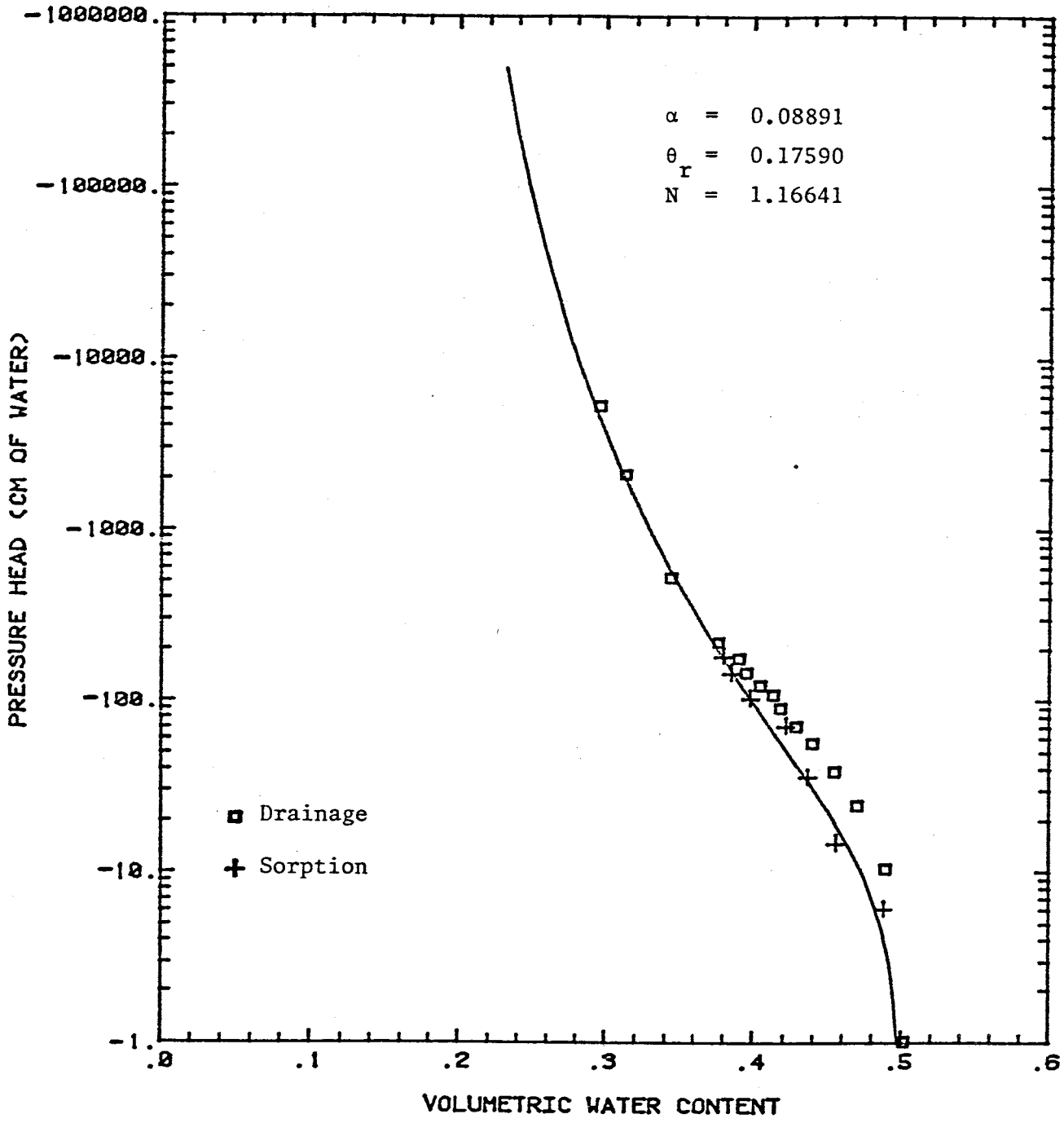

Figure 6. Moisture Characteristic Curve for the sample from an elevation of -30.5 cm. (Solid line is model fit to sorption data.)

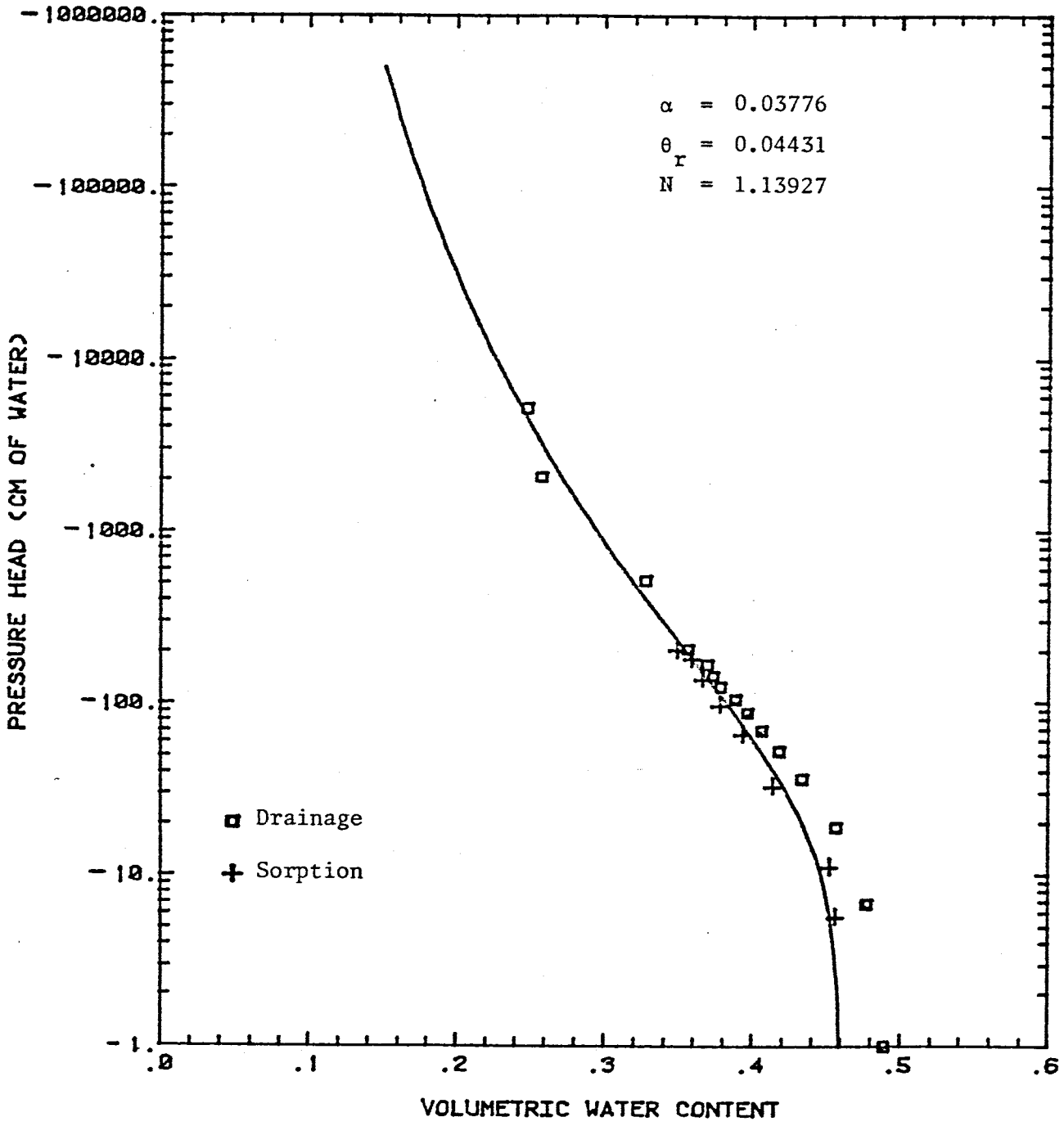

Figure 7. Moisture Characteristic Curve for the sample from an elevation of -50 cm. (Solid line is model fit to sorption data.)

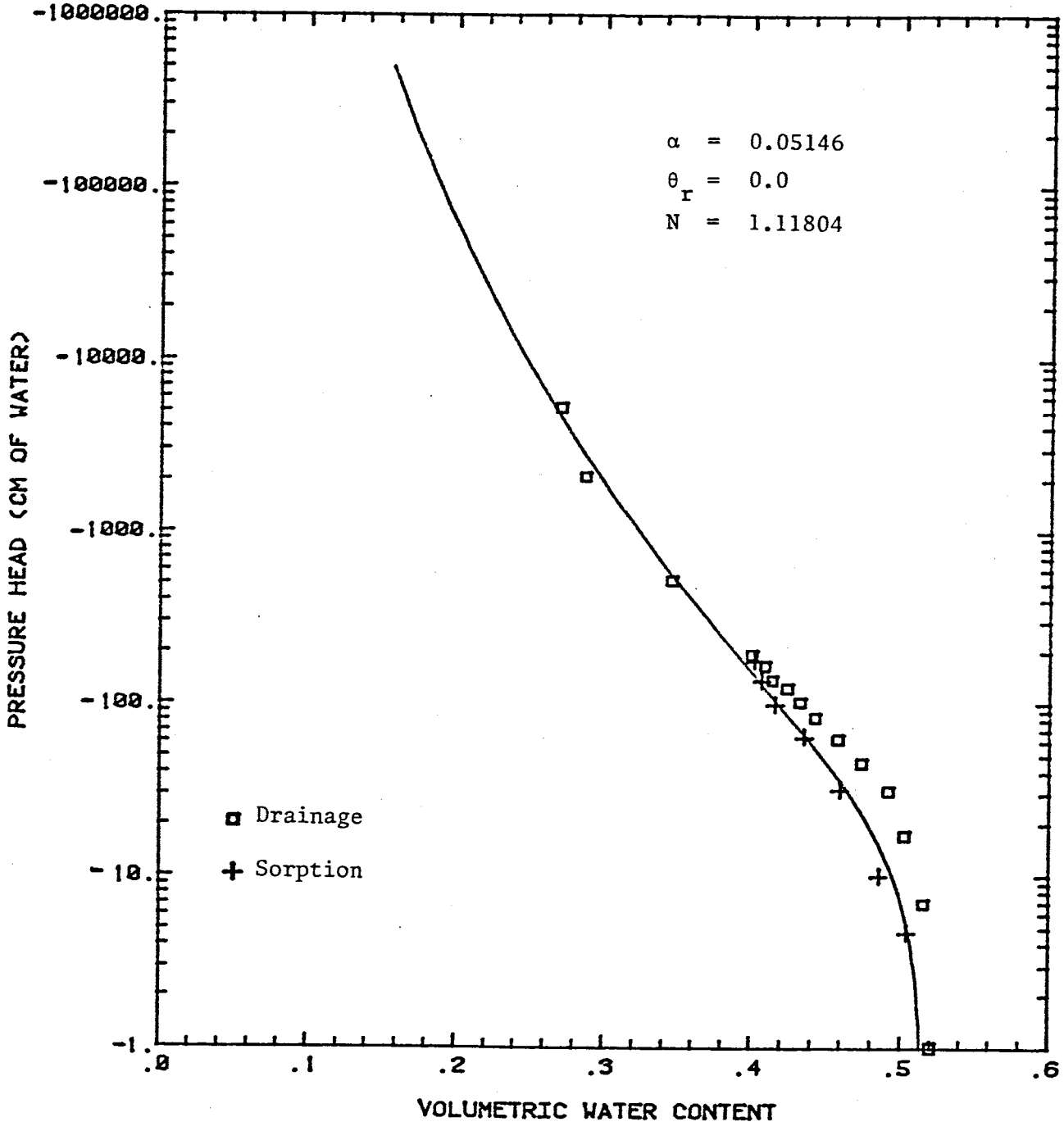

Figure 8. Moisture Characteristic Curve for the sample from an elevation of -75 cm. (Solid line is model fit to sorption data.)

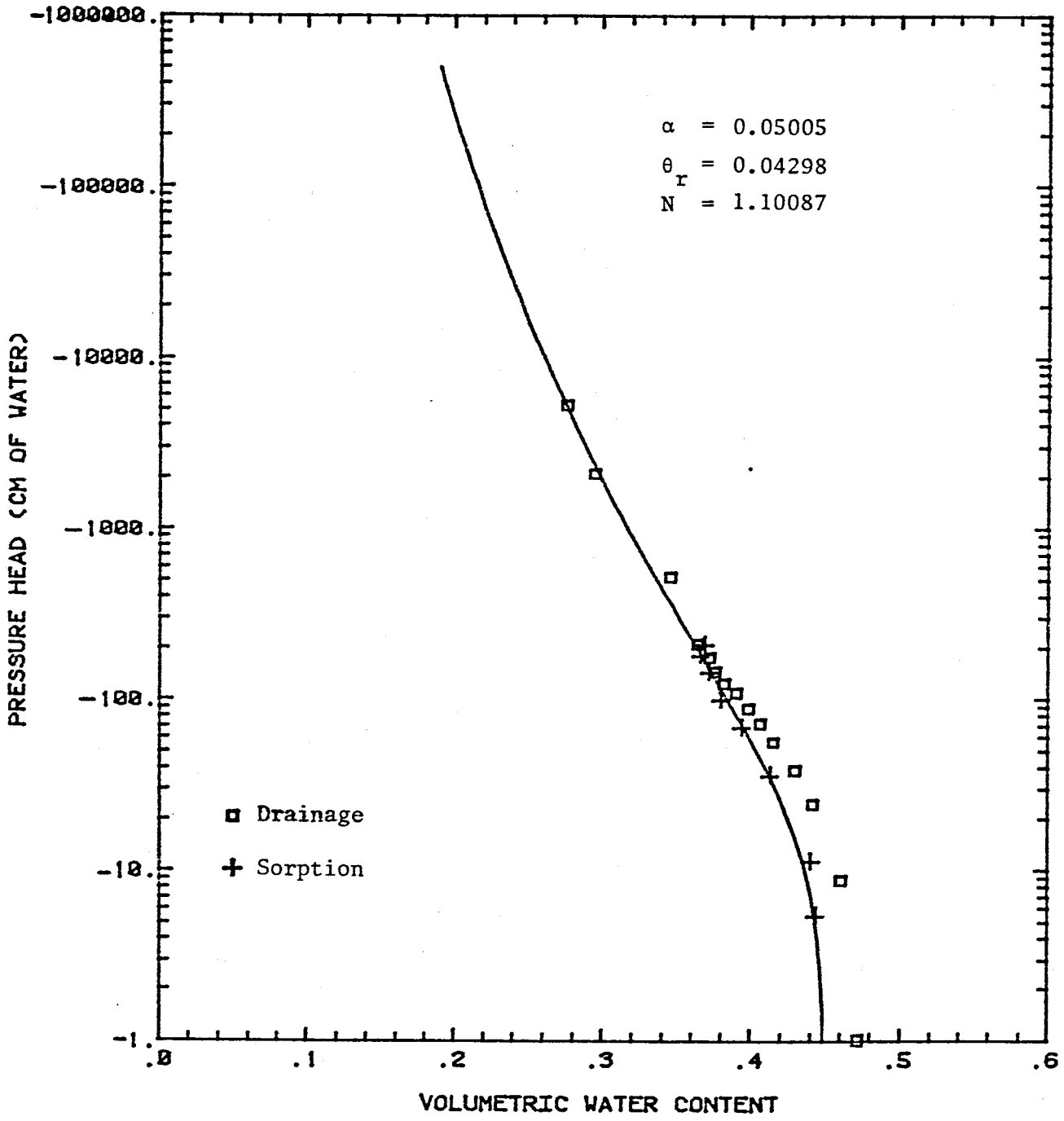

Figure 9. Moisture Characteristic Curve for the sample from an elevation of -100 cm. (Solid line is model fit to sorption data.)

3.3 Saturated Hydraulic Conductivity

Saturated hydraulic conductivity of the soil surrounding the borehole was estimated in the laboratory using shelby-tube permeameters. Vertically oriented shelby-tube permeameter samples were collected using a Mobile B-30 drilling rig. A total of four shelby tubes, which had been internally coated with a rust-inhibiting spray, were collected from the same hole at increasing depths. Each shelby-tube was approximately 61 cm in length. The first and second shelby-tubes retrieved full (55 cm) soil samples, while the third and fourth were only approximately 1/2 full with soil. The discrepancy between the length of 61 cm for each shelby-tube and the 55 cm length of soil sample exists because 6 cm are needed to attach the shelby-tubes to the drilling rig.

Excavation of the soil in the vicinity of the borehole had been previously conducted for purposes of removing tensiometers, neutron access tubes, temperature blocks, and also for retrieving samples for pressure head- moisture content curves. To insure that the shelby-tube samples were not taken from an area which had been previously excavated, the samples were taken at a radial distance of 315 cm from the borehole.

Shelby-tube samples were easily obtained to an elevation of -148 cm. At this elevation an extremely hard soil was encountered, and the drill rig was unable to push

the shelby-tube into this layer. Consequently, approximately one liter of water was poured down the hole in hopes of loosening the soil. The water seemed to work fairly well, as the drill rig was then able to retrieve a sample to an elevation of -173 cm.

The following field procedures were followed on each shelby-tube: 1) After each sample was pulled from the hole, the length of soil in the shelby-tube was compared to the depth of the bottom of the hole to detect any compaction that may have occurred during sampling (No compaction was evident in the samples taken). 2) The top and bottom of the tube were then taped with duct tape to avoid soil loss. Care was taken to keep each sample oriented in the vertical direction, just as they were removed from the ground, in order to avoid any redistribution of of soil.

In the laboratory, the shelby-tube samples were prepared in a manner that was similar to the method described in detail by Rabold (1984). Samples 1 through 3 were flooded with carbon dioxide for a period of 25 minutes each at a flow rate of 3.84 lpm, resulting in a total carbon dioxide volume of 96 liters. Shelby-tubes 1 and 2 (collected from elevations of -3.8 cm to -58.3 cm and -58.3 cm to -113.5 cm, respectively) had soil lengths of approximately 55 cm, and a cross-sectional area of 41.85 cm. Assuming a porosity of 0.50 from pressure head-moisture content data, one pore volume, defined as the bulk volume of soil tested multiplied by the porosity of the soil, for

these two tubes equal to approximately 1.15 liters. With a total volume of 96 liters injected, a total of approximately 80 pore volumes of carbon dioxide was injected into shelby-tube samples 1 and 2.

For sample 3, which had only 31.3 cm of soil and 29.7 cm of open space from the top of the tube down to the top of the soil, had approximately 140 pore volumes of carbon dioxide injected into it. However, as the data subsequently showed, a leak may have developed in the open space above the sample, which allowed the carbon dioxide to escape from the shelby-tube before having passed through the soil. The avenues of escape for the carbon dioxide include small diameter holes on the sides of the shelby-tubes, which are designed for manometer tubes to pass through. In the case of shelby-tube 3, the holes above the soil sample were taped with duct tape in an effort to plug them. It is possible that the taped holes developed leaks which allowed the carbon dioxide to escape.

Shelby-tube 4, which was attached to the permeameter immediately after tubes 1 through 3 were completed, had 28.3 cm of soil and 32.7 cm of open space above the sample. Having learned a lesson from shelby-tube 3, two rubber gaskets were placed over the manometer holes, and clamps placed over the rubber gaskets in order to insure that no leaks occurred during the carbon dioxide flood. These gaskets were successful in preventing leaks. However, due to the tightness of the soil in this tube, it was not

possible to push any carbon dioxide through the sample, even at flow rates as low as the flow valve would go. Even at the low flow rates, the back pressure in the shelby-tube was quickly able to prevent carbon dioxide from entering the tube. Consequently, this sample was run without the aid of carbon dioxide.

A constant head of water was maintained above the top of the samples while they were being tested. The constant head reservoir was supplied with tap water. The water level in the reservoir was governed by an overflow discharge hose out the side of the reservoir. Water was allowed to escape the system out the discharge hose and the bottoms os the shelby-tubes, while fresh tap water was constantly being added. Outflow (Q) from the bottom of the tubes was measured periodically beginning approximately twenty-four hours after water began to flow into the tubes. Changes in hydraulic gradient over segments of the tubes were measured by recording the rise of water on a graduated scale from manometers tapping the wall of the shelby-tubes (figure 10).

Figure 11 is a schematic representation of the data collected and method used to find Ks. The figure shows that small diameter copper tubes extended into the soil samples, providing a hydraulic connection between the manometers and the soil. Water levels in the manometer ttubes were initially put at a higher elevation than the water in the reservoir so that water was allowed to flow from the manometers into the soil rather than vice versa. We hoped

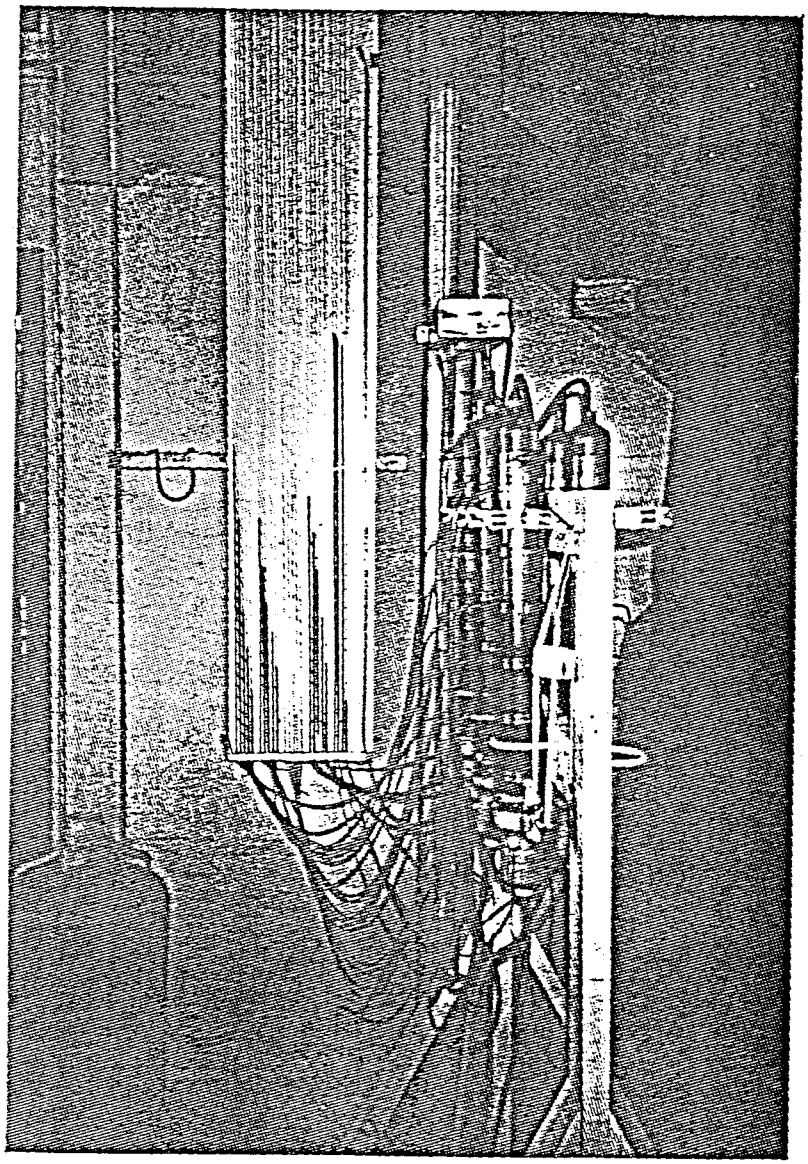

Figure 10. Shelby-tube Permeameter (from Rabold, 1984)

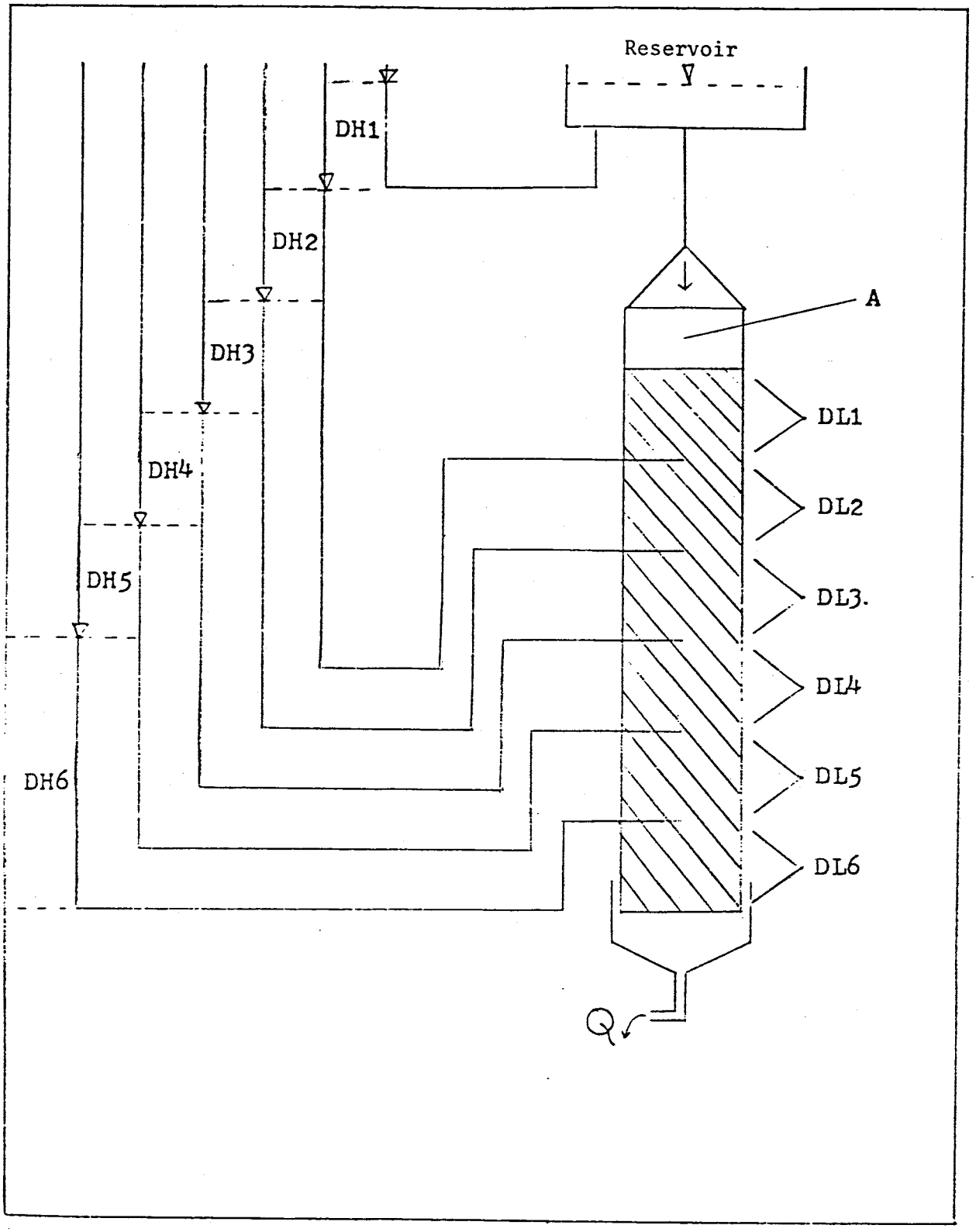

Figure 11. Schematic of Shelby-tube Permeameter (after Rabold, 1984)

that this would prevent clogging of the manometer tubes which might occur if water was initially allowed to flow from the shelby-tubes into the manometers.

Tap water was used as solvent in the shelby-tubes. Chemical analyses of the tap water and site field water show that the two water are very similar in chemical composition (Table 3). The similarity between the water suggests that the data obtained from the shelby-tube permeameter samples should be comparable to field data from the borehole infiltration test.

The saturated hydraulic conductivity for each segment was calculated using Darcy's Law:

$$Ks = Q / (A * i)$$

where Ks = saturated hydraulic conductivity (L/T)

Q = outflow per unit time (L^3/T)

A = cross-sectional area (L^2)

i = negative hydraulic gradient (unitless)

Over the first 5000 minutes of the test for shelby tubes 1 through 3, the copper tubes became clogged with soil. On three different occassions the copper manometers were removed from the soil and cleaned. The first two times this procedure was performed, the copper tubes subsequently became clogged again. On the third occassion, not only were the copper tubes cleaned, but the soil inside the shelby-tubes near the manometer holes was reamed out. This

Table 3. Water Chemistry Data

	Field Water January 1985	Tap Water March 1983
pH	7.5	8.05
CO_3 (ppm)	0.0	*
HCO_3 (ppm)	159	161
Cl (ppm)	15	78
SO_4 (ppm)	35	29
NO_3 (ppm)	3.2	1.6
F (ppm)	*	0.41
Na (ppm)	55	60
K (ppm)	4.6	3.0
Mg (ppm)	4.1	6.5
Ca (ppm)	14	16
Conductivity (μmhos)	300	320
TDS (ppm)	211	243
Hardness (ppm $CaCo_3$)	36	*

*: These data not measured

Analyses performed by the New Mexico Bureau of Mines and Mineral Resources

process worked fairly well, with a total of ten out of thirteen manometers functioning properly by the end of the test. Where a particular manometer did not function properly, the change in hydraulic head between neighboring manometers was used to calculate Ks over the interval between the properly functioning manometers. For shelby-tube 4, the process of cleaning out manometers was carried out twice over the first 2500 minutes of the test before the manometer at an elevation of -154 cm functioned properly.

The results of the shelby-tube permeameter experiments are shown on figures 12 and 13, which indicate the changes in saturated hydraulic conductivity (Ks) with time for each depth. Figure 12 shows the changes in Ks obtained from shelby-tubes 1 through 3. In the interest of clarity, the results from shelby-tube 4 are presented in figure 13. In general, the curves show a decrease in Ks over time, which can be explained by swelling of the clays over time, resulting in reduction of permeability as discussed by Hillel (1980).

The hydraulic conductivity at elevations of -113.5 cm to -117.8 cm varies over the first 7000 minutes of the test, with a net decrease in Ks, followed by a steady increase in Ks from 7000 minutes to the end of the test. Christiansen (1944) found similar decreases in Ks followed by increases due to entrapped air. This suggests that shelby- tube 3 was not effectively flooded with carbon dioxide before

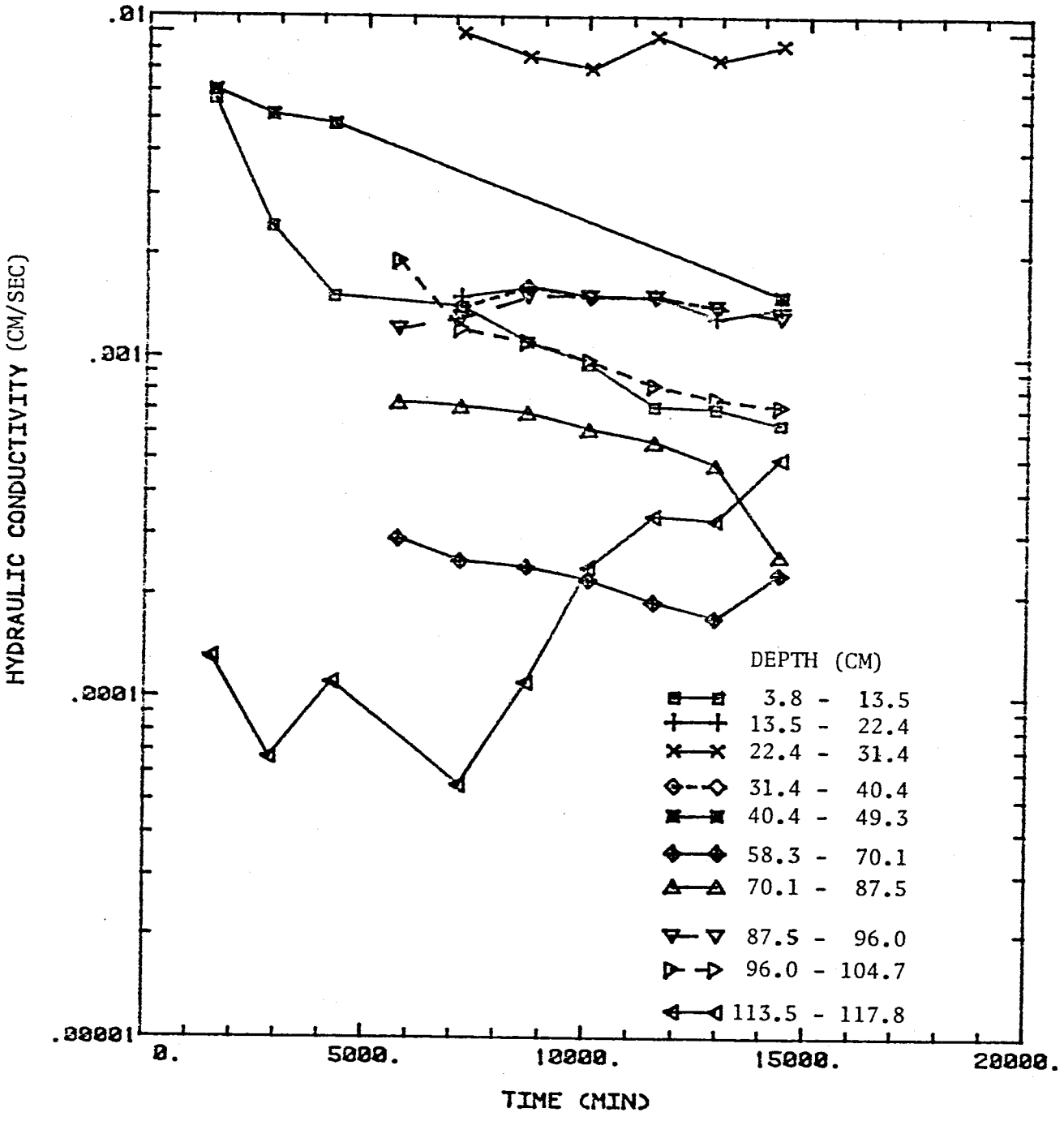

Figure 12. Hydraulic Conductivity versus Time for Shelby-tube Permeameter samples #1 through #3

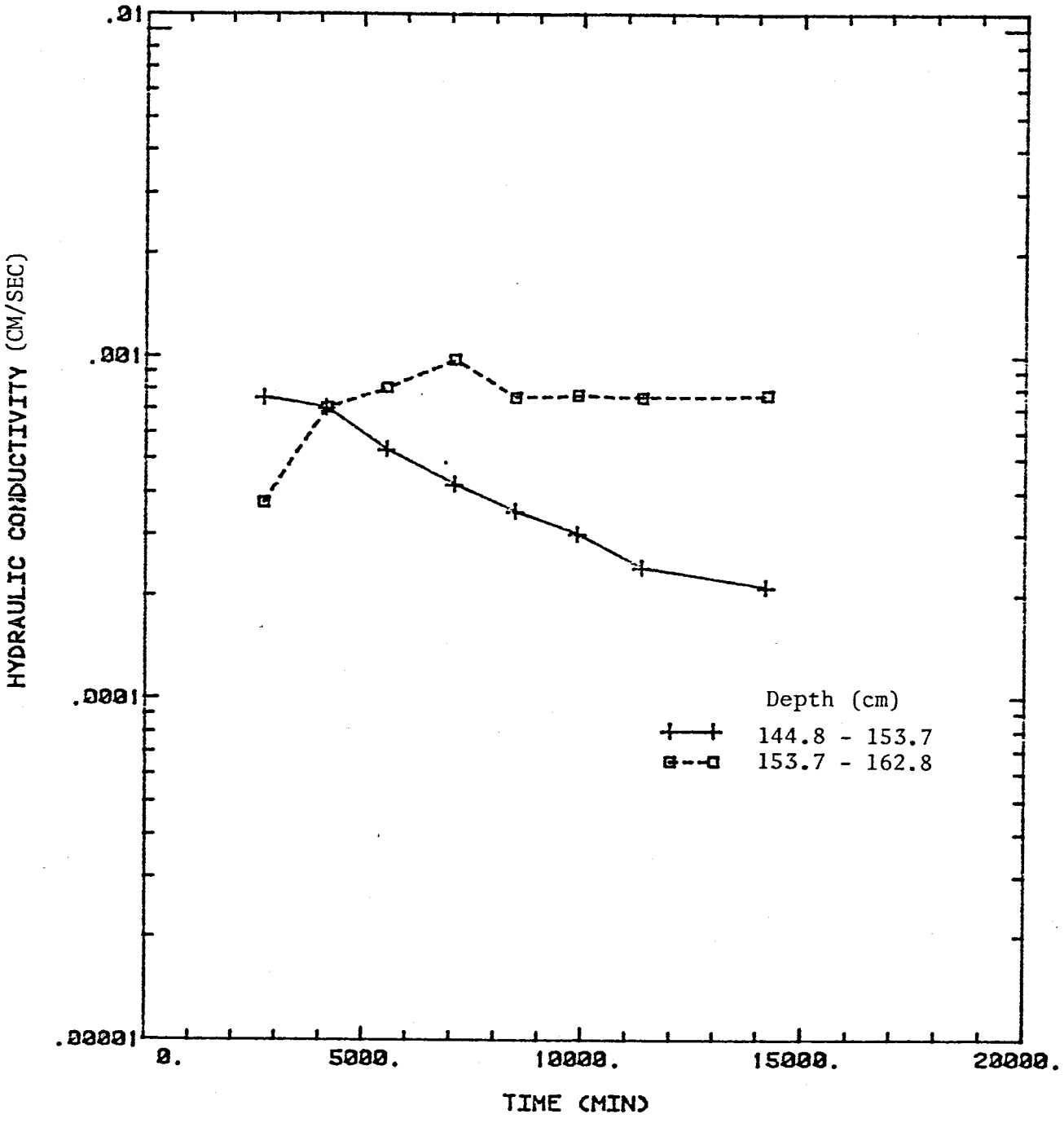

Figure 13. Hydraulic Conductivity versus Time for Shelby-tube Permeameter sample #4

beginning infiltration with water. The increase in Ks in shelby-tube 4 at elevations of -153.2 cm to -162.8 cm may also due to entrapped air.

Temperature readings were not made concurrently with outflow readings. Subsequently, temperature measurements were made at various times of the day, and the temperature of the infiltrating water was found to vary by only 2 degrees celsius. Since the readings from the shelby-tubes were made at approximately the same time of the day, temperature effects should not have caused the variations in Ks. Similar variations in Ks at early times were observed by Rabold (1984) in some shelby-tube permeameters. Various factors, such as swelling of the soil and entrapped air may be the cause of the fluctuations.

The results presented in figures 12 and 13 are not corrected to 20 degrees celsius. However, the temperature of the infiltrating water was found to be approximately 23 degrees celsius. Consequently, the values of Ks from the shelby-tubes are likely to be approximately 6% higher than Ks at 20 degrees celsius.

Figure 14 shows the final saturated hydraulic conductivities from the shelby-tube permeameters plotted as a function of elevation. The borehole is also shown, as is the water level maintained in the borehole for the borehole infiltration test. The material from an elevation of approximately -15 cm to -50 cm is seen to have a much higher Ks than most of the rest of the material.

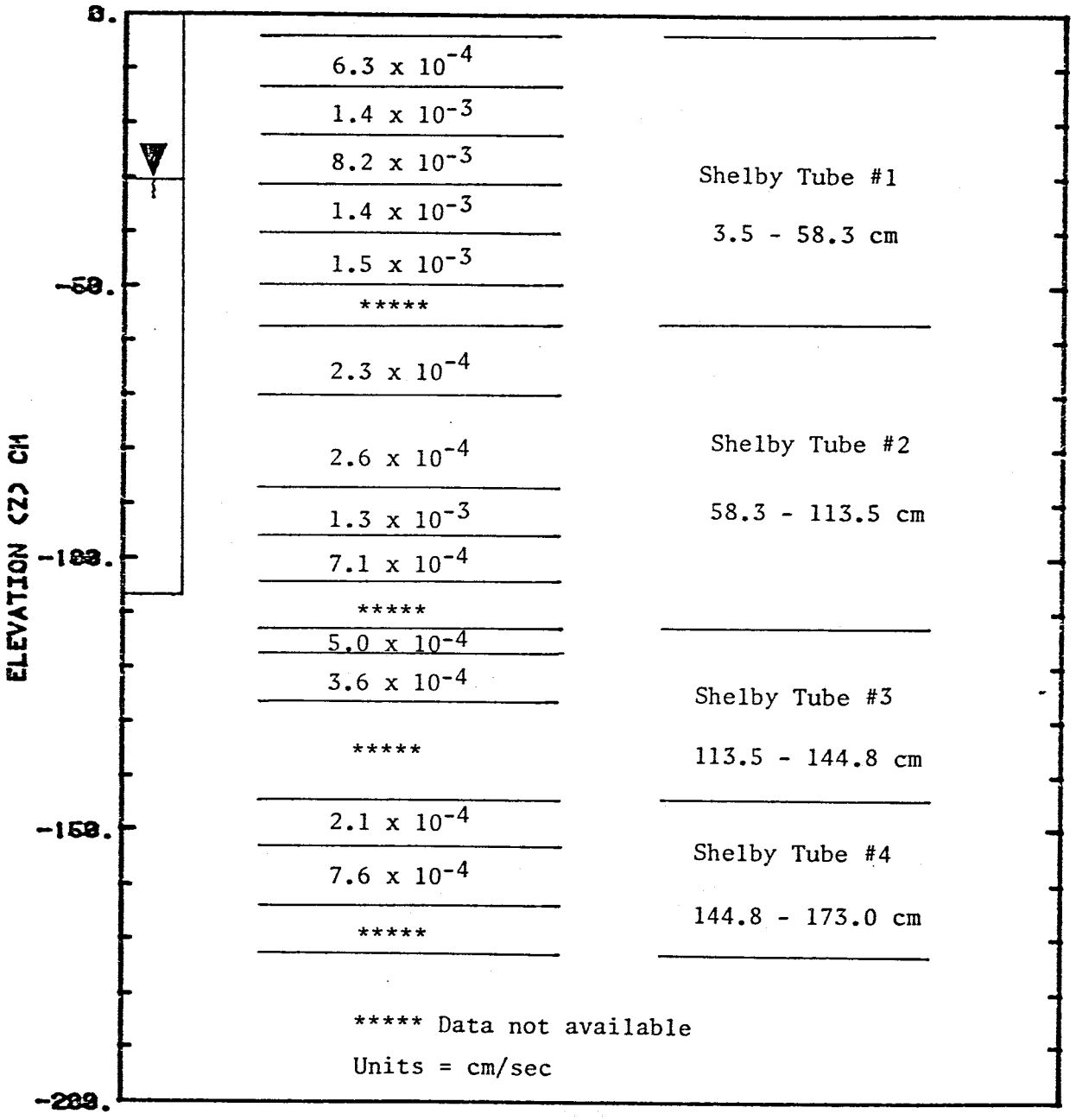

Figure 14. Final Hydraulic Conductivity versus Elevation for Shelby-tube Permeameter samples

At elevations from -85.7 cm to -104.7 cm, the shelby-tube permeameters provide saturated hydraulic conductivities from 1.3 x 10-3 cm/sec to 7.1 x 10-4 cm/sec. Stephens and Neuman (1982b) point out that flow rate out of the borehole increases more or less linearly with depth. In light of this, one might expect the saturated hydraulic conductivity obtained from the borehole infiltration test would be from 1.3 x 10-3 cm/sec to 7.1 x 10-4 cm/sec, or at least higher than the average of 2.45 x 10-4 cm/sec exhibited from elevations of -58.3 cm to -85.7 cm.

4. INSTRUMENTATION

Instrumentation for S9T1 was approximately the same as that for tests S5T3 through S5T8 (Lambert, 1983). This way comparisons could be made between the results of S5T3 through S5T8, which were conducted in fine sands, to S9T1, which was conducted in a silty-loam to loamy soil (Boyle, 1984).

4.1 Borehole

The borehole at S9T1 was augered by hand to an elevation of -106.7 cm and cased with a plastic Johnson well screen having a diameter of 10.2 centimeters and 0.02 cm slots. The well screen was 168.2 cm in length, which left 61.5 cm of well screen projecting above land surface. The upper 92 cm of well screen was sealed using duct tape, leaving 76.2 cm open to the soil. Approximately a 1.5 cm annular space was created between the screen and the borehole wall during augering. The annular space was backfilled with the same soil that was augered out of the hole. The casing was shaken slightly during the backfilling process in an attempt to settle the backfill material.

4.2 Tensiometers

Two days into the test, tensiometers were installed at radii of 25, 50, 75, 100, and 150 cm from the borehole center. Seven days into the test, tensiometers were installed at a radius of 10 cm from the center of the borehole. Mercury manometers were constructed for reading values of total hydraulic head with respect to a land surface datum. The formula for determining the distance from the mercury reservoir to the zero total hydraulic head mark on the manometer scale, b, is calculated from:

$$b = c * (pw) / (pHg - pw) \qquad (2)$$

here "c" is the height of the mercury level in the reservoir above the datum (land surface), pHg is the densities of mercury, and pw is the density of water. Values of 13.55 g/cc and 1.0 g/cc were used for pHg and pw, respectively.

Total head values were calculated from the manometer scale readings by equation 3:

$$TH = a * (1 - pHg / pw) \qquad (3)$$

where "TH" is the total hydraulic head in centimeters of water, and "a" is the rise of mercury in centimeters above the zero mark. Pressure head is then calculated using equation 4:

$$PH = TH - z \qquad (4)$$

where "PH" is the pressure head in centimeters of water, and z is the elevation of the center of the tensiometer cup (positive values of z increase upward). Table 4 lists the radius and depth of each tensiometer used in S9T1. Figure 15 is a plan view of the instrumentation.

4.3 Neutron Probe

Instrumentation for the neutron probe included aluminum access tubes installed to an elevation of approximately -400 cm. Neutron probe readings taken during the infiltration test were subsequently converted to actual moisture contents by developing a calibration curve. Confidence intervals were also subsequently estimated.

4.3.1 Neutron Access Tubes

Aluminum access tubes having an outside diameter of 5.08 cm were installed at radii of 45, 75, 100, 155, and 200 cm from the borehole center. The holes for the access tubes were augered by hand with an auger of the same outside diameter as the access tubes, which meant that backfilling around the access tubes was not necessary as it had been in previous borehole tests (Lambert, 1983). The top of each access tube was leveled off at a pre-set height of 19.5 cm above land surface, from which the neutron probe depths had

been calibrated. The bottoms of the access tubes were set at an approximate elevation of -427 cm (-14 ft).

Moisture content was monitored by a neutron probe (Campbell Pacific Nuclear Corp., model 503, Pachero, Cal.), which had a 50 millicurie Americium-Beryllium source. The neutron probe emits fast neutrons from the source, which randomly interact with the surrounding soil. Hydrogen has nearly the same mass as the neutrons; consequently, hydrogen in the soil causes the fast neutrons to lose energy through collisions with the hydrogen, resulting in slow neutrons. The slow neutrons are counted by the detector, which sends electrical impulses to a ratemeter. The ratemeter is then read by the operator, or the neutron probe can be programmed to store the data itself. The more hydrogen present in the soil, i.e., the higher the moisture content, the more slow neutrons are created and detected.

The sphere of influence of the neutron probe ranges from a radius of 10 cm a wet soil to more than 25 cm in a dry soil (Hillel, 1980). This limits the use of the neutron probe to elevations greater than -20 to -30 centimeters.

The location of the borehole, tensiometers, and neutron access tubes for S9T1 are shown of figure 15.

4.3.2 Calibrating the neutron probe

In order to define the relationship between the neutron probe readings taken during the test and the actual moisture content, the following procedure was performed:

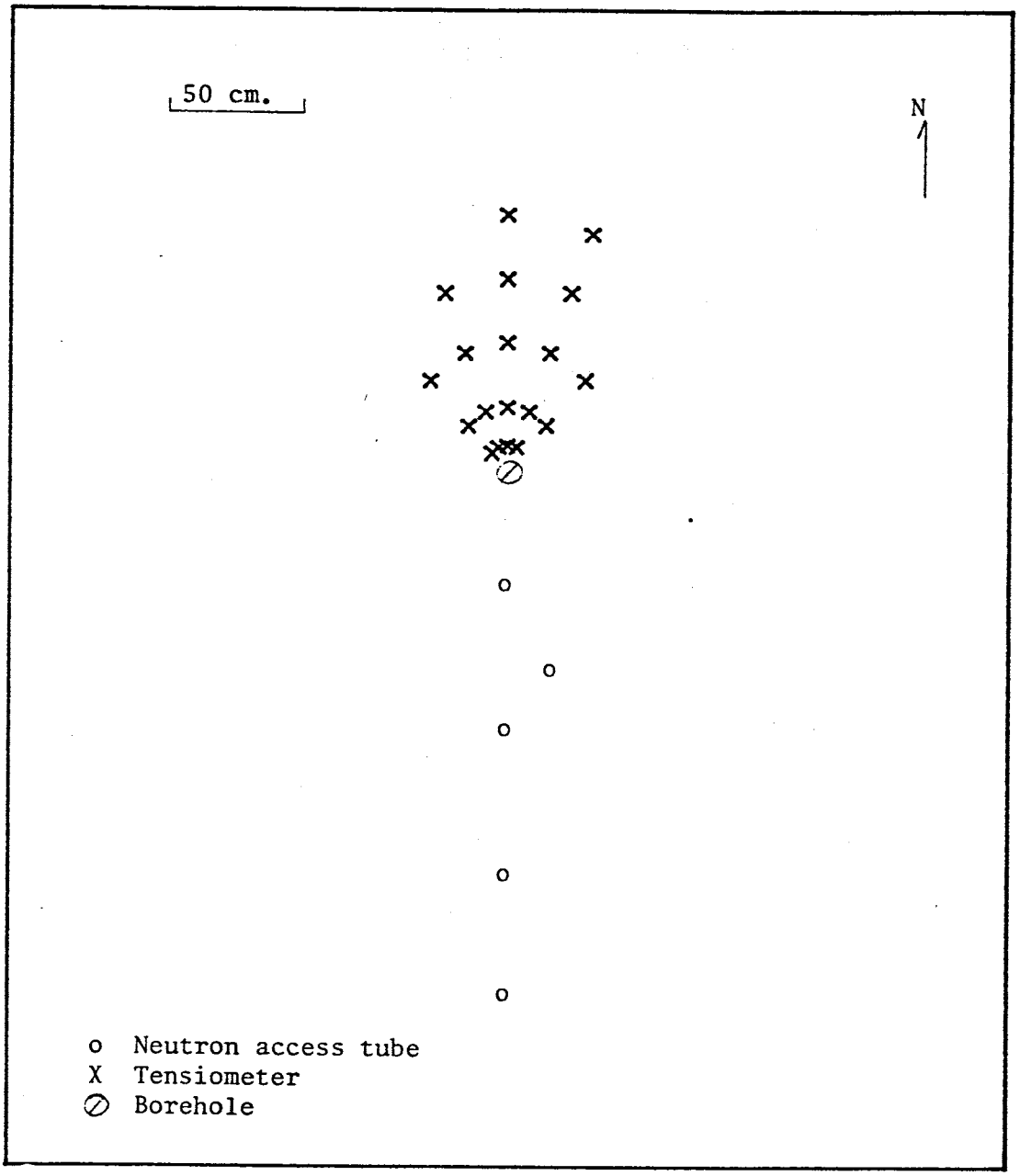

Figure 15. Location of Instrumentation for S9T1

Approximately two weeks after the conclusion of S9T1, the neutron probe was used to record moisture contents in soil surrounding the neutron access tubes used in S9T1. Immediately following the completion of all of the neutron probe measurements, 100 cubic centimeter soil samples were taken at elevations corresponding to neutron probe measurements. Samples were taken from two sides of each access tube. The samples were brought to the laboratory, where they were weighed and then oven dried. After oven drying, the samples were again weighed. The loss of weight in each sample was assumed to be due to a loss of water from the sample.

The gravimetric moisture content for each sample was calculated, as was the dry bulk density. The volumetric moisture content was then calculated by equation 5:

$$\theta = (w) \cdot (pb) \; / \; (pw) \qquad (5)$$

where 'θ' = volumetric moisture content, 'w' = gravimetric moisture content, 'pb' = dry bulk density (M/L^3), 'pw' = density of water (M/L^3) (assumed equal to 1).

The data from S9T1 were combined with data taken at the Sevilleta National Wildlife Refuge in a fine sand for purposes of calibration. The combined data were used to define a calibration curve shown in figure 16. The calibration curve has the following equation 6:

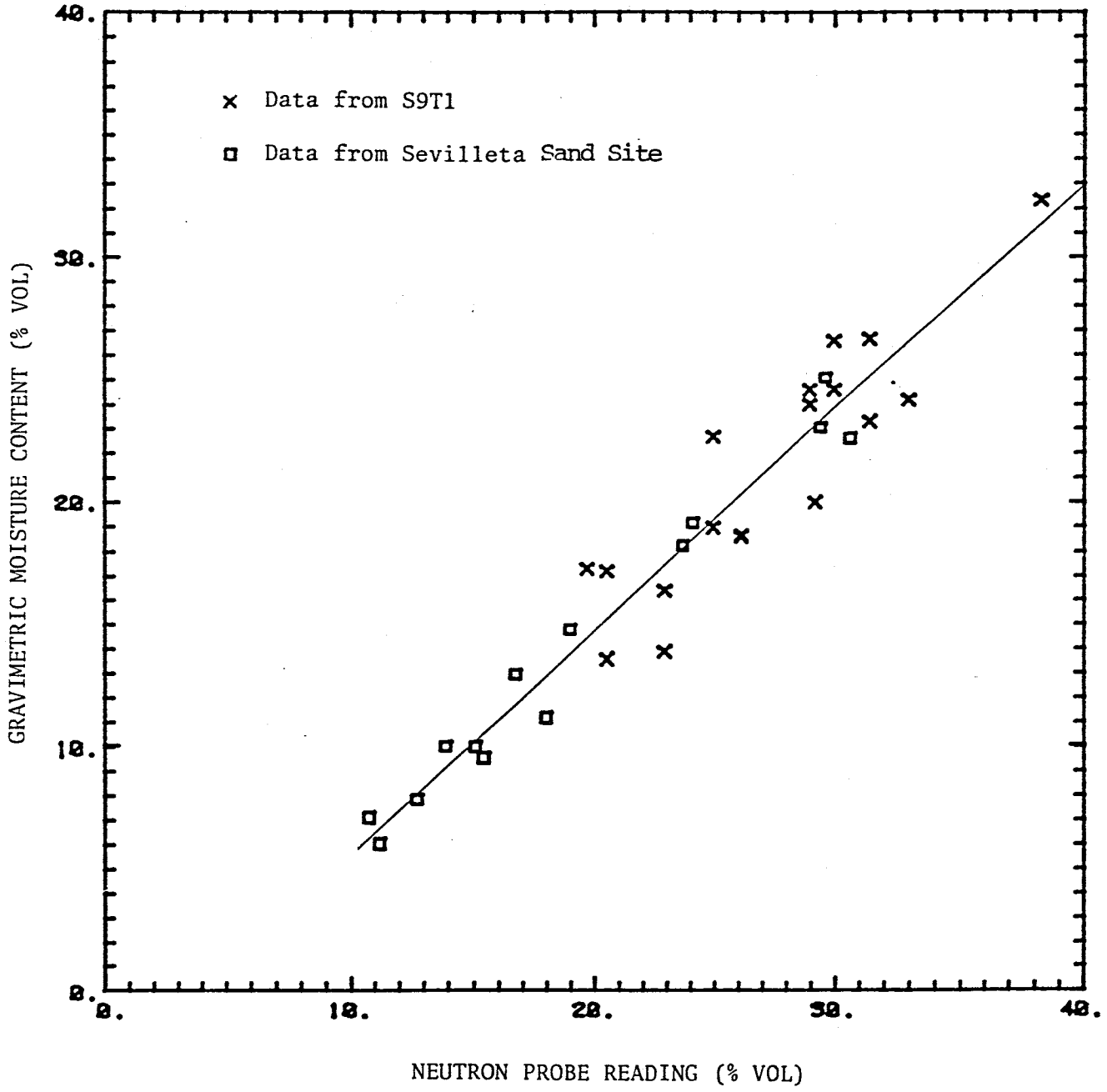

Figure 16. Neutron Probe Calibration Curve

$$\text{Actual} = 0.926\ (\text{N.P.}) - 0.0392 \qquad R^2=0.848 \qquad (6)$$

where 'N.P.' is the neutron probe reading (% vol) in decimals. This calibration curve was used to convert all neutron probe readings in S9T1 to actual moisture contents. Notice that the calibration curve does not extend below approximately 10% volume N.P. It is probable that the calibration curve below 10% volume differs from the calibration curve developed for S9T1.

4.3.3 Confidence intervals for the neutron probe

Both 4 second and 16 second neutron probe count rates were used in S9T1. In order to estimate the errors associated with the two count rates, the following experiment was carried out:

A series of fifty 16 second counts were recorded at a particular elevation in an aluminum access tube which had been previously installed outside the laboratory. Immediately following the sixteen second counts, and at the same depth, a series of fifty 4 second counts were recorded. The mean and standard deviation for both the 16 second counts and the 4 second counts were computed, assuming a normal distribution. We found that for the 16 second count rate, there exists a 68% confidence that any one reading will be within 0.205% volume of the actual moisture content, and a 95% confidence that any one reading will be within 0.41% volume of the actual value. For the 4 second count

rate, there exists a 68% confidence that any one reading will be within 0.404% volume of the actual moisture content, and a 95% confidence any one reading will be within 0.808% volume of the actual value.

4.4 Thermistors

The temperature of infiltrating water and soil water was recorded using model MC-312 thermistors (Soiltest, Inc., Evanston, Ill.) The accuracy of the thermistors is approximately ±1 degree Fahrenheit. A thermistor was attached to the bottom of the float valve in the borehole to monitor the temperature of the infiltrating water, and another thermistor was placed just below land surface. Other thermistors were placed at a radius of 50 centimeters from the borehole center at elevations of -100 and -200 cm.

4.5 Water Supply

Field water used in S9T1 was obtained from a well located in Blue Canyon (figure 3). Chemistry of the water is shown in Table 3. The water was pumped into two 400 liter barrels which were thoroughly cleaned and rinsed with distilled water. After the barrels were filled with water, the openings on the tops of the barrels were sealed with rubber stoppers and the water transported to the site by a departmental vehicle. At the site, the water was siphoned

out of these two barrels and into two 400 liter barrels used for water storage.

The two 400 liter barrels, previously used for water storage were previously used for borehole test S8T1 (Rabold, 1984). The barrels were cleaned out and internally coated with a rust-inhibiting coating before being placed on a table at site S9T1. Piping and valves were used to connect the barrels to the same float valve apparatus as designed by Rabold (1984). The valving system was designed to allow either one or two barrels to be used at any time. Manometers were placed along the side of each barrel, from which the volume of water discharged from one barrel could be found by equation 7:

$$V_d = 2.55 * (\Delta w) \qquad (7)$$

where 'V_d' equals volume discharged and 'Δw' equals decline in water level in the manometer (cm). When both barrels were discharging simultaneously, the calibration was doubled to 5.10. By dividing the volume discharged by the duration of the discharge, the rate of infiltration could be found, assuming a constant head of water in the borehole.

4.6 Float Valve

The float valve apparatus used in this borehole test was one which had been designed by Rabold (1984) for use in

test S8T1 (figure 17). Rabold (1984) includes specifications for design. Styrofoam was used as the flotation device. The float valve was calibrated in the laboratory, and this calibration was subsequently used to set the height of water in the borehole at the desired level.

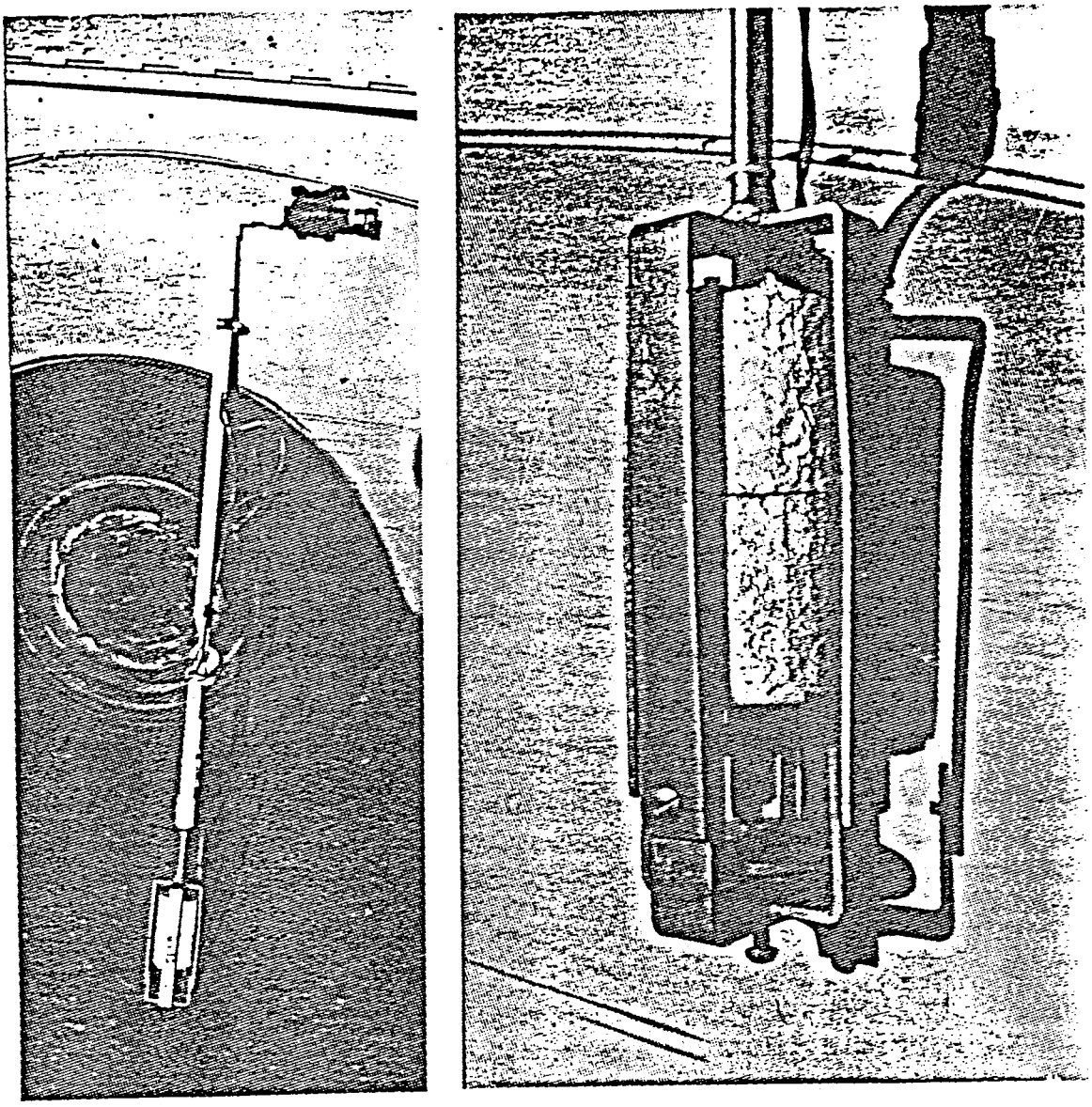

Figure 17. Float Valve (from Rabold, 1984)

5. FIELD PROCEDURES

Borehole infiltration test S9T1 began on September 5, 1984. In the days preceeding September 5, the borehole casing, thermistors, neutron access tubes, and water storage barrels had been emplaced. On September 5, approximately one and one half hours before water was allowed to enter the borehole, carbon dioxide was injected into the borehole to reduce entrapped air in the soil (Lambert 1983, Stephens, et al, 1983). The equipment used to inject the carbon dioxide into the borehole and surrounding soil included; a tank filled with carbon dioxide, a Victor number VTS 400D pressure regulator, a Victor 4000 psi inflow gauge, and a Marsh Safecase discharge gauge. These were connected to a Sho-Rate Flowmeter (Model 1355, Brooks Instrument Division, Emerson Electric Company, Hatfield, PA.) via tygon tubing. The flow rate of the carbon dioxide was determined from the rise of a steel ball in a graduated glass cylinder of the flowmeter by:

$$Q\ (LPM) = (G - 0.04) / 0.51 \qquad (8)$$

where 'G' equals the gauge reading (Rabold, 1984). Knowing elapsed time and flow rate "Q" enabled the determination of volumes of carbon dioxide injected.

Connected to the flowmeter was a discharge tube which

extended into the borehole. After flooding the borehole with carbon dioxide for five minutes in order to remove some of the air in the borehole, the borehole was sealed off with a rubber stopper and duct tape, leaving only the tubing extending into the borehole. Carbon dioxide was then forced into the soil surrounding the borehole. The gauge was kept approximately at a level of 2, which resulted in a flow rate of approximately 3.84 liters per minute. Carbon dioxide was injected for a total time of 95 minutes, for a total volume injected of 364.8 liters of carbon dioxide.

While the borehole was flooded with carbon dioxide, background moisture content readings were taken at the various radii. No tensiometers were in place as of yet, because it was feared that the pressure heads would exceed the air entry value of the tensiometer cups. Background soil-water temperatures were recorded, as well as the initial water levels in the water storage barrels.

After flooding the borehole with carbon dioxide for 95 minutes, the carbon dioxide was cut off and the tubing removed from the borehole. The valves leading from the water storage barrels to the float valve were opened and water was allowed to enter the borehole. The borehole did not immediately fill. It took approximately 66 minutes for the water level in the borehole to reach the desired 76.2 cm above the bottom of the borehole.

Tensiometers were emplaced at radii of 25, 50, 75, 100, and 150 cm from the borehole center on day 2 of the test.

They were given one day to equilibrate before data were recorded. On day 7, tensiometers were installed at a radius of 10 cm from the center of the borehole to accurately define the total and pressure heads near the borehole. These tensiometers were also given one day to equilibrate before readings were recorded.

Moisture content, temperature, total head and pressure head, height of water in the borehole, and infiltration rates were all monitored periodically throughout the test. Whenever the water in the water storage barrels became low, they were refilled with fresh field water from Blue Canyon (figure 3). The tensiometer manometer stands and the tensiometers themselves were covered with plywood between readings in order to minimize evaporation and temperature fluctuations. Occassionally, the manometers were purged of air bubbles in the tubes by pushing distilled, de-aired water throught the manometer tubes.

On September 20, 1984 (t=21,972 min), the infiltrating water was switched from field water to tap water in order to study changes in chemistry. A subsequent chemical analysis of the two waters revealed they were similar, however, as shown on Table 3.

Borehole test S9T1 was ended on September 26, 1984 due to a constant rain which made access to the site impossible. This test lasted approximately 28,000 minutes, making it the longest borehole infiltration test to date at New Mexico Institute of Mining and Technology.

5.1 Carbon Dioxide Flood

A total of 364.8 liters of carbon dioxide were injected into the borehole before beginning infiltration into S9T1. One pore volume is defined as the volume of carbon dioxide injected divided by the void volume of the soil sampled during the borehole infiltration test. The volume of soil sampled can be found using Bouwer's (1978) equation :

$$Ss = 0.4\ H^3 \qquad (9)$$

where Ss = volume of soil sampled, and "H" is the height of water in the borehole. For S9T1, H = 76.2 cm, resulting in a value of 176,980 cubic centimeters for Ss. Assuming a porosity of 0.5 from laboratory samples, the void volume of the soil sampled is 88,490 cubic centimeters. The number of pore volumes injected into the soil can be found by dividing the total volume of carbon dioxide injected (364,800 cubic centimeters) minus the borehole volume (14,000 cubic centimeters) by the void volume (88,490 cubic centimeters). This results in 4 pore volumes being injected into the soil.

The effectiveness of 4 pore volumes of carbon dioxide in reducing entrapped air is unclear. Lambert (1983) varied the number of pore volumes injected to study the effect of carbon dioxide on infiltration rates and cumulative infiltration. Figure 18 shows his results as far as cumulative infiltration is concerned. Notice that

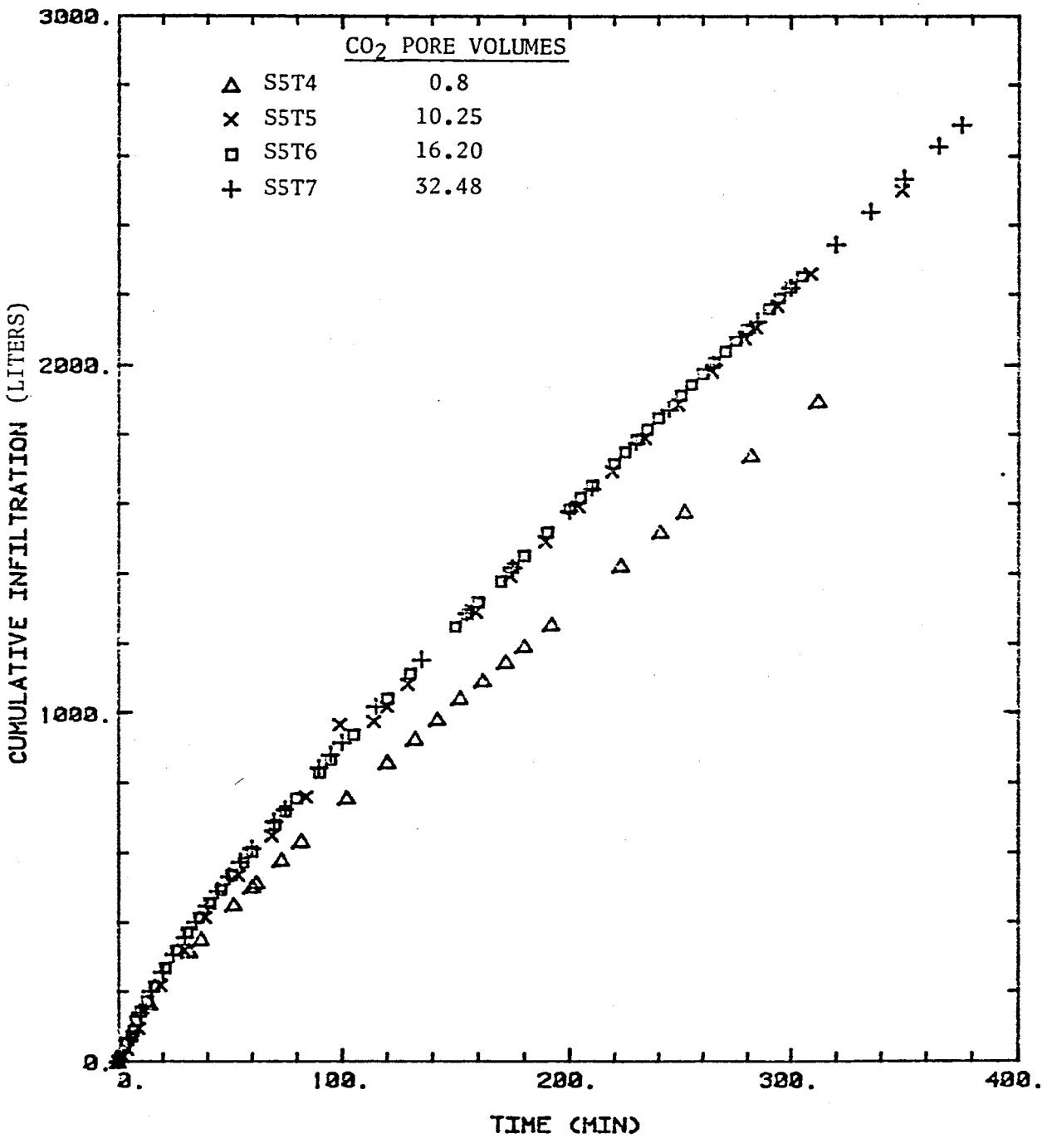

Figure 18. Cumulative Infiltration versus Time for Borehole Infiltration Tests S5T4 through S5T7

increasing the number of pore volumes from 0.8 to 10.25 did affect the cumulative infiltration, but increasing the number of pore volumes above 10.25 did not affect it.

It is unclear whether 4 pore volumes would lie intermediate to S5T4 and the other tests, or if it would lie along the same curve as S5T5-S5T7. It is also unclear whether the results from Lambert are applicable to the finer-grained soil of S9T1.

5.2 Correcting infiltration rates for viscosity changes

Infiltration rates into the borehole vary with temperature due to changes in the viscosity of the infiltrating water. As in previous borehole infiltration tests (Rabold, 1984, Watson, 1983, Lambert, 1983, Tyler, 1982), temperature readings were taken concurrently with infiltration rate readings. However, after the first day of testing in S9T1, both infiltration rate and temperature readings were taken only one or two times daily. This made it necessary to estimate temperature fluctuations over time in order to correct infiltration rates for changes in viscosity. The infiltration rates were all corrected to 20 degrees Celsius.

Assistance in estimating temperature fluctuations was obtained from the National Weather Service Forecast Office in Albuquerque, New Mexico, who were kind enough to send data which listed the high and low temperatures for Socorro, N. M. over the period in which S9T1 was being conducted. These data were then used to correct infiltration rates using the following formula:

$$Q_C = Q_O * (u_O/u) \qquad (10)$$

where:

Q_C = the infiltration rate corrected to 20 degrees Celsius

Q_o = the observed infiltration rate (L^3/T)

u_o = the viscosity of water at 20 degrees Celsius

u = the viscosity of water at the average infiltrating temperature

The average infiltrating temperature was obtained by finding the average temperature of the infiltrating water between two field readings. In order to do this, the following assumptions were made:

1) The temperature of the infiltrating water was in equilibrium with the surrounding air.

2) The high and low temperatures occurred at 1600 and 0500 hours respectively.

3) The temperature varied linearly between the two extremes.

4) The temperature at the field site was the same as the temperature in the city of Socorro.

6. RESULTS

We do not believe precipitation had a significant effect on the results of the test. Variations in horehole water level caused changes in infiltration rate, total head and pressure head, and hydraulic gradient. Comparison of infiltrating water temperature to soil water temperature indicates entrapped air may have impeeded infiltration rate and thus the value of saturated hydraulic conductivity. Cumulative infiltration exceeded the maximum volume recommended by the United States Bureau of Reclamation (USBR). Moisture content, total head, and pressure head data indicate infiltration was affected by variations in soil stratigraphy near the borehole. A comparison of hydraulic gradients to infiltration rate supports the hypothesis of entrapped air influencing infiltration rate. Estimates of saturated hydraulic conductivity (Ks) from the infiltration test were approximately 2 to 5 times lower than Ks values obtained from laboratory shelby-tube permeamter tests. Empirical equations developed by Stephens, et al (1983) to account for unsaturated flow do not differ significantly from equations which neglect unsaturated flow.

6.1 Precipitation during the infiltration test

When conducting a borehole infiltration test of this length (approximately 28,000 min), precipitation and

6.2 Water Level in the Borehole

Water level in the borehole was maintained by a float valve designed by Rabold (1984). The water level was maintained at about 76.2 cm above the bottom of the borehole. Figure 19 shows that about 66 minutes elapsed before the water level in the borehole reached the desired level of 76.2 cm. Prior to t=66 min, the soil was able to receive the water more quickly than the float valve was able to deliver it.

As figure 20 shows, the float valve worked fairly well, with five obvious malfunctions. After approximately t=24,000 min, the styrofoam used in the float valve from the beginning of the test was replaced with fresh, dry styrofoam. It was thought that the first set of styrofoam had become water-logged, which led to the malfunction of the float valve. Also, some scaling was evident on the float valve, which may have contributed to its failures at various times.

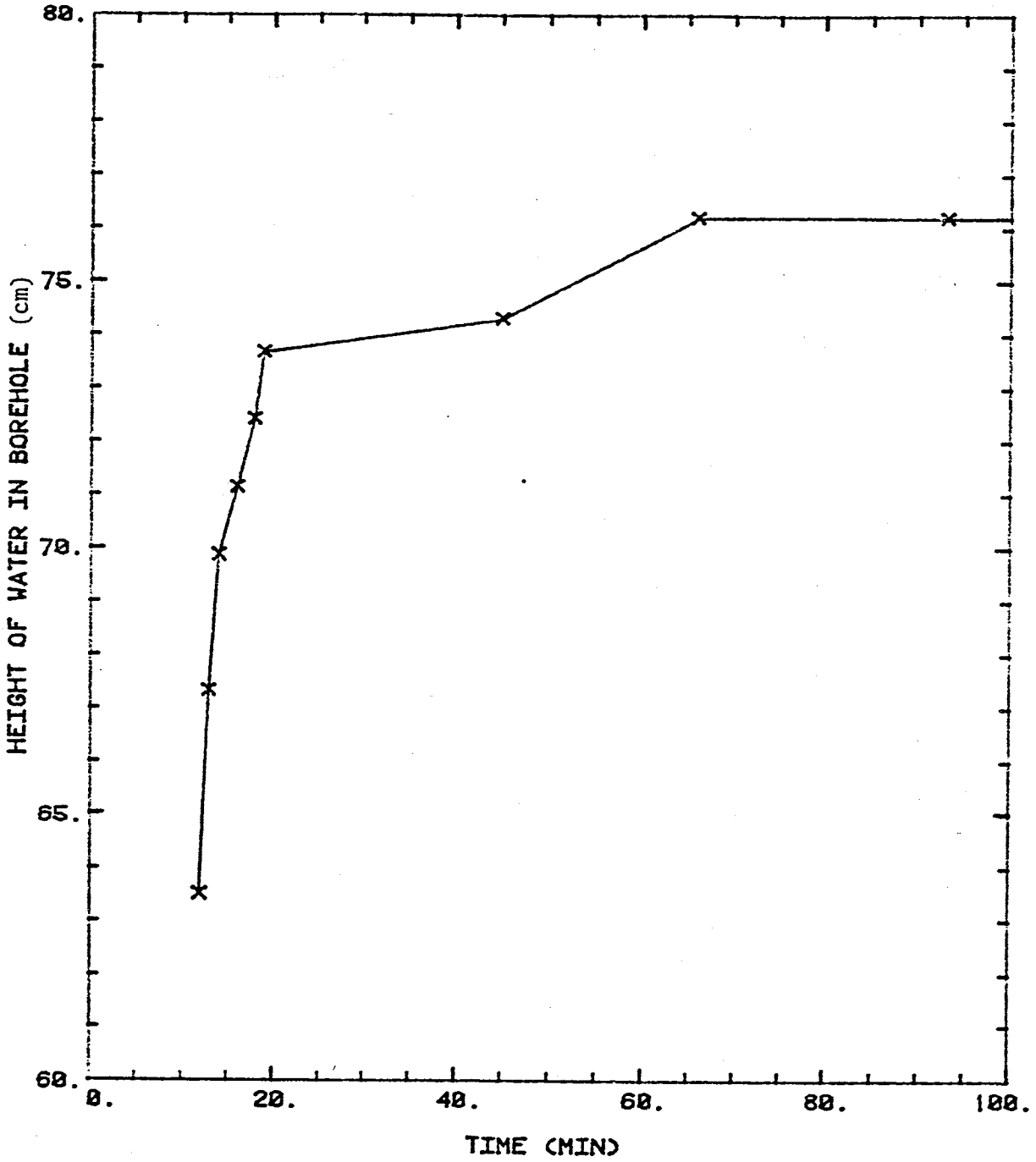

Figure 19. Height of Water in the Borehole versus Time for the first 100 minutes of S9T1

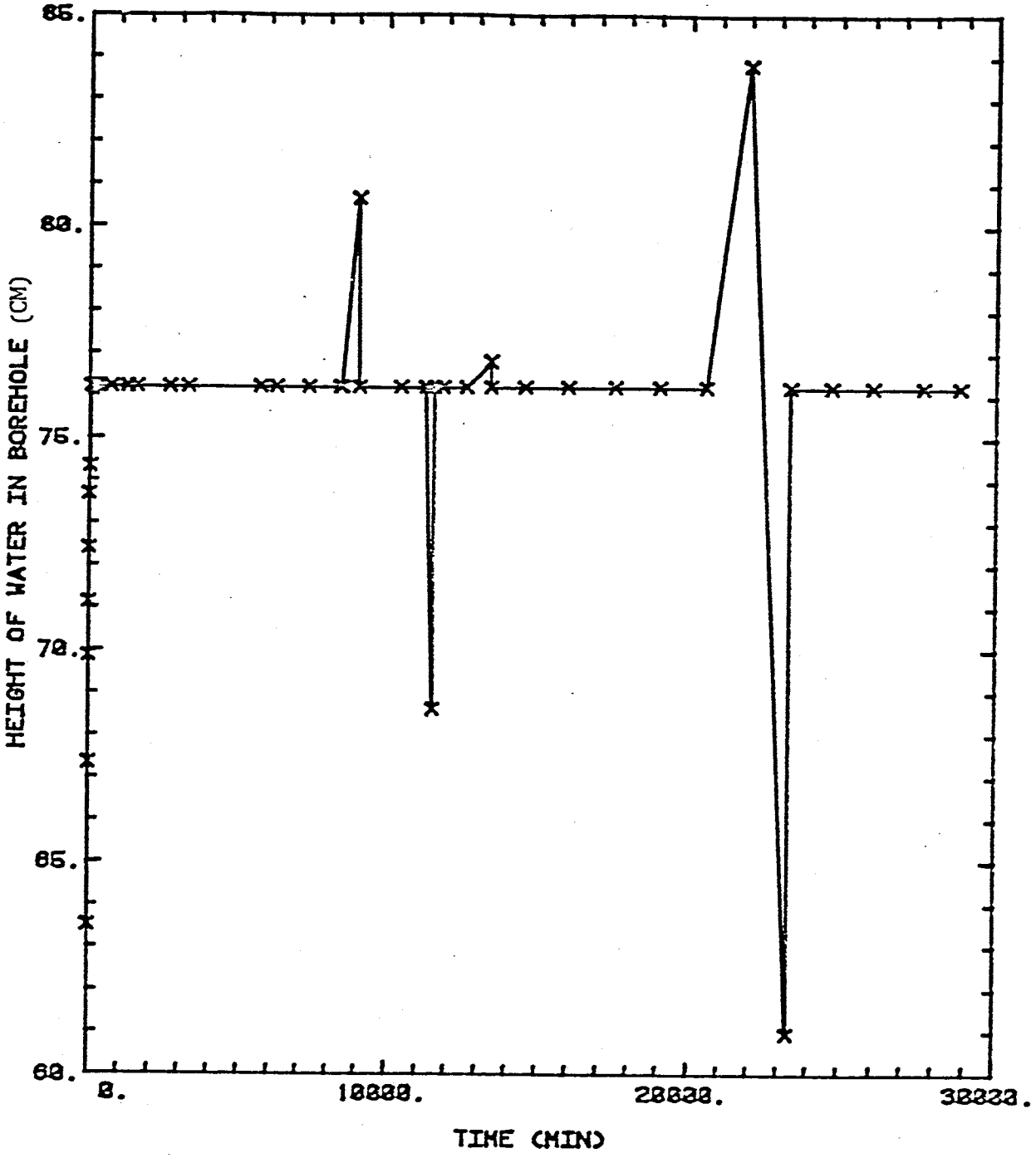

Figure 20. Height of Water in the Borehole versus Time for S9T1

6.3 Temperature in the Borehole

Temperature in the borehole versus time is presented in figure 21. The temperature in the borehole was recorded by attaching a thermistor to the bottom of the float valve. Temperature of the infiltrating water fluctuates with the time of day, since the water supply barrels were in contact with the atmosphere. The temperature data should be viewed as possibly informative, but not definitive. Some of the variations in temperature are the result of readings taken just after refilling the water supply barrels with fresh well water. Assuming a constant temperature for the well water, adding it to the water supply barrels could significantly raise or lower the temperature of the water, depending on the time of day the water was added. Also, readings were sometimes taken 24 hours apart. While the temperature would be approximately the same for both readings, this does not imply that the temperature remained constant between the readings.

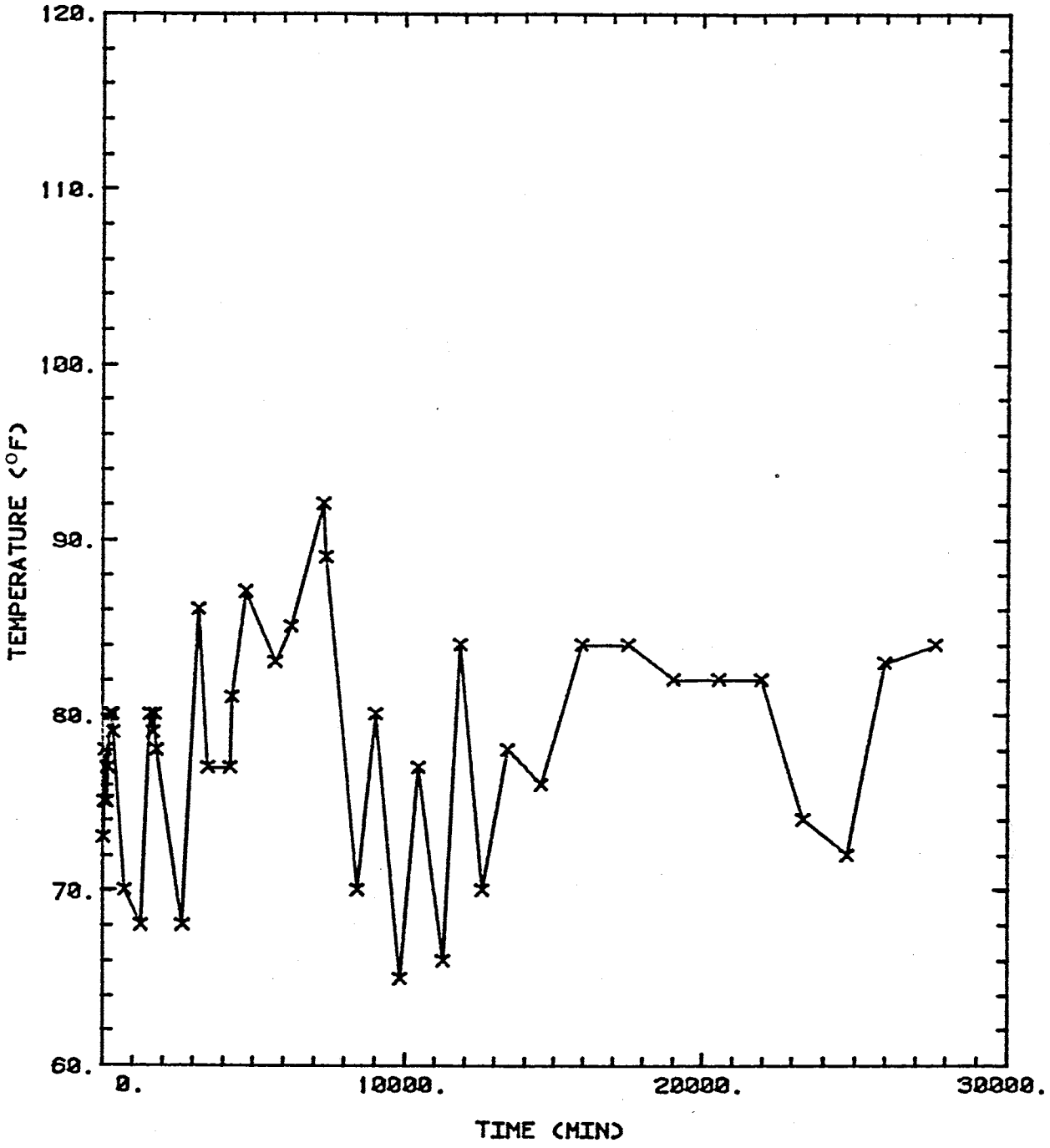

Figure 21. Temperature in the Borehole

6.4 Soil-Water Temperature

Two temperature blocks were installed for S9T1. Both were at a radius of 50 cm from the borehole, at elevations of -100 cm and -200 cm. The changes in soil-water temperature over time are presented in figure 22.

The soil-water temperature increased from t=0 to approximately t=7000 min. The rise in temperature was caused by the introduction of infiltration water having a higher temperature than the insitu soil water. The soil-water temperature decreased after t=15,000 min, due to a decrease in the mean air temperature (National Weather Forecasting Service, Albuquerque, N.M.). Lower mean daily temperature may have lowered the mean temperature of the infiltrating water, and resulted in the decrease in soil-water temperature. Borehole temperature readings (figure 21) do not indicate a similar decrease in temperature, probably because borehole temperature was more sensitive to the air temperature at the time of reading than to the mean daily temperature.

The soil-water temperature values were accurate only to within 1 degree Fahrenheit, which may explain some of the short term variations seen in figure 22. The general trend of increased temperature, constant temperature, and then decreased temperature are probably not caused by this accuracy problem.

Figure 23 is a plot of soil-water temperature at an

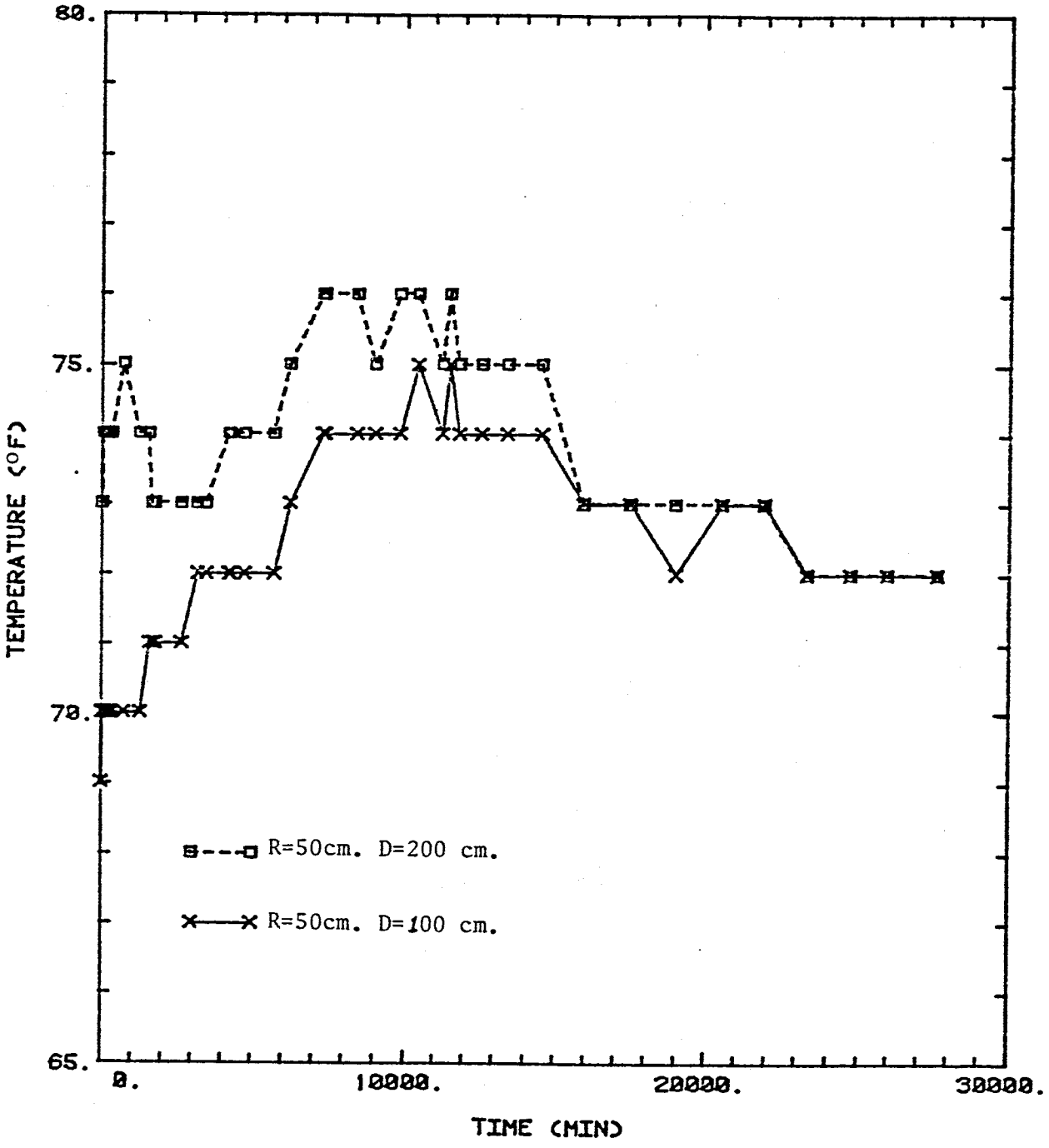

Figure 22. Soil-water Temperature versus Time

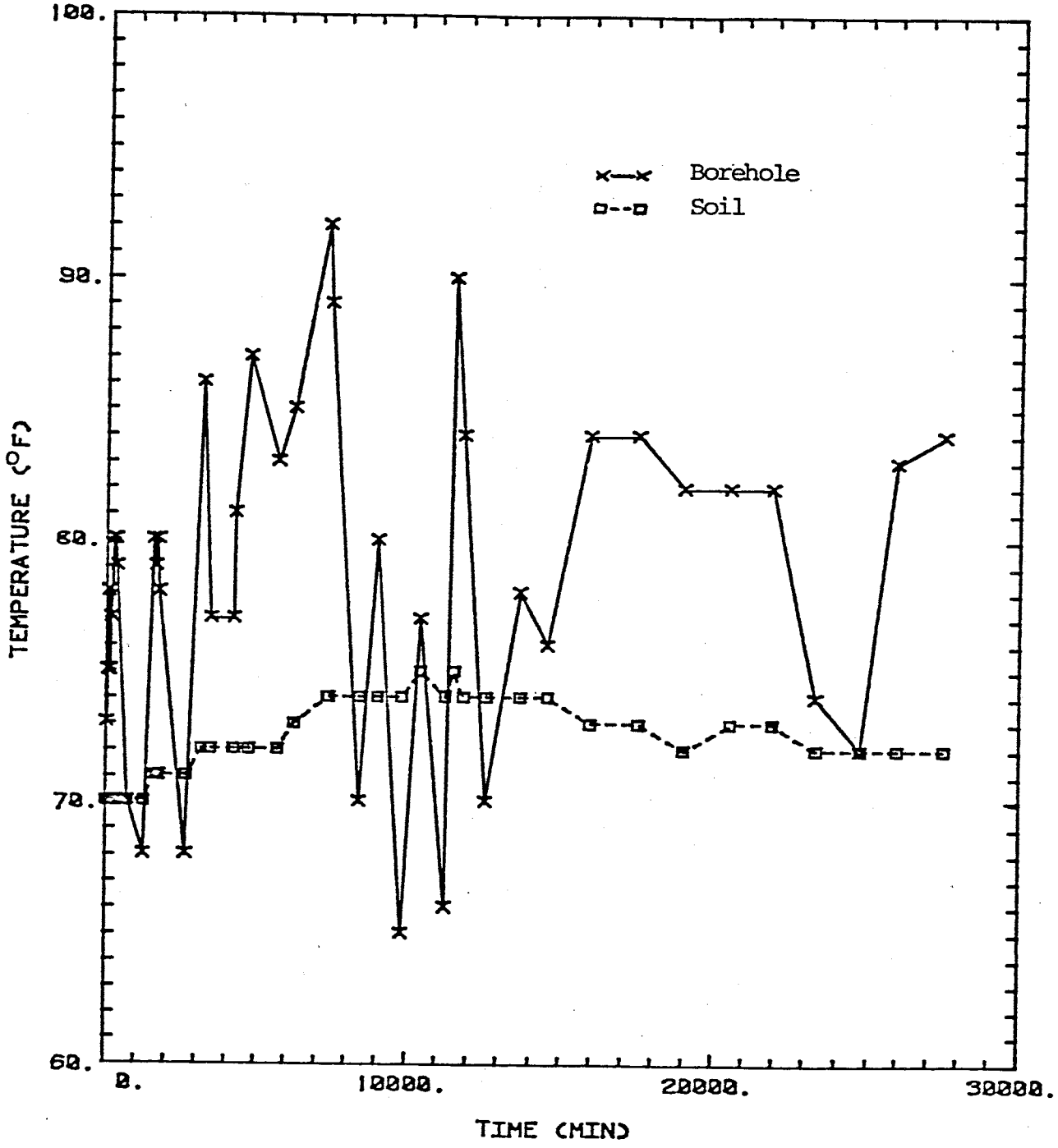

Figure 23. Temperature of Soil-water at R=50 cm and an elevation of -100 cm from land surface datum versus borehole temperature

elevation of -100 cm and borehole temperature. The periods when borehole temperature is below soil-water temperature represent early morning readings. Stephens, et al (1983) indicated borehole temperatures below soil-water temperatures favor the formation of entrapped air in the soil profile. Figure 23 suggests that entrapped air may have been present in S9T1.

6.5 Infiltration Rate

Figure 24 is a plot of infiltration rate (Q) versus time for S9T1. The two obviously anamolous points are explained as follows: The data point at t=2682 min (pt. 1) was recorded just after refilling the water storage barrels. Perhaps some surging of the float valve was caused by refilling the barrels. The data point at t=11,576 min (pt. 2) is explained by a malfunction of the float valve which allowed the water level in the borehole to drop by 10%. The float valve was repaired and the water level allowed to rise to its proper level before this reading was taken. The excess water needed to return the water level to its proper position resulted in the high value of infiltration rate.

Between t=11,533 min and t=13,423 min Q remained relatively low. This is thought to be due to entrapped air in the soil after the 10% decrease in head in the borehole. Between t=13,423 min and t=14,533 min it is possible that the a portion of the entrapped air was removed from the soil, and Q increased.

The sudden decrease in Q at t=11,533 min creates problems in picking a value for steady infiltration rate. Q varies by 25% between t=14,533 min and t=20,532 min. If the relatively low values of Q between t=11,533 min and t=14,533 min are excluded, the slope of the decrease in Q between t=14,533 min and t=20,532 min seems to follow the slope of the decrease prior to t=11,533 min.

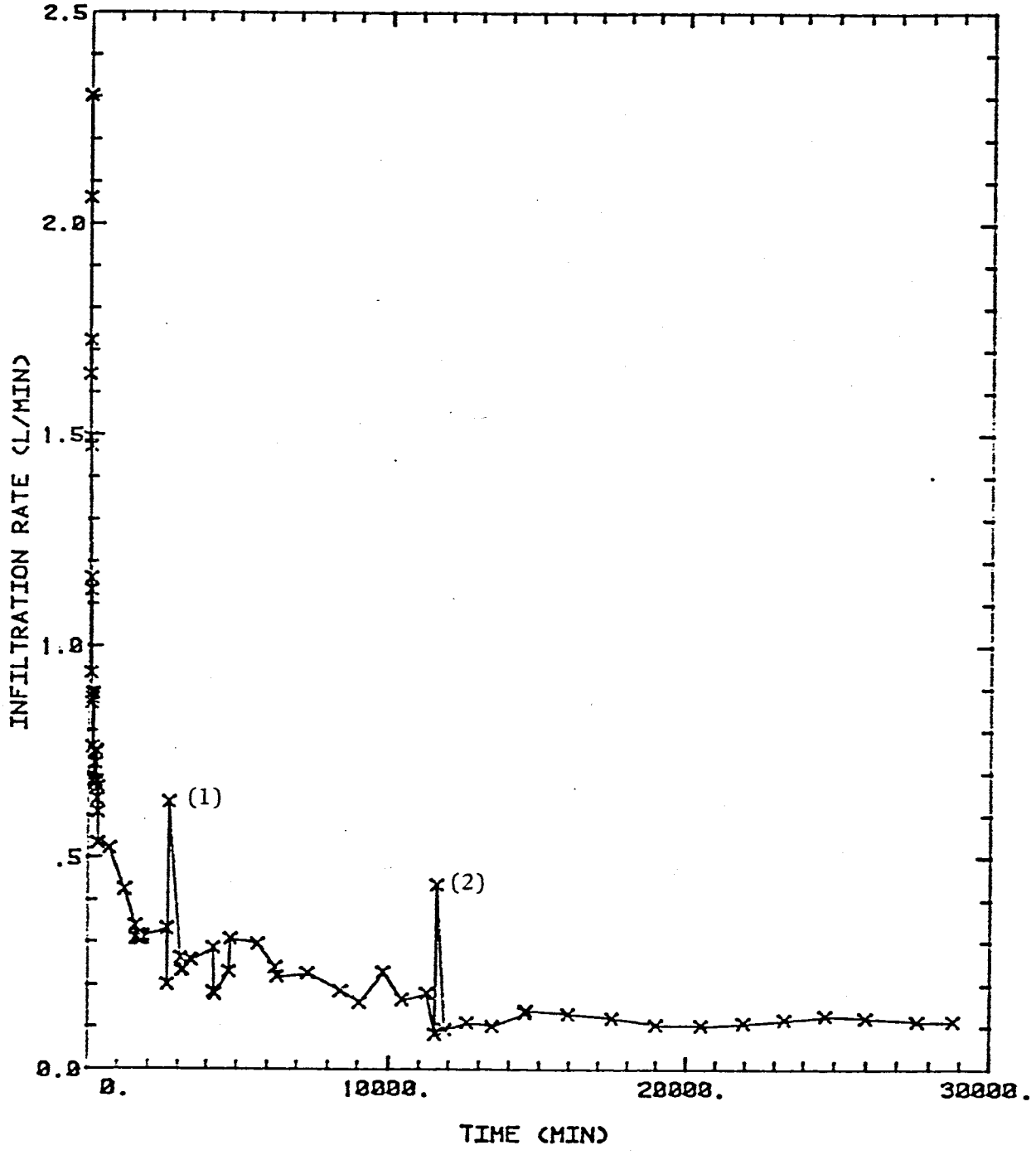

Figure 24. Infiltration Rate versus Time

However, Q does vary after t=20,532 min, alternately increasing and decreasing. For purposes of this study, steady infiltration rate is assumed to have been reached at t=14,533 min, with an infiltration rate of 0.12 lpm averaged from the data between t=14,533 min and t=28,802 min.

The infiltrating water was changed from field water to tap water at t=21,972 min. No drastic change in Q occurred after the change in water for S9T1. The chemistries of the tap water and field water were very similar (Table 3), which caused Q to remain steady. In contrast, Rabold (1984) reported a drastic change in infiltration rate after changing the chemistry of the supply to tap water from on-site groundwater.

6.6 Cumulative Infiltration

Cumulative infiltration versus time is presented on figure 25. The slope of the curve decreases steadily as time progresses, until steady-state is reached. At steady-state and beyond, the slope of the line becomes more or less constant. This constant slope begins at approximately t=14,000 minutes, which coincides with the beginning of steady-state observed on the graph of infiltration rate vs. time (figure 24). The time to reach steady infiltration rate is approximate, and could be as early as 11,000 minutes.

According to the USBR (Earth Manual, 1974), the minimum volume of water needed to reach a steady value of infiltration rate (Vmin) is given by equation 11:

$$V_{min} = 2.09 * Sy * H^3 * \left(\frac{2}{\sinh^{-1}(H_D) - 1} \right)^{3/2} \qquad (11)$$

where Sy is the specific yield of the soil being tested and is defined as porosity minus residual water content. Assuming a porosity of 0.47 from a laboratory sample from an elevation of -100 cm and a residual volumetric moisture content of 0.25 from the pressure head-moisture content curve, the specific yield is equal to 0.22. For S9T1, "H" was 76.2 cm and "r" was 5.08 cm. Using these values, Vmin is 155 liters.

The USBR (Earth Manual, 1974) also recommends that a

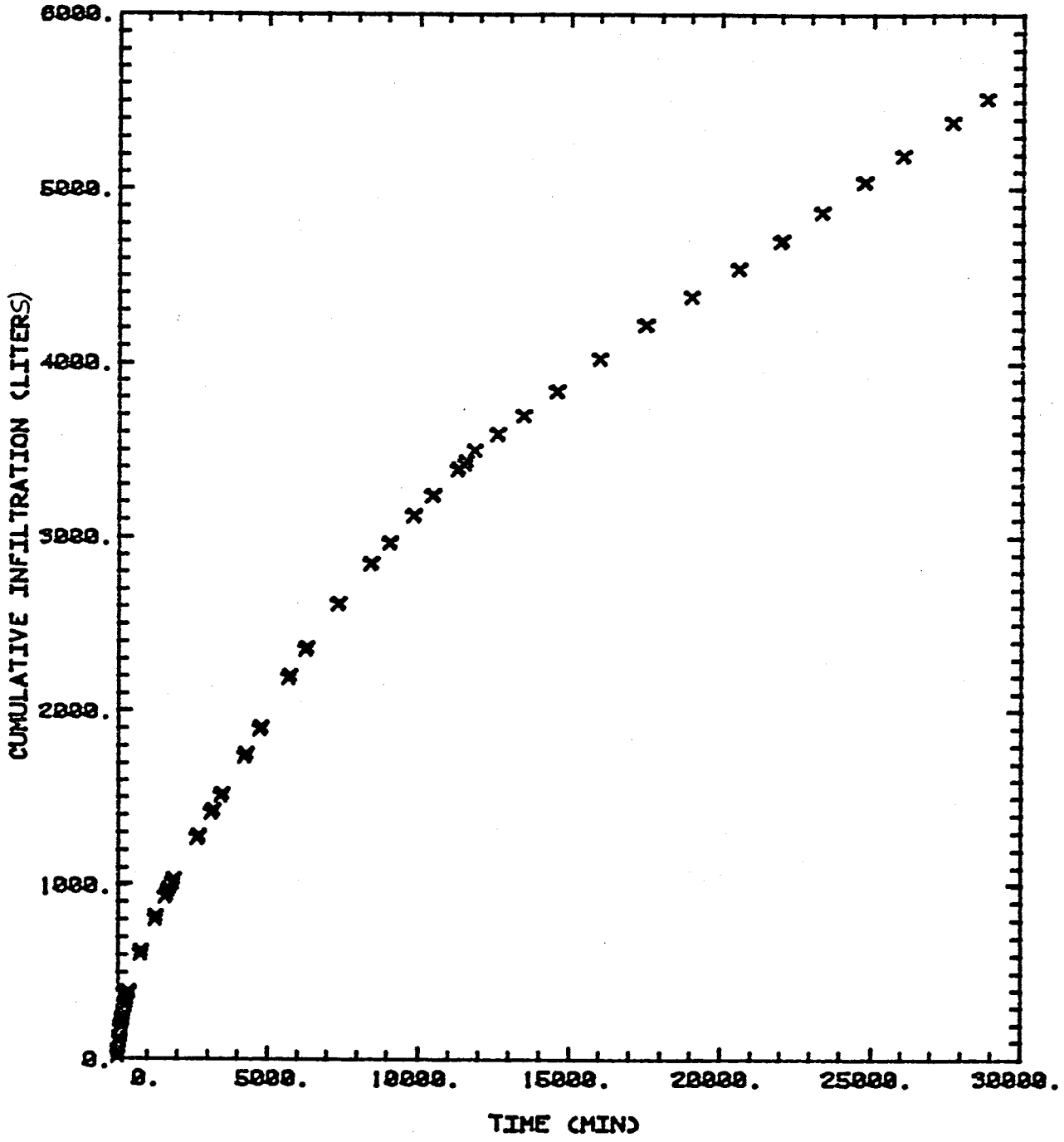

Figure 25. Cumulative Infiltration versus Time

maximum volume of water not be exceeded in a borehole infiltration test. The value of Vmax is 2.05 times greater than Vmin; with Vmin equal to 155 liters, Vmax is found to be 317 liters. Vmin and Vmax occur at t=88 min and t=262 min, respectively. At Vmax, infiltration rate is aproximately 6.1 times higher than the infiltration rate at steady state.

Both Vmin and Vmax occur well before steady state was reached. The volume of water needed to reach steady-state was approximately 3850 liters, which is 12 times greater than the 317 liters recommended by the USBR.

6.7 Moisture Content

Moisture content profiles for various times were generated using a contouring routine called NCAR (National Center for Atmospheric Research, Scientific Computing Division Graphics System, May 1983). All moisture content readings have been corrected to actual moisture contents. The borehole is included in each profile, as well as the water level in the borehole.

Figure 26 is a profile of background (t=0) moisture content. These data were taken just before beginning the borehole infiltration test. The profile shows that the soil between elevations of approximately -200 cm and -350 cm was slightly dryer than adjacent strata. Sieve analyses indicate soil below -180 cm was more uniform in grain size and coarser in d10 size. Coarser-grained soils would be expected to have lower moisture contents than finer-grained soils.

Cuttings obtained when augering holes for the neutron probe aluminum access tubes had revealed the presence of an organic layer at an elevation of -360 cm. The organic layer was about 253 cm below the bottom of the borehole, and was not considered to affect the infiltration rate of the borehole infiltration test.

Figure 27 shows the vertical variability in moisture content. Figure 27 shows the highest value of moisture content to occur at an elevation of approximately -140 cm.

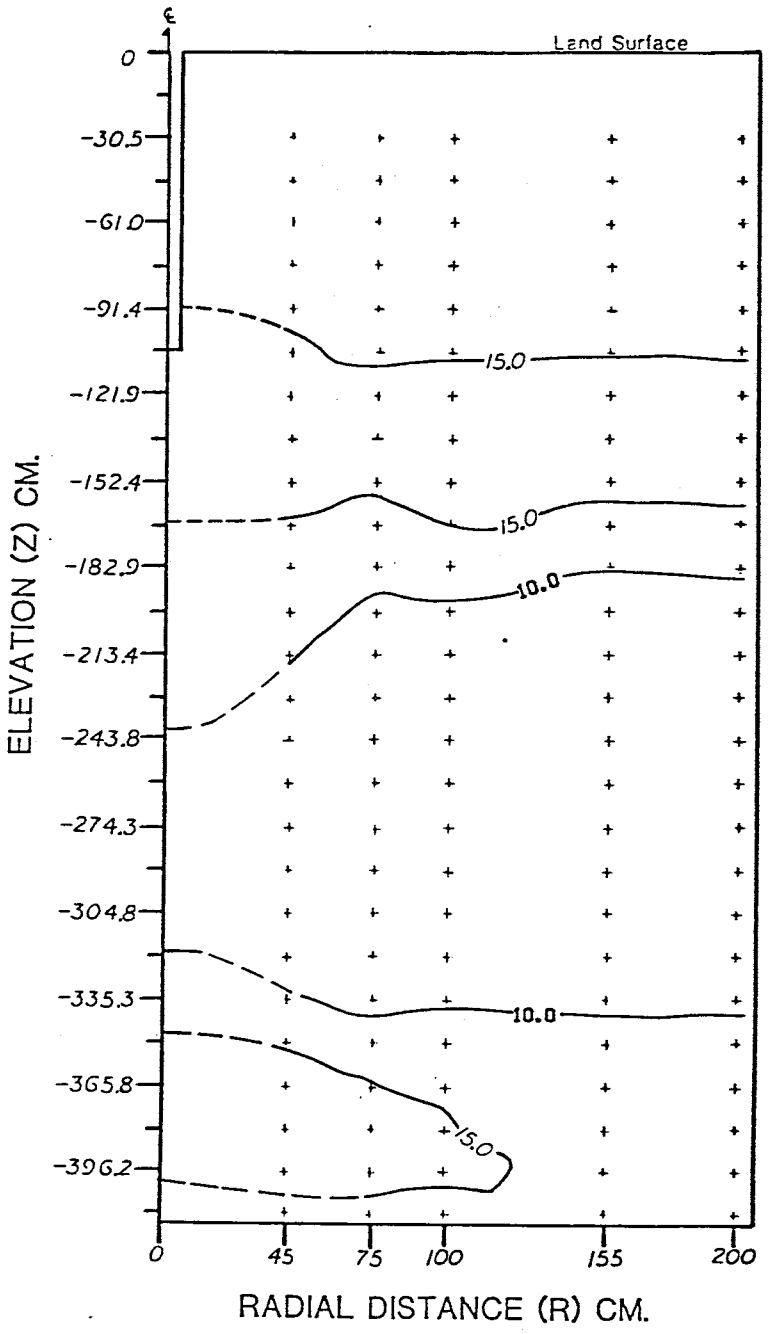

Figure 26. Moisture Content Profile at t=0 minutes

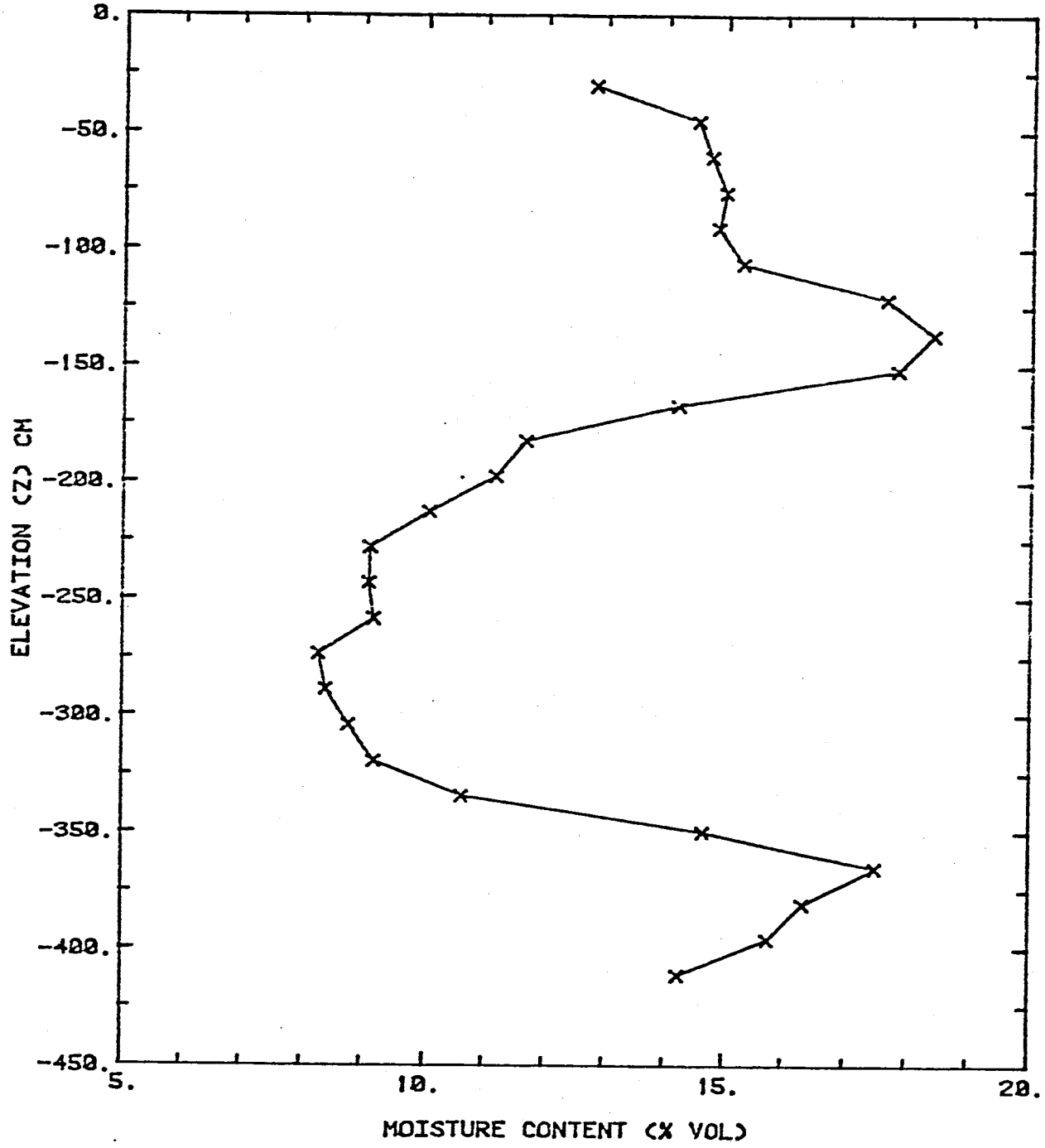

Figure 27. Moisture Content versus Elevation at R=45 cm and t=0 minutes

Figure 28 shows the moisture content profile at t=252 min. The wetting front has already reached a radius of approximately 85 cm from the borehole center at elevations of approximately -75 cm to -120 cm. The moisture content profile inside the wetting front (less than 15% vol) is fairly concentric around the borehole at this time. By t=1224 min (figure 29), the wetting front has extended both laterally and vertically. The profile inside the wetting front is still fairly concentric around the borehole.

Clay expansion or soil swelling may have occurred during S9T1. By t=90 min of the test, a fracture at the soil surface extended from the borehole to approximately a radius of 60 cm. In the following two days, two more fractures were observed. The fractures appeared to lengthen in response to radial distance to the wetting front. The fractures were at 90 degrees from one another, with a total of three fractures. No fracture extended from the borehole towards trench T-3 (figure 4). The fractures were approximately 1.5 cm in width, with a pencil or finger being easily pushed into fractures.

Figure 30 (t=2632 min) shows that the wetting front has moved still farther radially. However, the 30% moisture content contour has not extended nearly as much as the other contours. The 20% and 25% countours show evidence of water mounding above the coarser layer at an elevation approximately -180 cm. The 30% contour does not show evidence of mounding probably due to the air entry value of

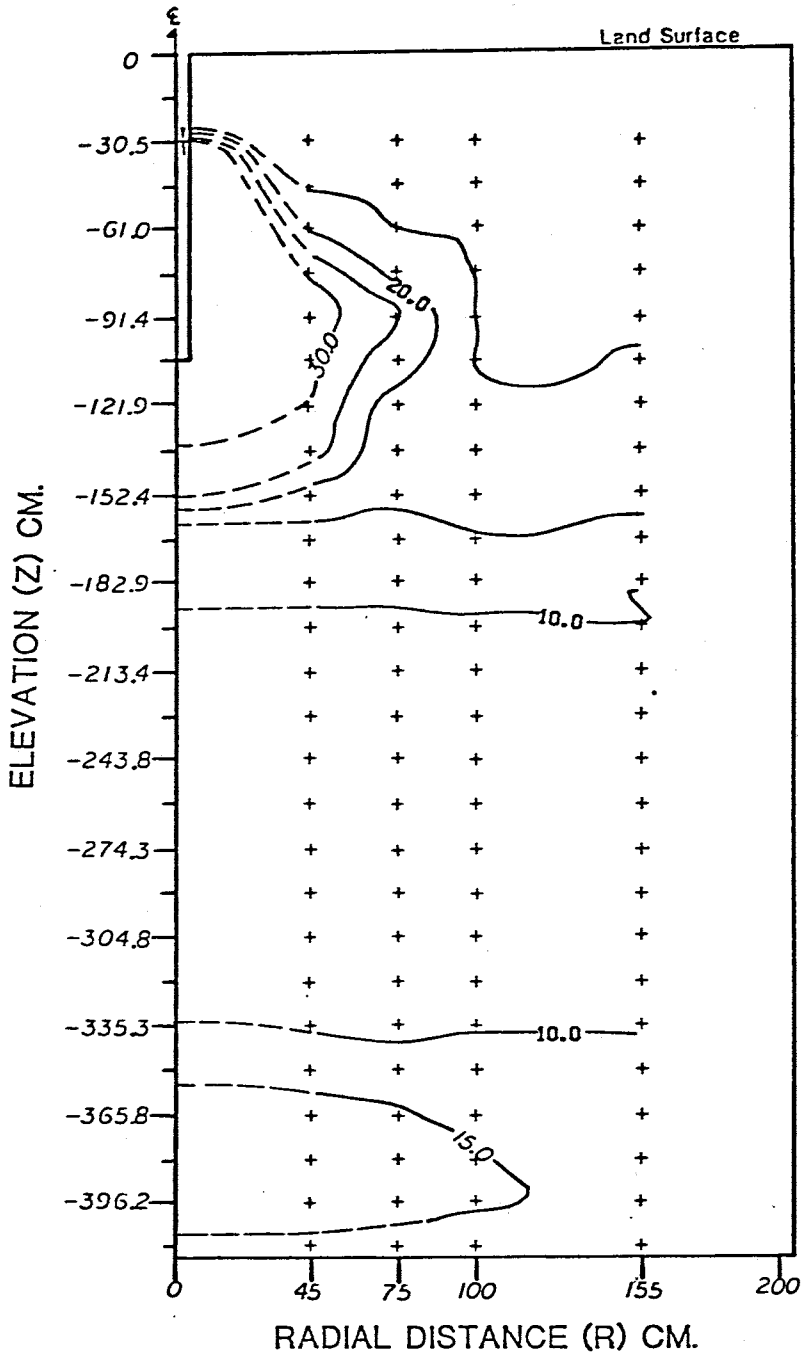

Figure 28. Moisture Content Profile at t=252 minutes

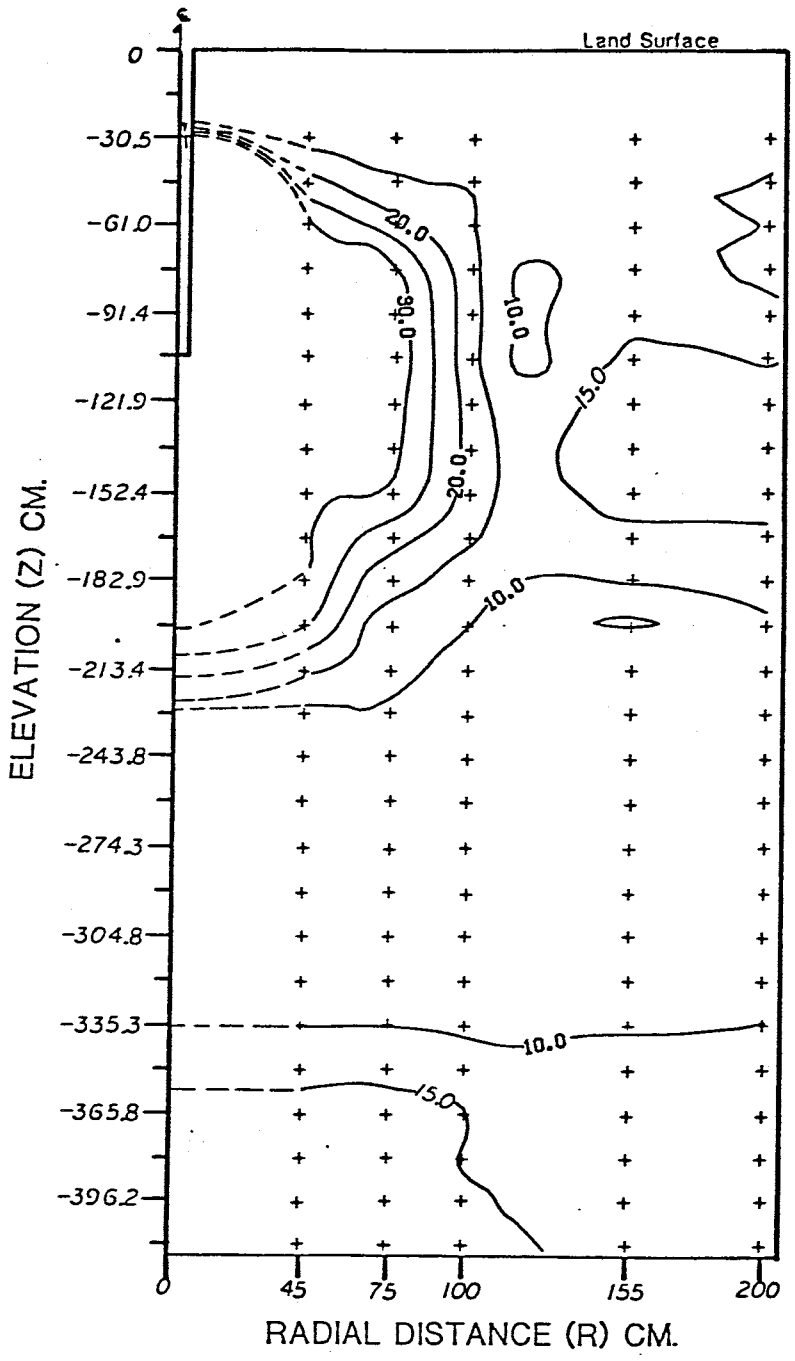

Figure 29. Moisture Content Profile at t=1224 minutes

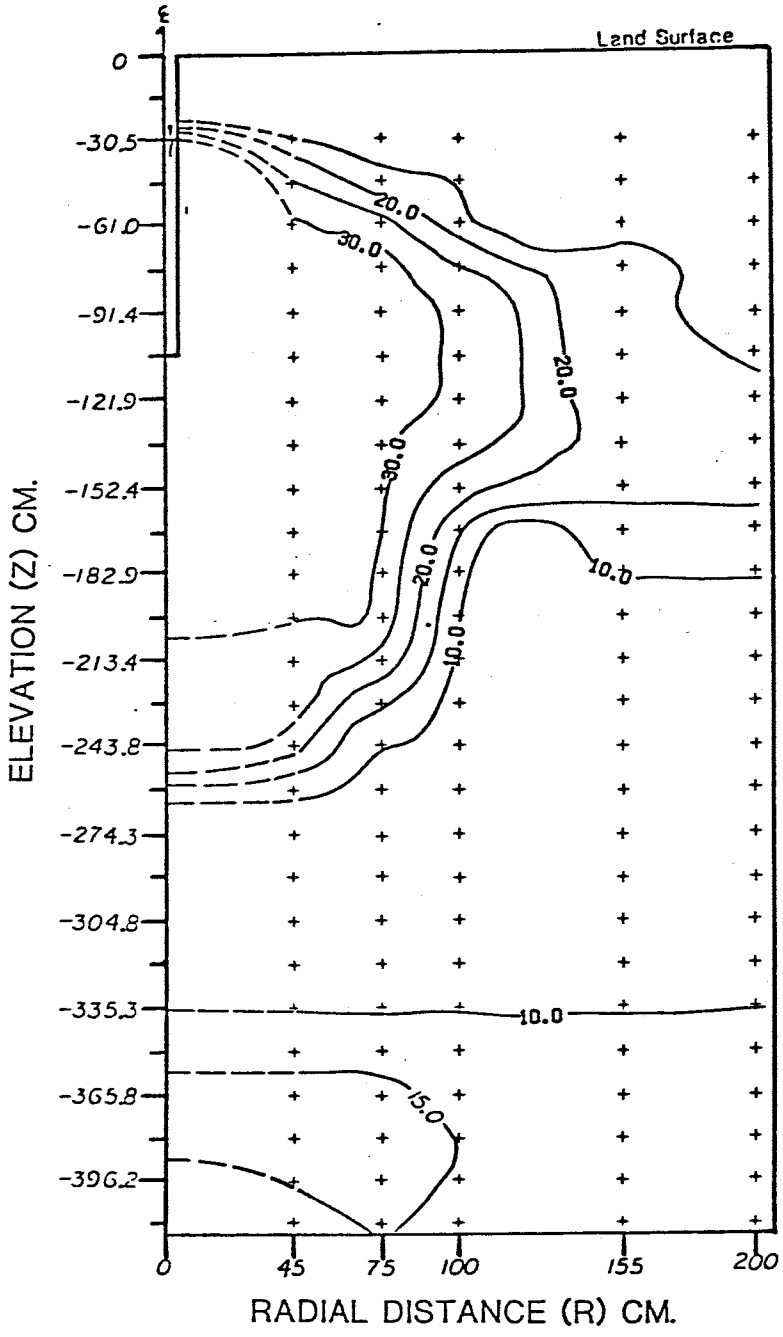

Figure 30. Moisture Content Profile at t=2632 minutes

the coarse layer having been exceeded, allowing water to percolate downward from the finer layer to the coarser layer.

Figures 31 and 32 (t=4267 to t=5742 min) show a finger of the 30% contour extending to an elevation of approximately -270 cm at a radius of approximately 60 cm. By t=8397 min (figure 33), the 30% contour has broken into separate segments, one at depth and another nearer the borehole. Hillel (1980b) recognized this type of phenomenon, which he called "wetting front instability."

By t=9827 min (figure 34), while the wetting front had continued to expand vertically and horizontally, the region enclosed by the 30% contour had shrunk in size somewhat. In figure 35 (t=11,282 min) the region enclosed by the 30% contour has expanded again both laterally and vertically. Two separate regions are again enclosed by the 30% contours, suggesting a similar process of wetting front instability as described above. By this time, the fractures seen on the land surface were extending to a distance of approximately 200 cm from the borehole, while the fractures near the borehole (<45 cm) were closed.

Figure 36 shows the moisture content distribution at t=12,572 min. The size of the region enclosed by the 30% contour is again reduced. The reduction may have been caused by a lower water level the borehole due to a malfunction of the float valve sometime between t=11,282 min and t=11,532 min. A lower water level the borehole reduced

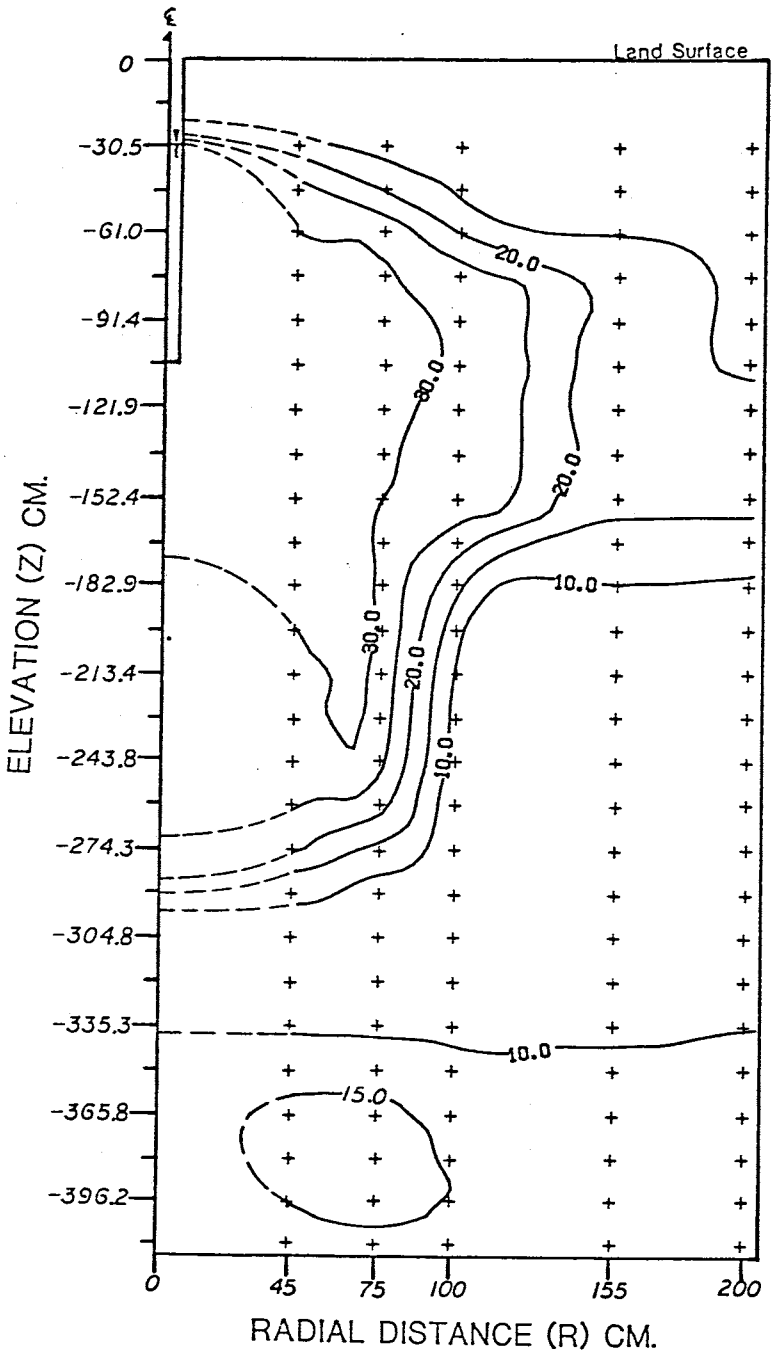

Figure 31. Moisture Content Profile at t=4267 minutes

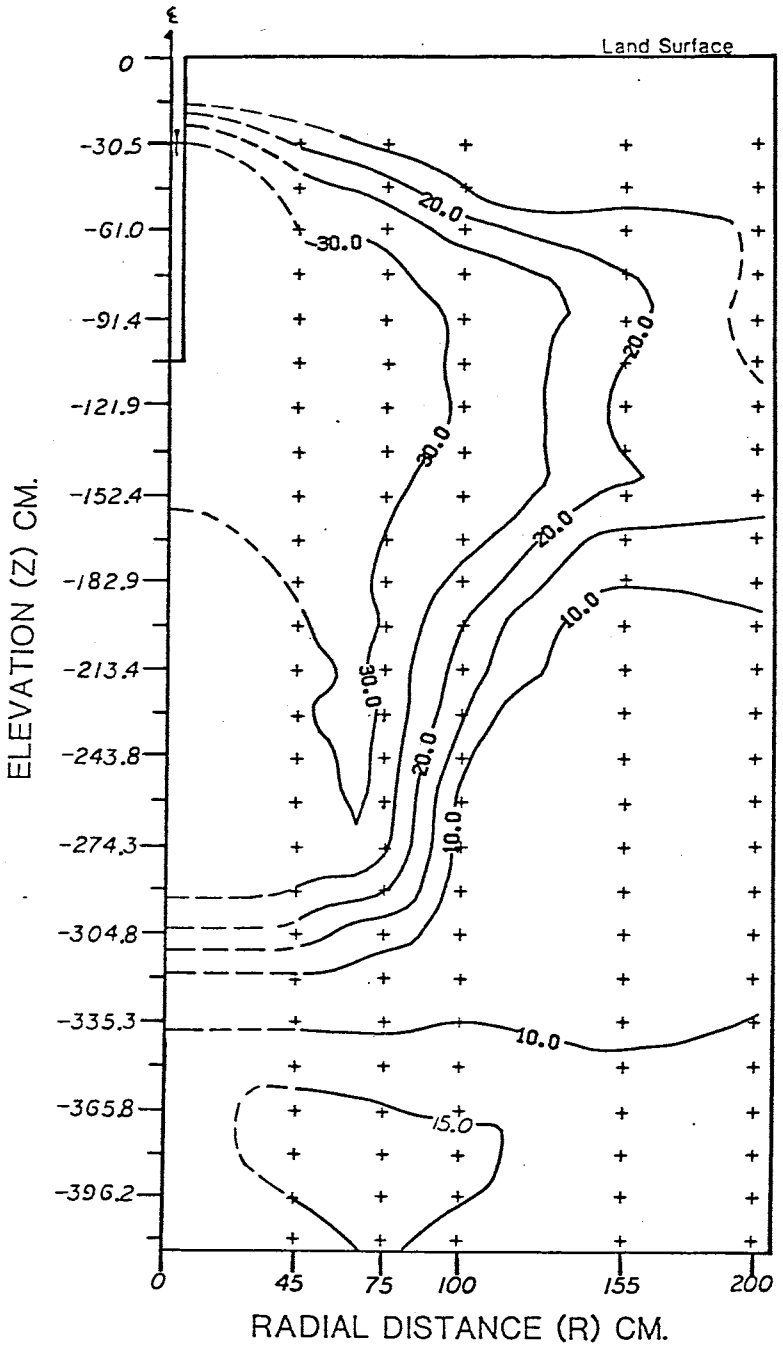

Figure 32. Moisture Content Profile at t=5742 minutes

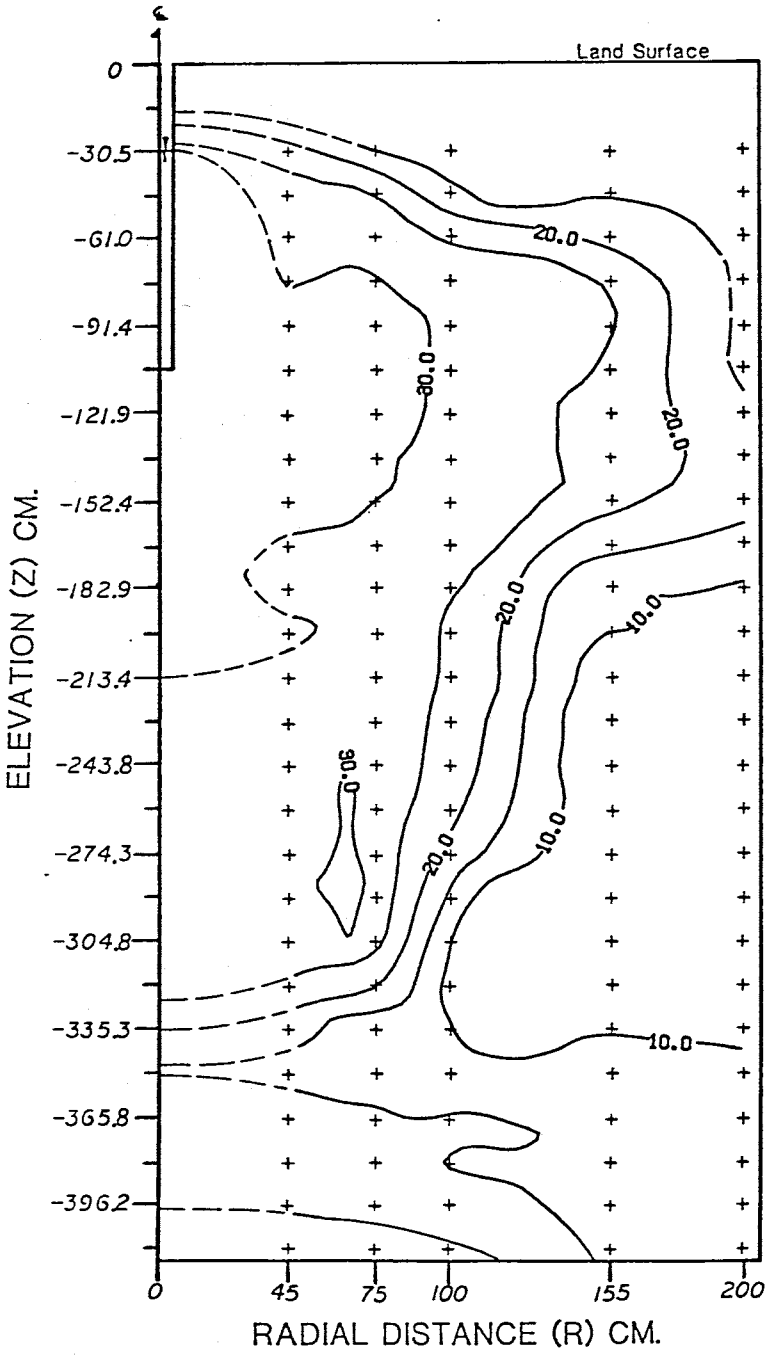

Figure 33. Moisture Content Profile at t=8397 minutes

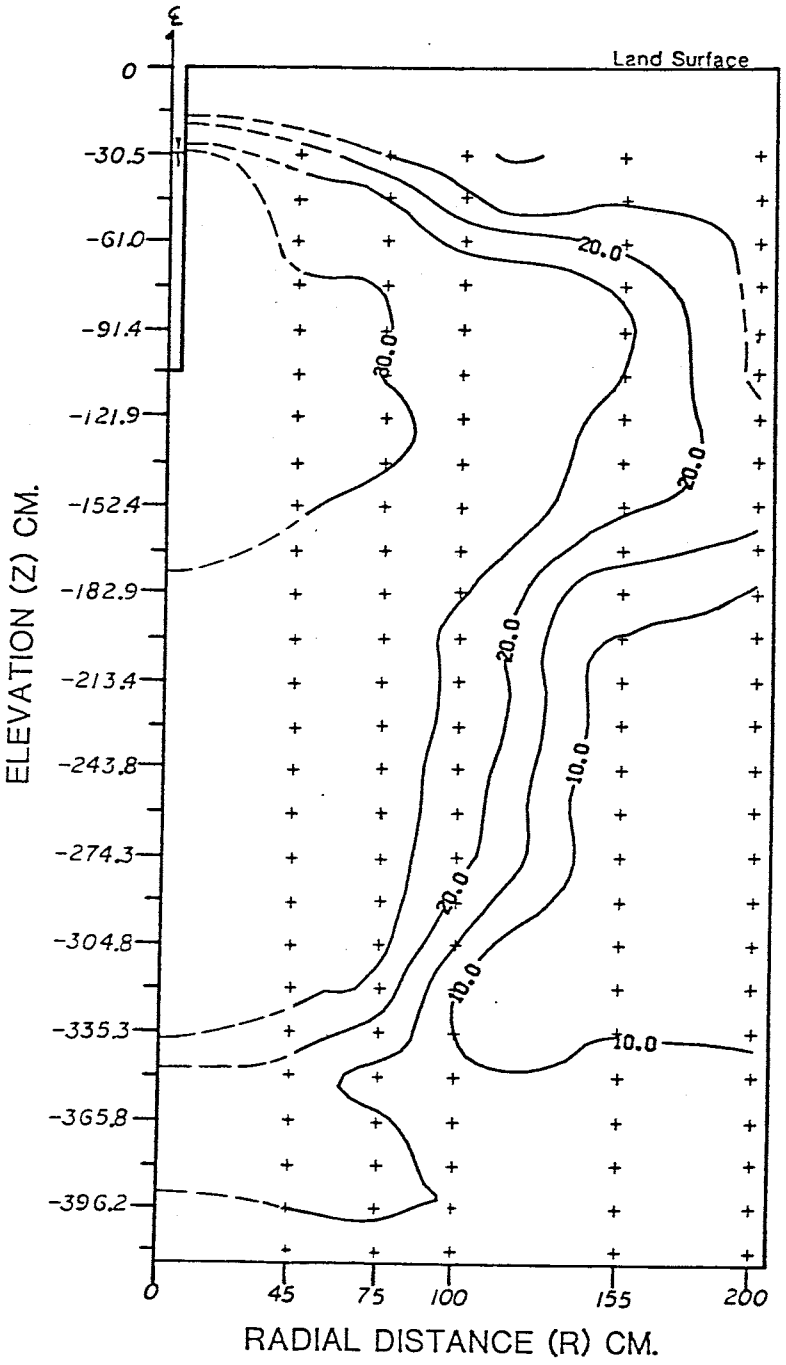

Figure 34. Moisture Content Profile at t=9827 minutes

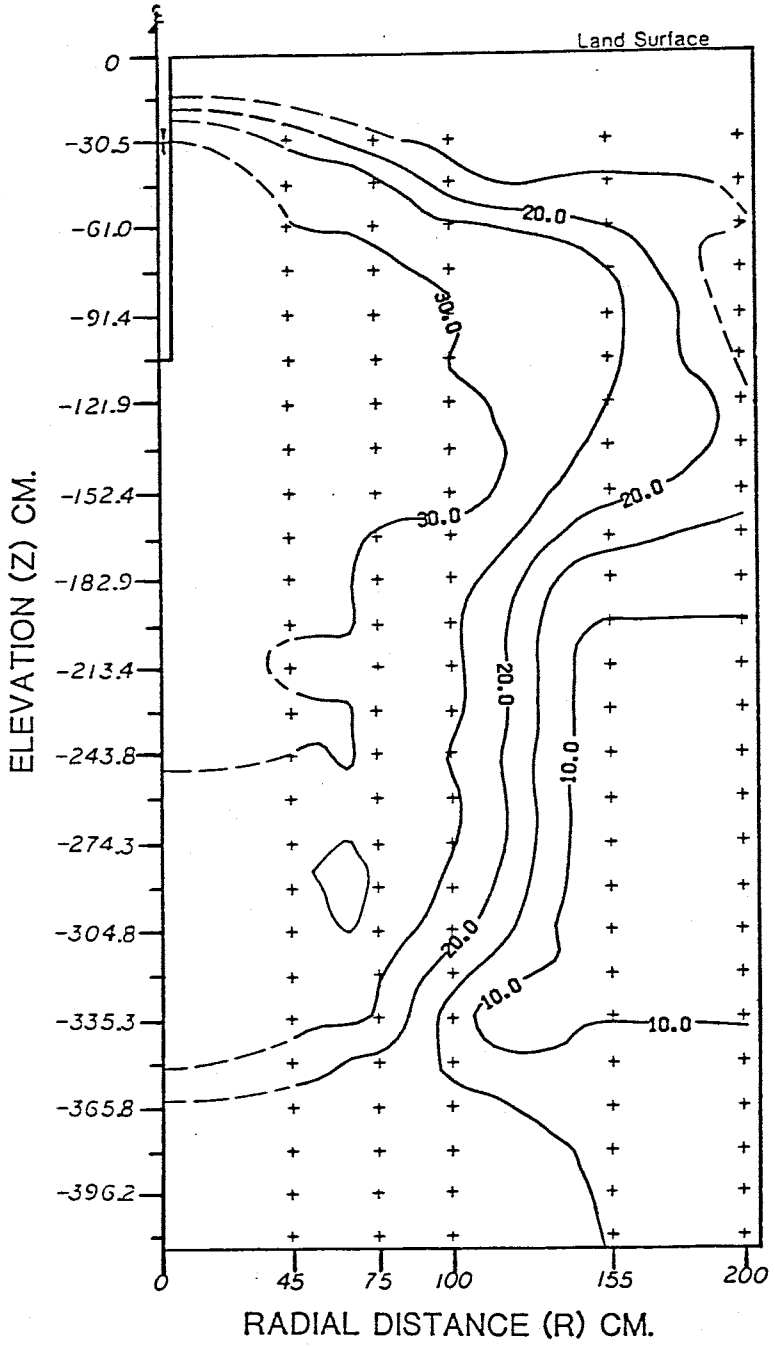

Figure 35. Moisture Content Profile at t=11,282 minutes

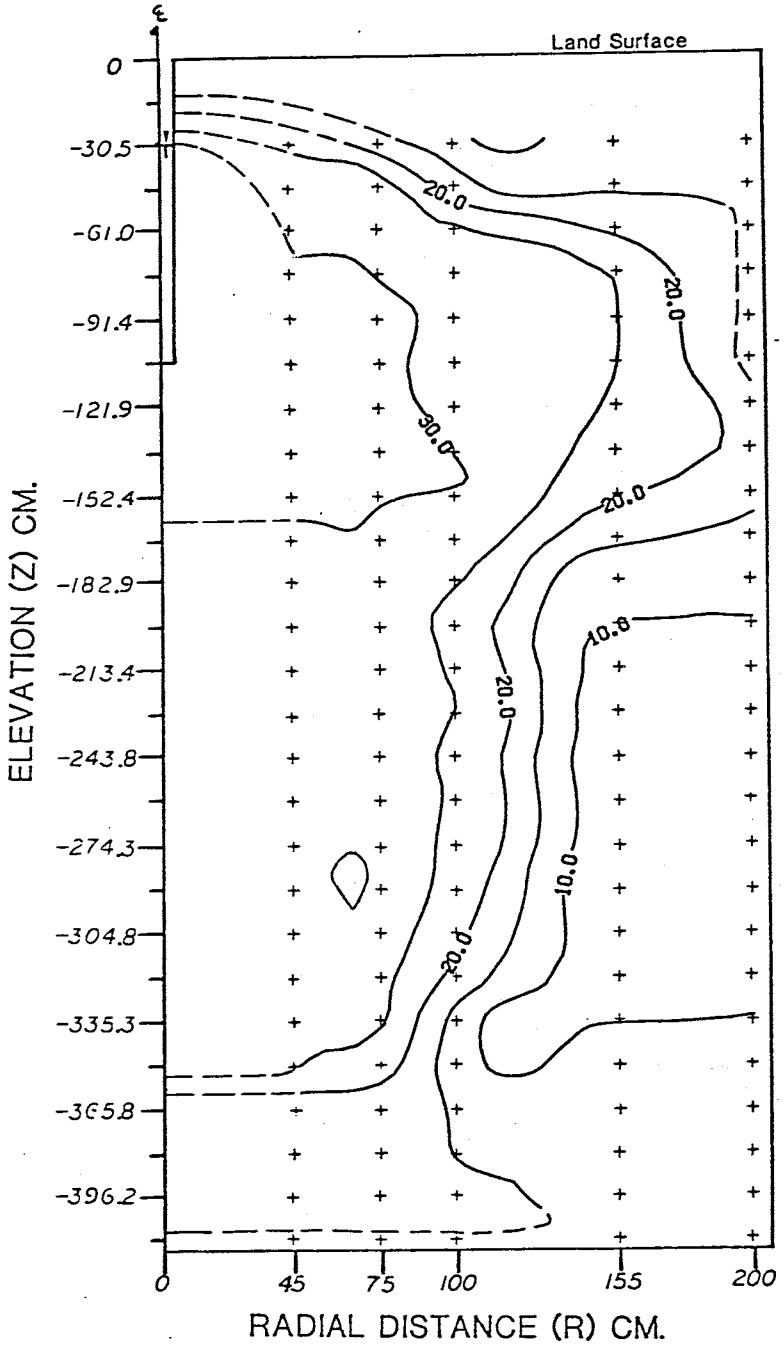

Figure 36. Moisture Content Profile at t=12,572 minutes

infiltration rate (Q) out of the borehole. Watson (1983) found that Q was proportional to the square of the height of water in the borehole. So, a small decrease in head in the borehole can affect Q. The reduction in Q caused the soil to dry slightly, resulting in lower moisture contents in the soil enclosed by the 30% contour.

Figure 37 shows the profile of moisture content at steady state infiltration. Water is again seen to be mounding on top of the coarse layer at an elevation of approximately -180 cm.

Between t=14,537 min and the end of the test (figures 37 through 44), the region enclosed by the 30% contour alternately expands and contracts, and appears irregular. This may have been caused to a degree by malfunctions in the float valve, which allowed a 10% increase of the water level in the borehole between t=20,532 min and t=21,947 min, and a 20% decrease in the water level between t=21,947 min and t=23,347 min. Another possible cause of the irregular moisture content profiles was a change in count rates for the neutron probe from 16 second rates prior to t=12,572 min to 4 second count rates after t=12,572 min. Subsequent error analysis has shown the 95% confidence interval for the 16 second count rate to be ±0.404% volume, while the 95% confidence interval for the 4 second count rate is ±0.808% volume. However, Stephens, et al (1983) observed similar expansion and contraction during borehole infiltration tests, and attributed these cycles to temperature

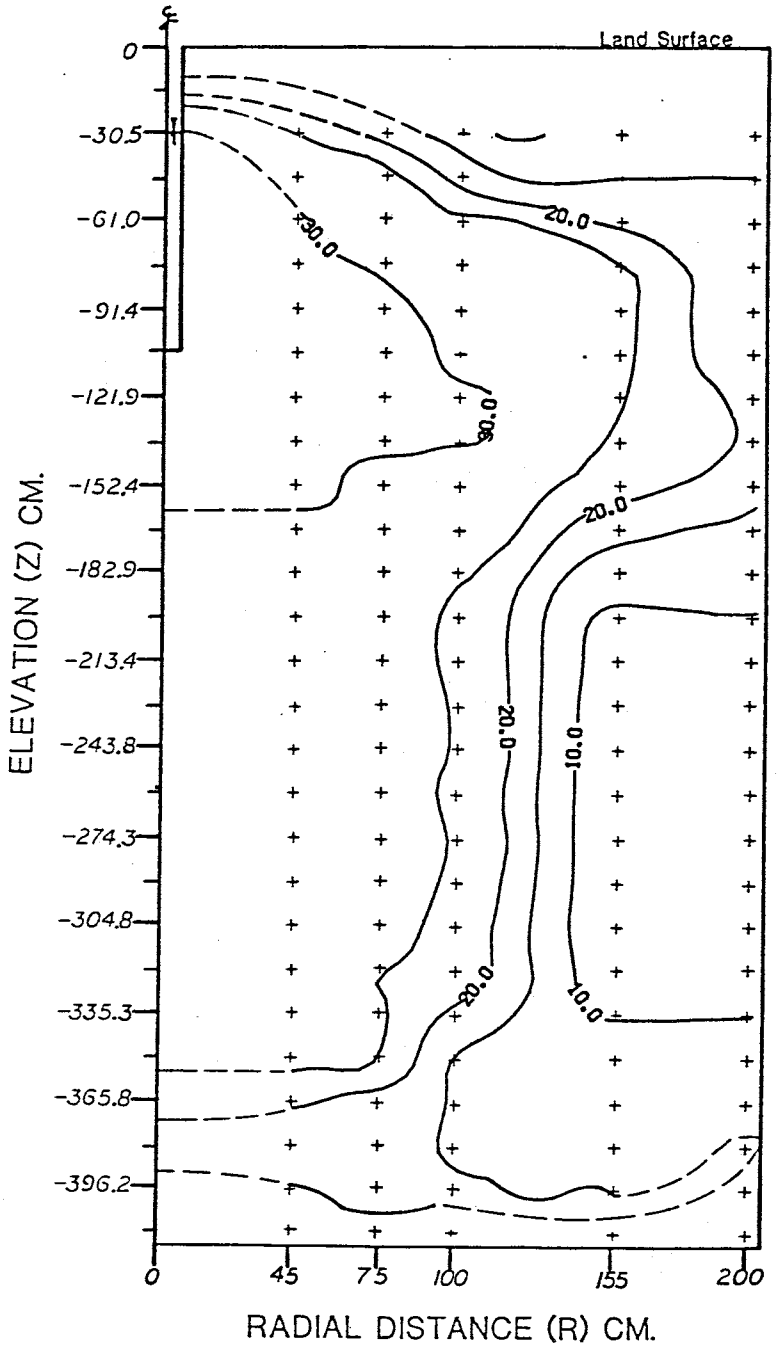

Figure 37. Moisture Content Profile at t=14,537 minutes (Steady State)

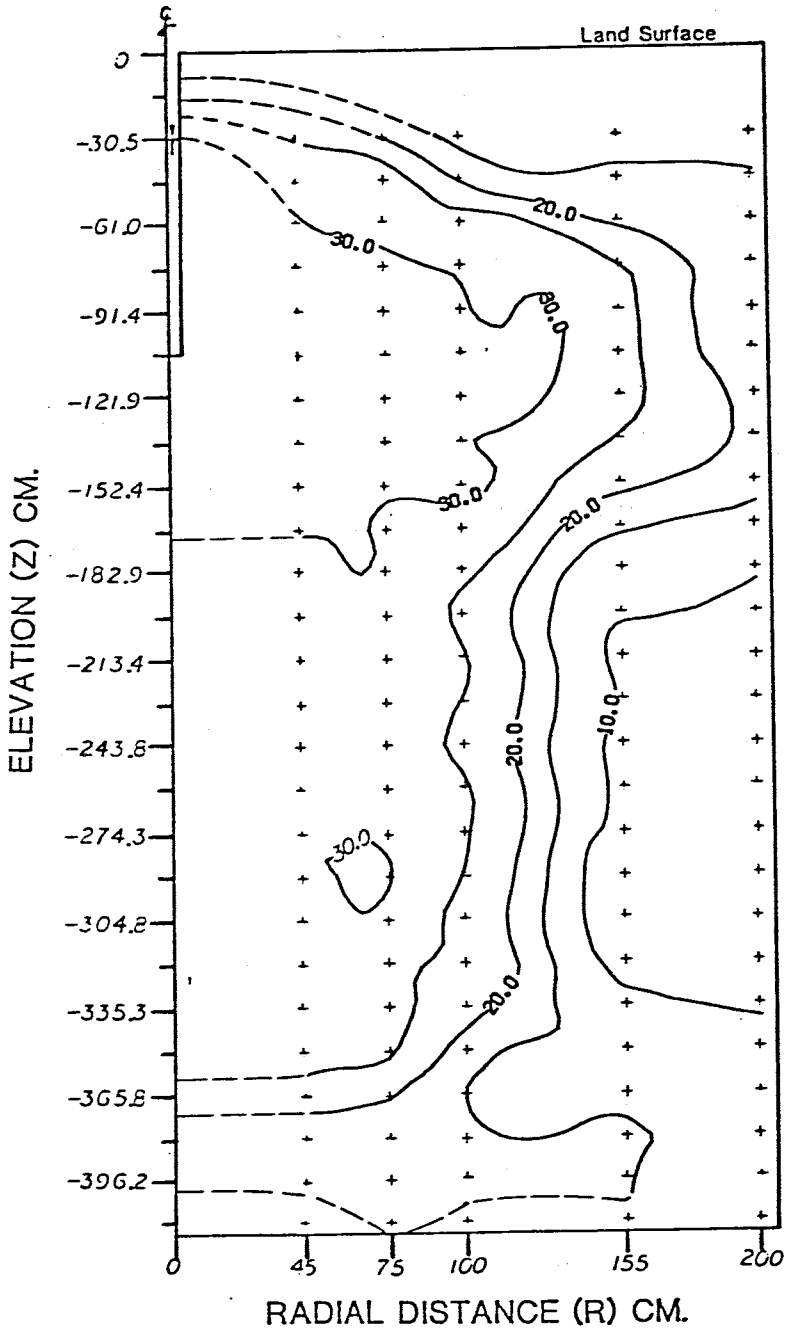

Figure 38. Moisture Content Profile at t=15,962 minutes

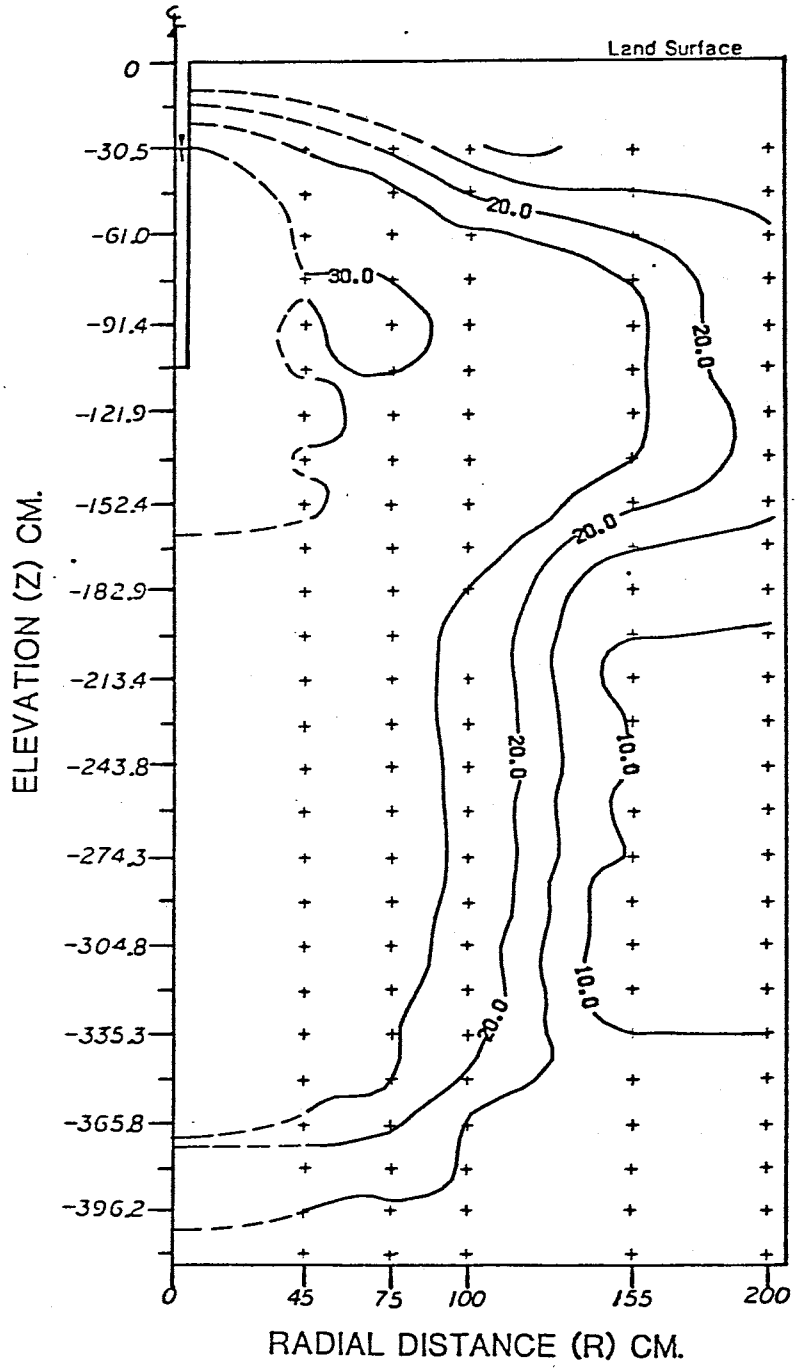

Figure 39. Moisture Content Profile at t=17,512 minutes

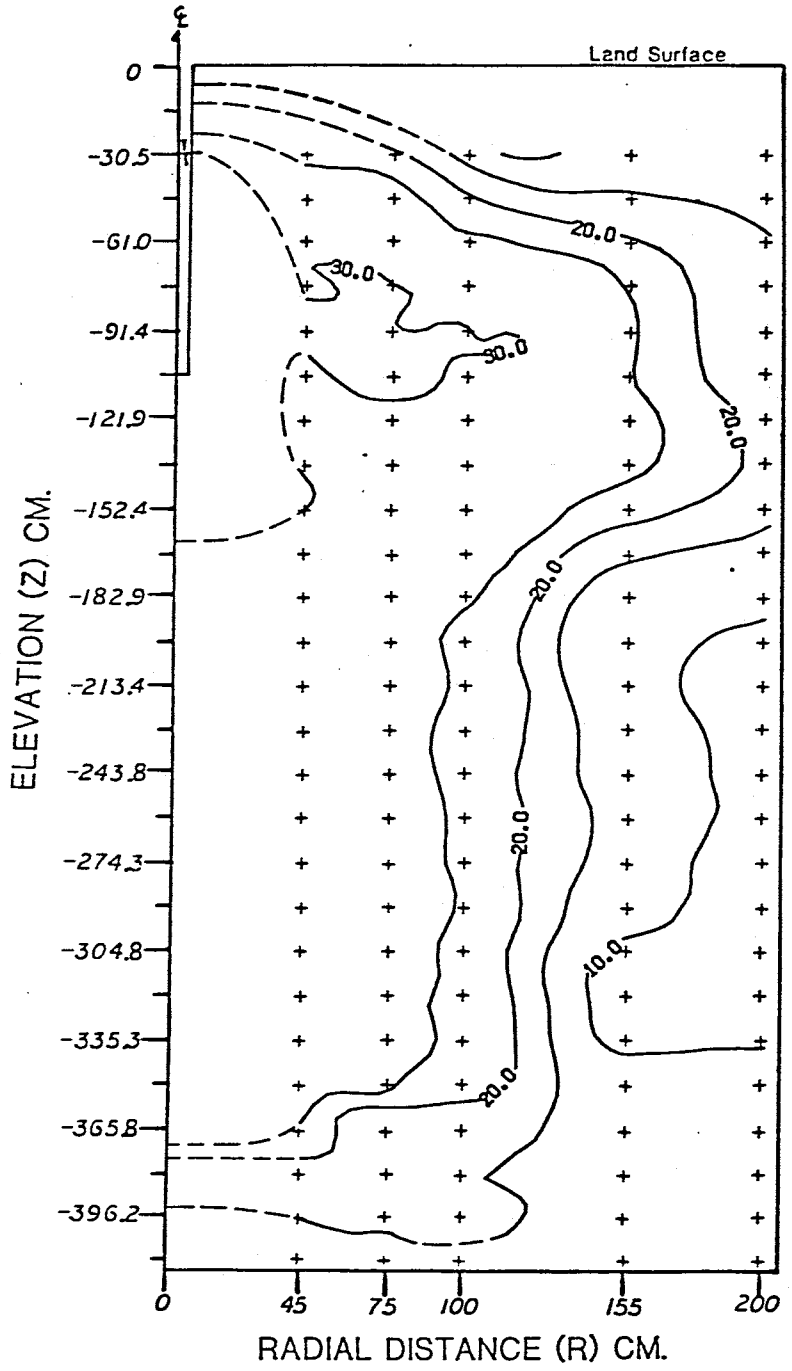

Figure 40. Moisture Content Profile at t=20,542 minutes

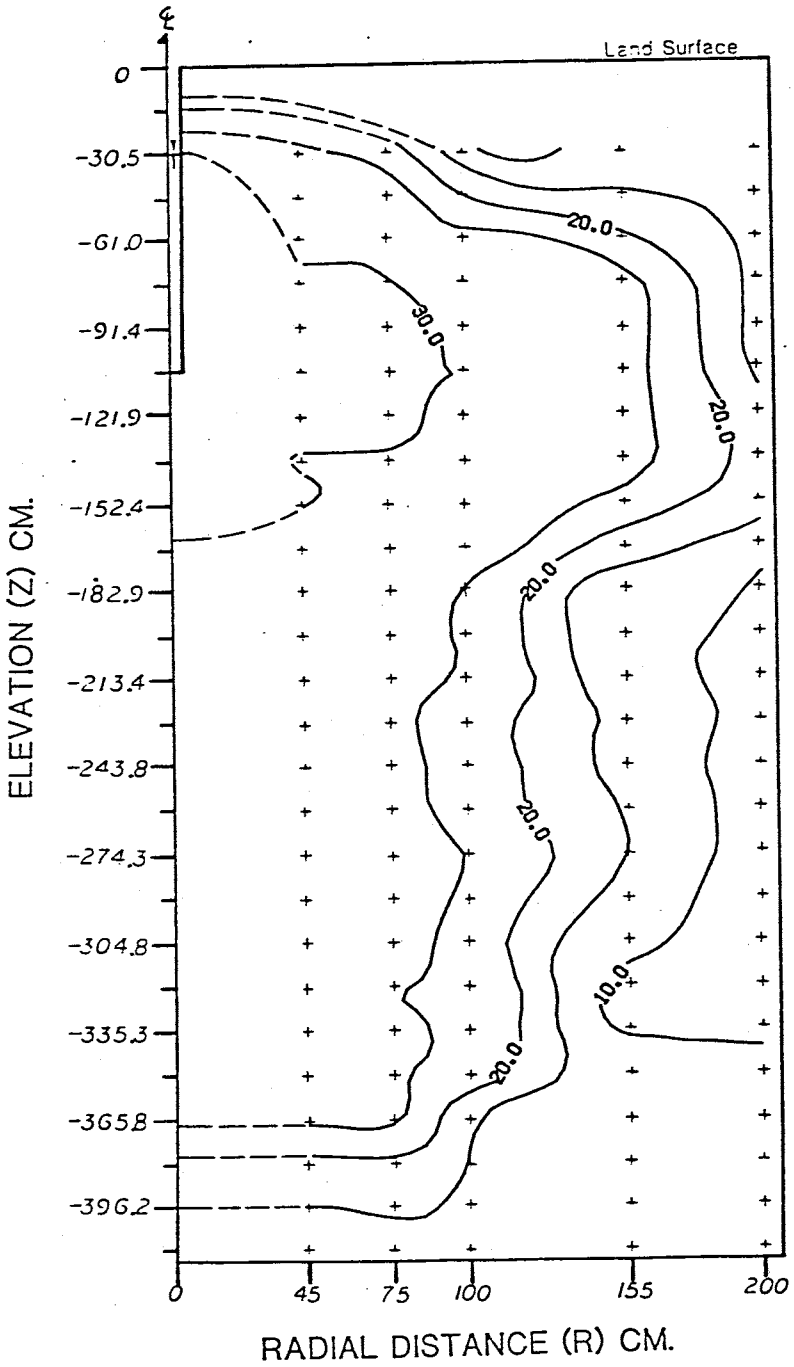

Figure 41. Moisture Content Profile at t=21,987 minutes

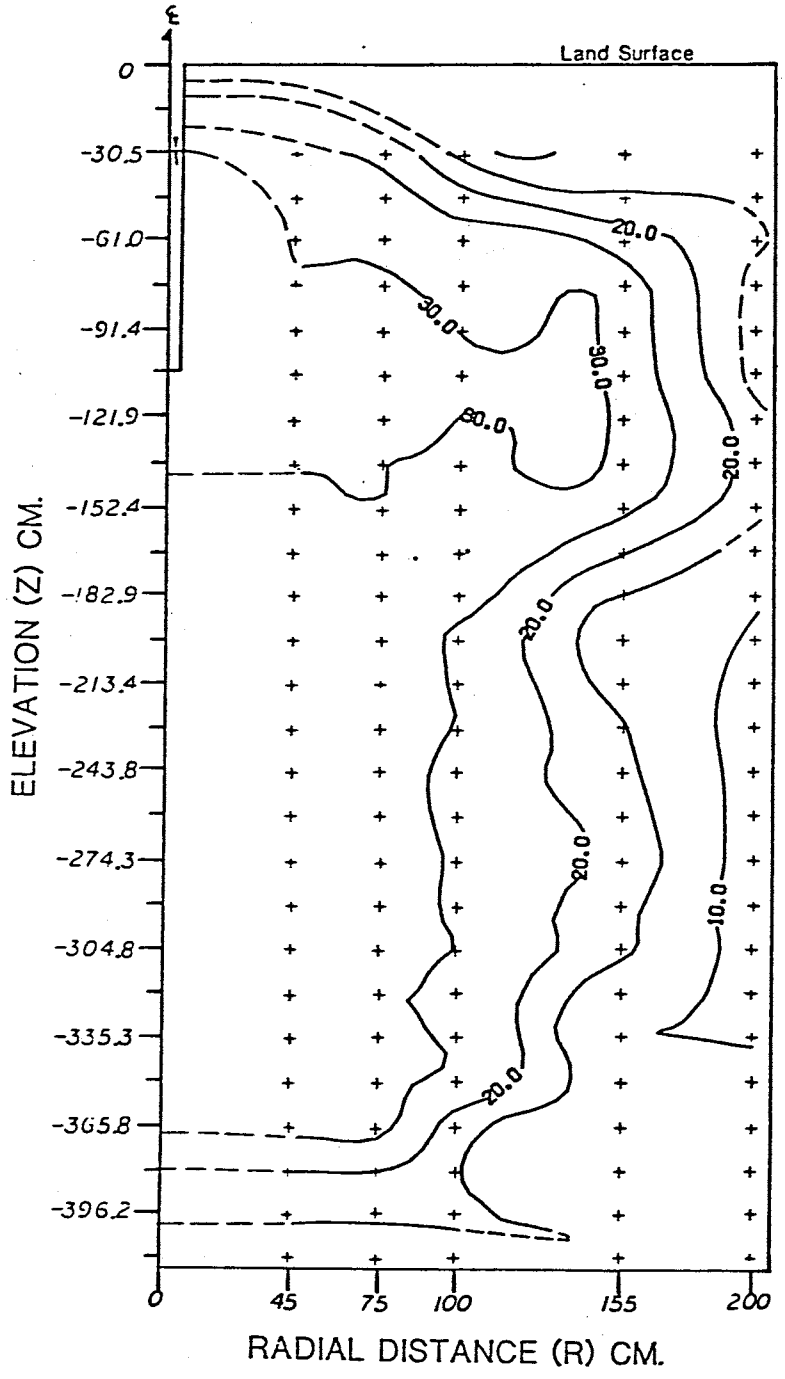

Figure 42. Moisture Content Profile at t=24,717 minutes

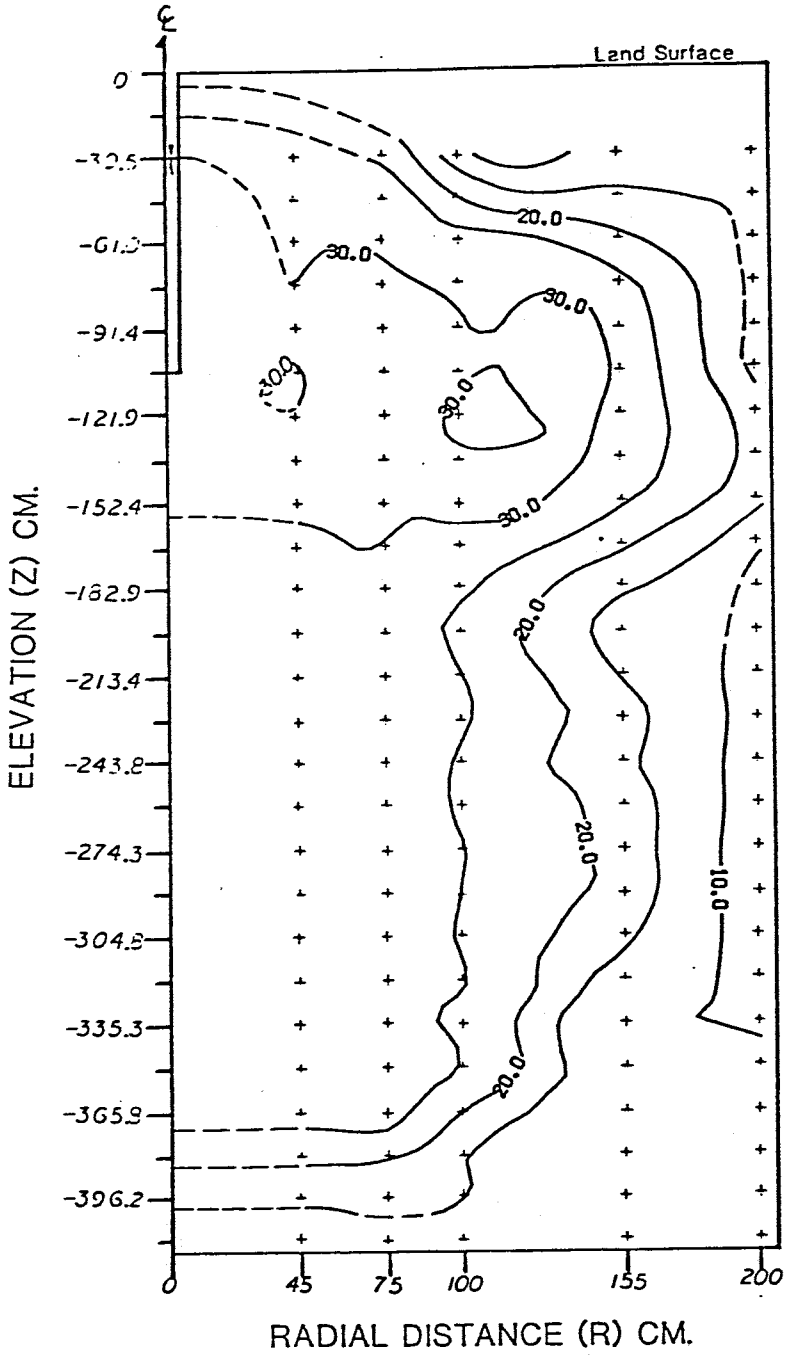

Figure 43. Moisture Content Profile at t=25,972 minutes

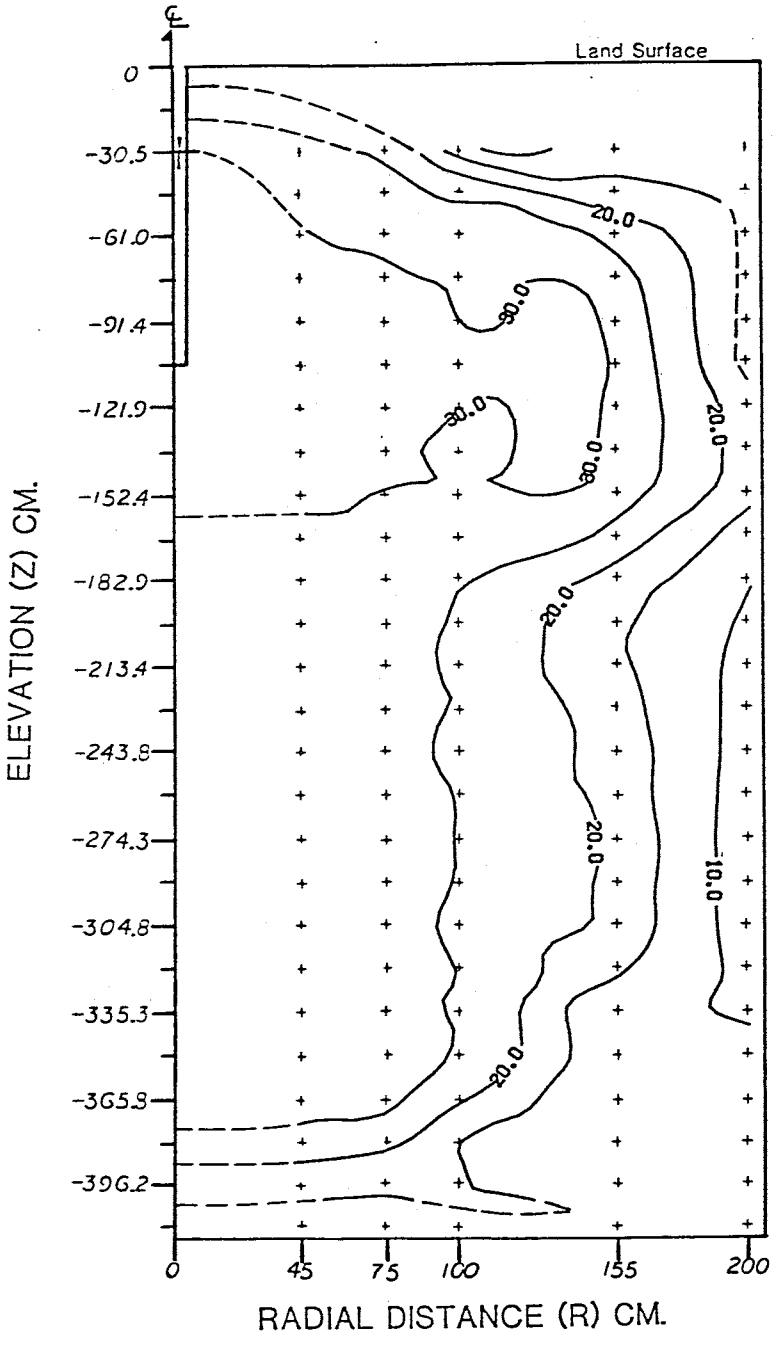

Figure 44. Moisture Content Profile at t=27,627 minutes

fluctuations which affected the volume of entrapped air. All of these phenomenon may have contributed to the alternating moisture content profiles observed.

6.8 Pressure Head

Pressure head profiles were generated using the same contouring routine as for the moisture content profiles, namely NCAR (National Center for Atmospheric Research, Scientific Computing Division Graphics System, May 1983). Contours between the borehole and the first tensiometer data points (either a radius of 25 cm or 10 cm) were drawn in by hand.

Tensiometers were not emplaced until day 2 of the test, and were not read until day 3 (t=4267 min). Mercury manometers were connected to the tensiometers from which values of total head were recorded.

Figure 45 shows the pressure head profile at t=4267 min. Pressure head gradients at radii of 50, 75, and 100 cm at elevations of -30.5 cm, -50 cm, and -75 cm, respectively are still quite high, indicating the limit of the wetting front.

In figures 46 through 48 (t=4772 min to t=5742 min, respectively) the gradients at radii of 75 cm and 100 cm are decreased due to the soil becoming wetter. Of particular interest in figures 46 through 48 is the apparent saturation of the soil at an elevation of -150 cm and a radius of approximately 30 cm. As previously discussed, sieve analyses revealed the soil at an elevation of about -180 cm to be of coarser texture than the soil above. In unsaturated flow conditions, water often mounds on top of

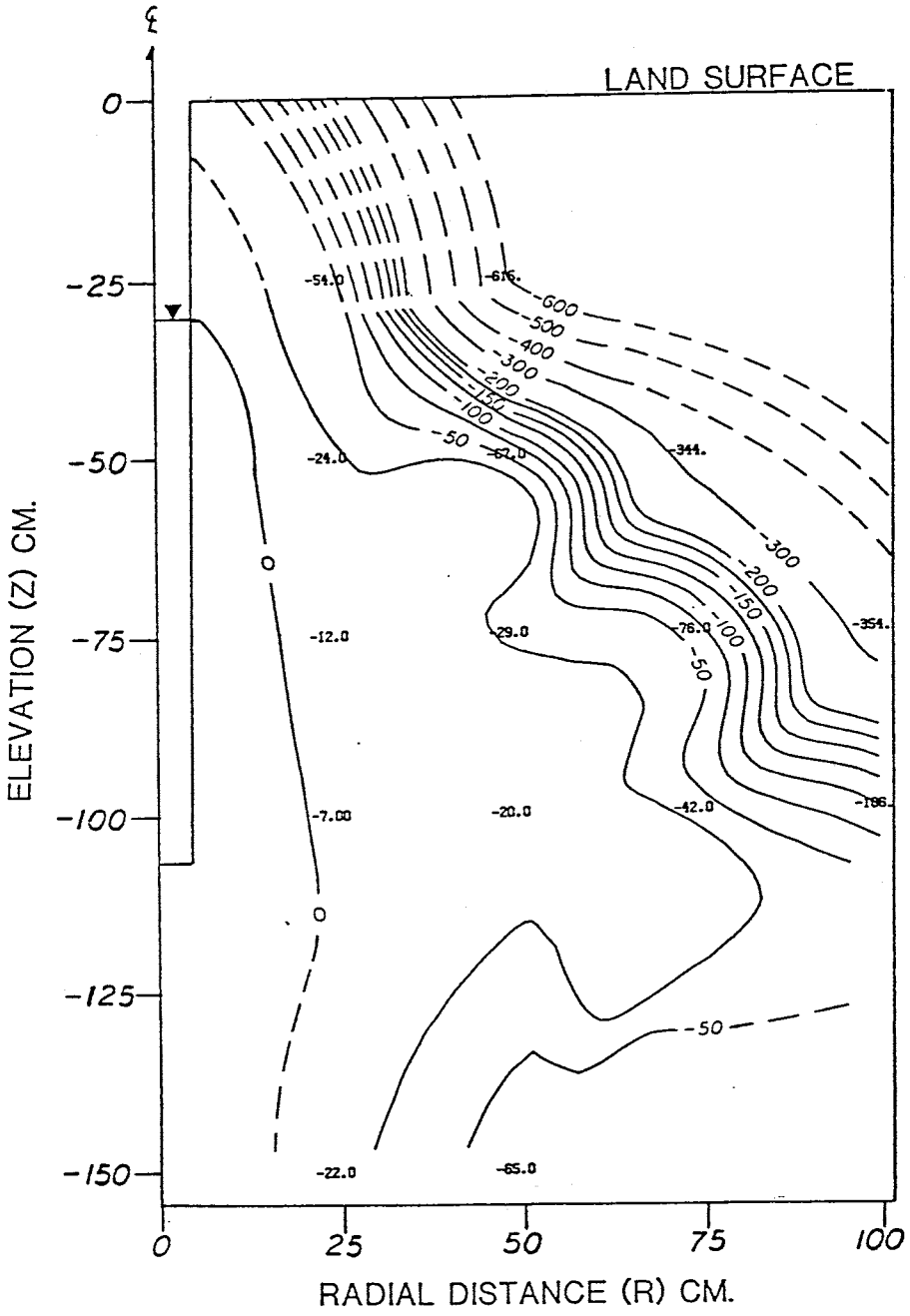

Figure 45. Pressure Head Profile at t=4267 minutes

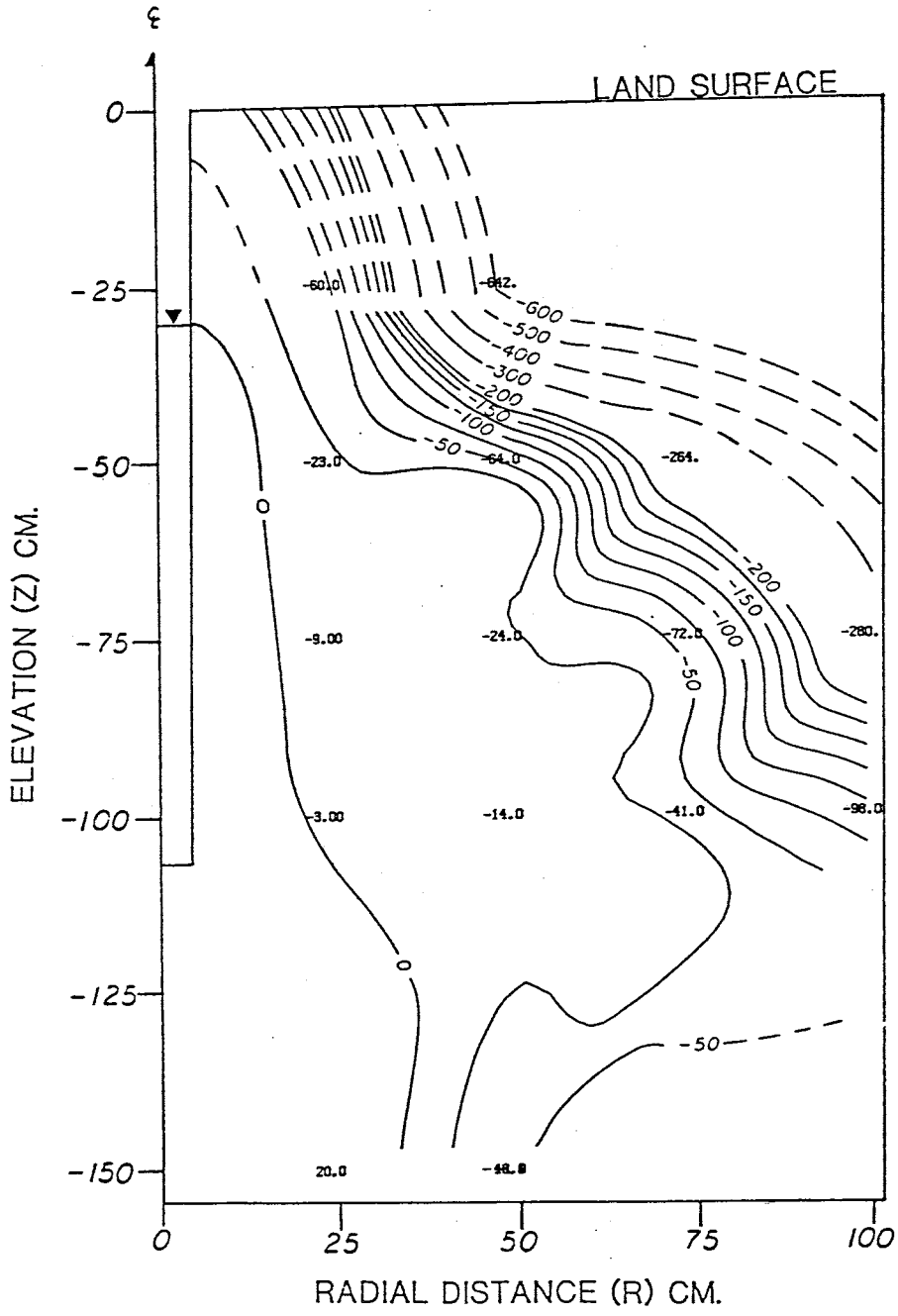

Figure 46. Pressure Head Profile at t=4772 minutes

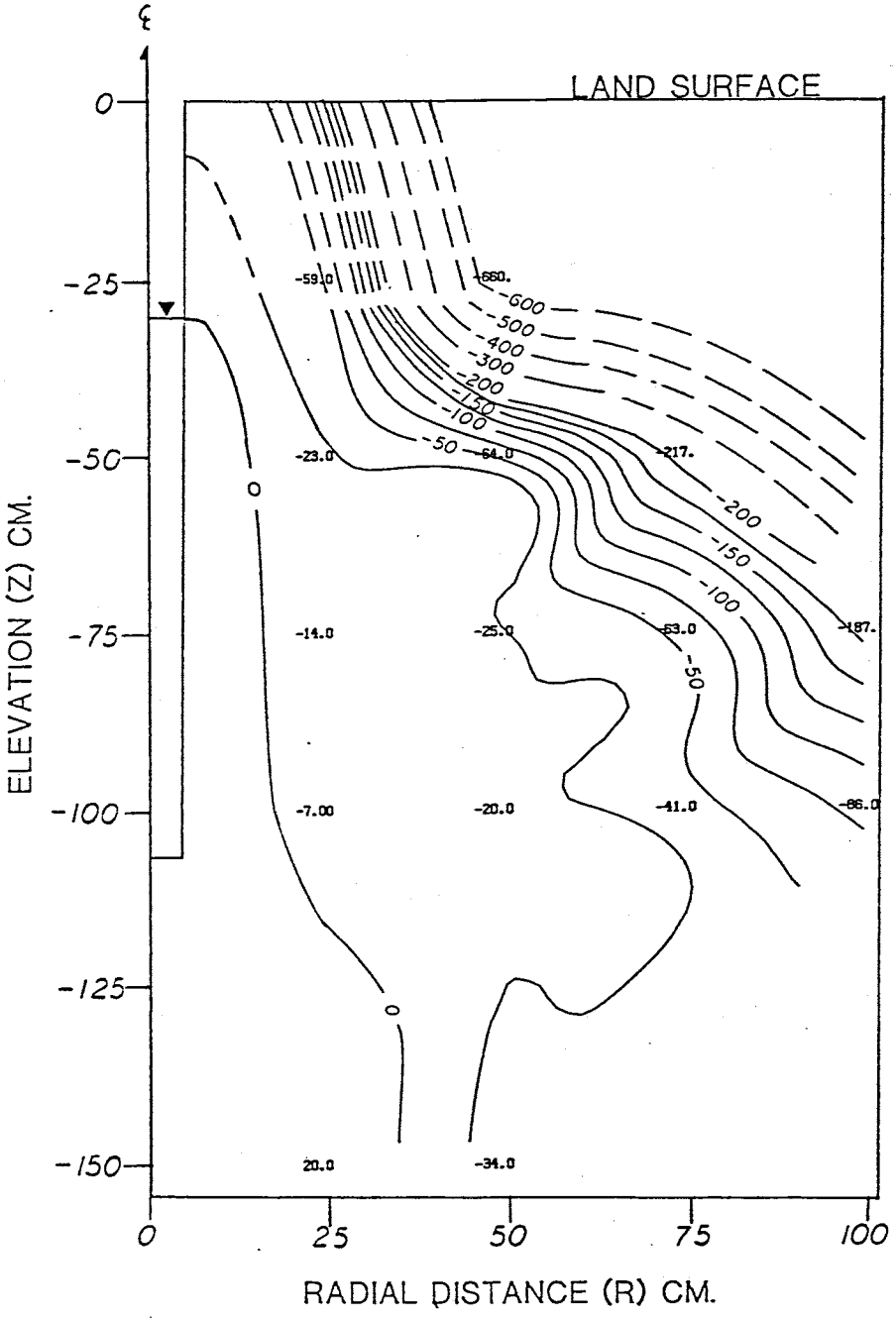

Figure 47. Pressure Head Profile at t=5692 minutes

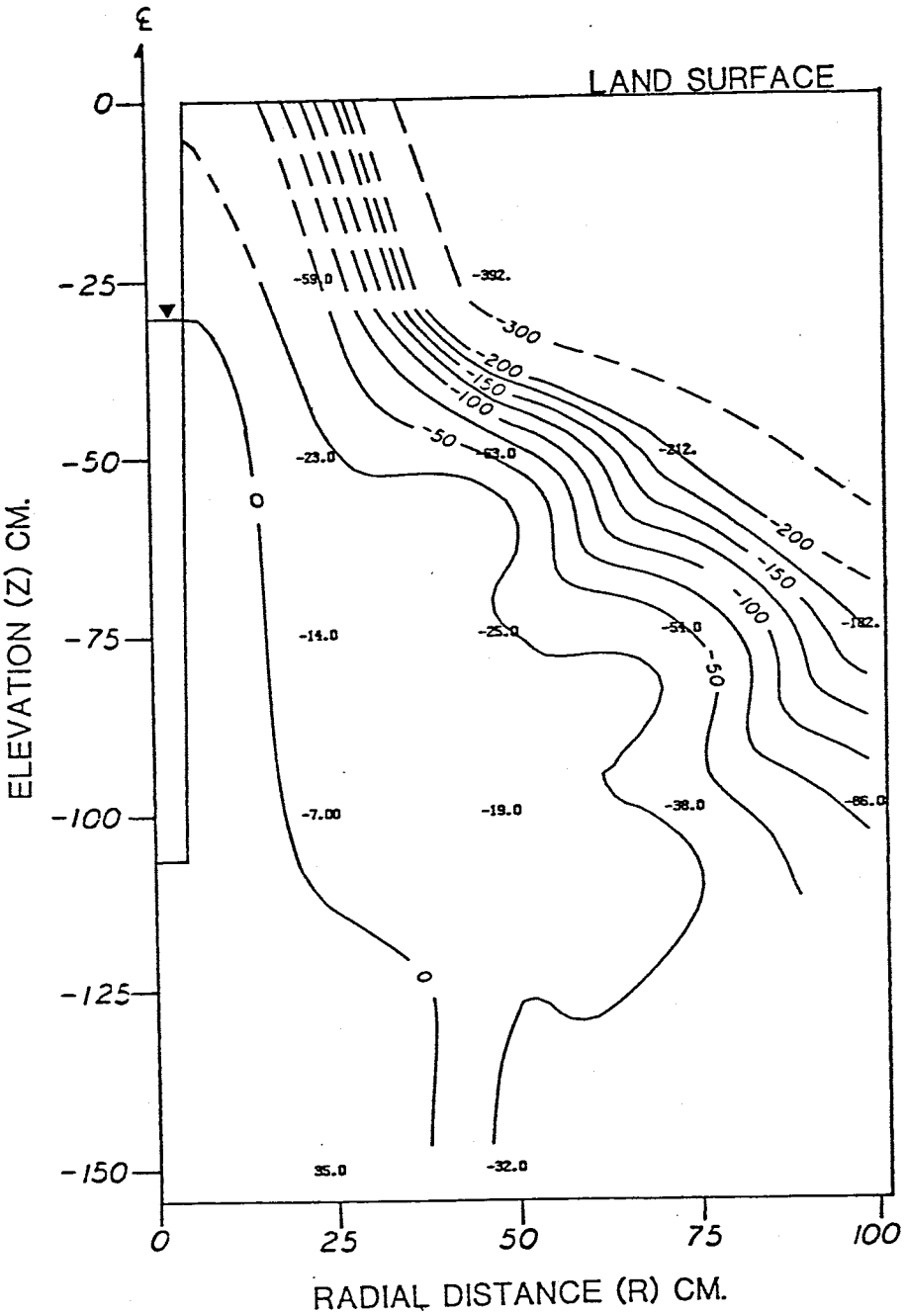

Figure 48. Pressure Head Profile at t=5742 minutes

the coarser grained soil until its water-entry value is exceeded.

By t=8397 min (figure 49) the zone of enhanced wetness above an elevation of -150 cm no longer existed. This implies that the water was able to drain into or through the coarser grained soil. Periods of drainage through the coarser grained soil were also inferred from moisture content profiles, which showed "fingering" of water into the coarser layer. In figure 49 the gradients at radii of 75 cm and 100 cm have decreased considerably from figure 46 (t=4772 min). However, the zone of saturation as defined by the zero pressure head contour is essentially the same at t=8397 min as it was at t=4772 min. Stephens (1979) realized that a finite zone of saturation would develop in three dimensional infiltration, and the pressure head data from S9T1 tend to support this.

Between t=8397 min and t=11,282 min (figures 49 through 54), the profile remains essentially constant near the borehole, with tensiometers at radii of 75 cm and 100 cm continuing to wet up. Figure 55 (t=11,532 min) shows that soil wetness decreases near the borehole. This drying may have been caused by a reduction of water level in the borehole due to a malfunction of the float valve between t=11,282 min and t=11,532 min. The reduction in water level reduced infiltration rates out of the borehole, and this decreased pressure heads near the borehole. The decrease in pressure heads resulted in an increase in hydraulic

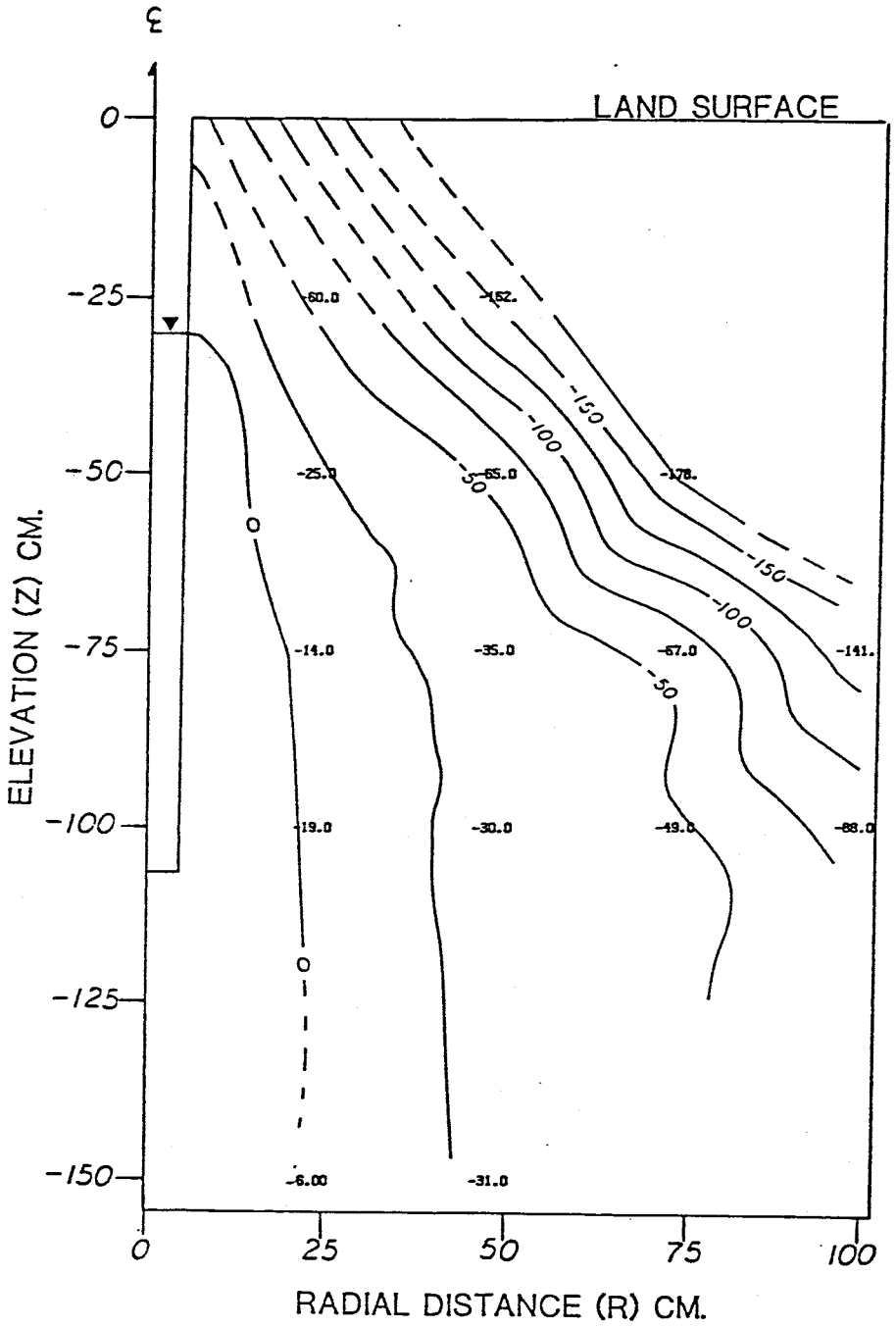

Figure 49. Pressure Head Profile at t=8397 minutes

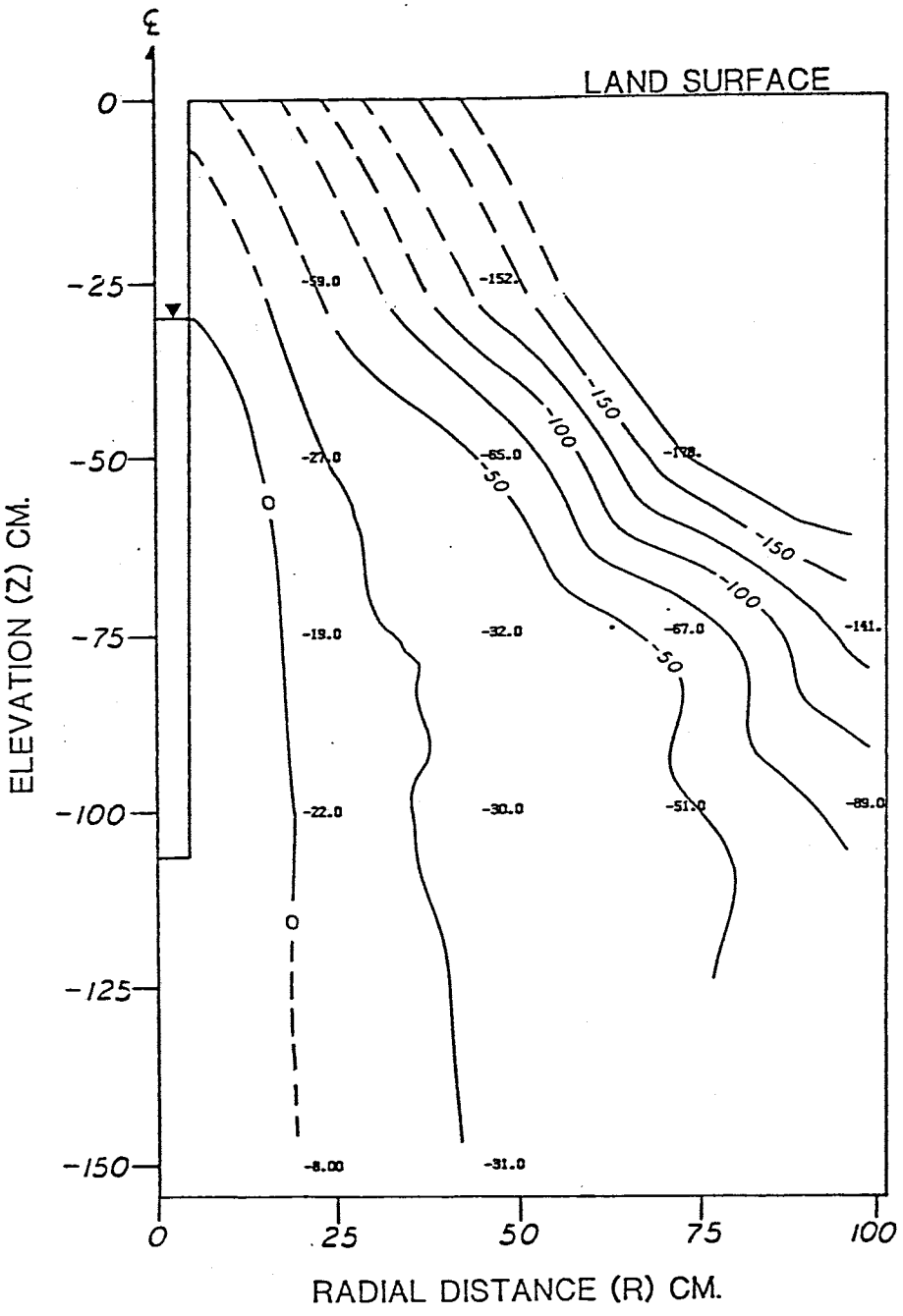

Figure 50. Pressure Head Profile at t=8447 minutes

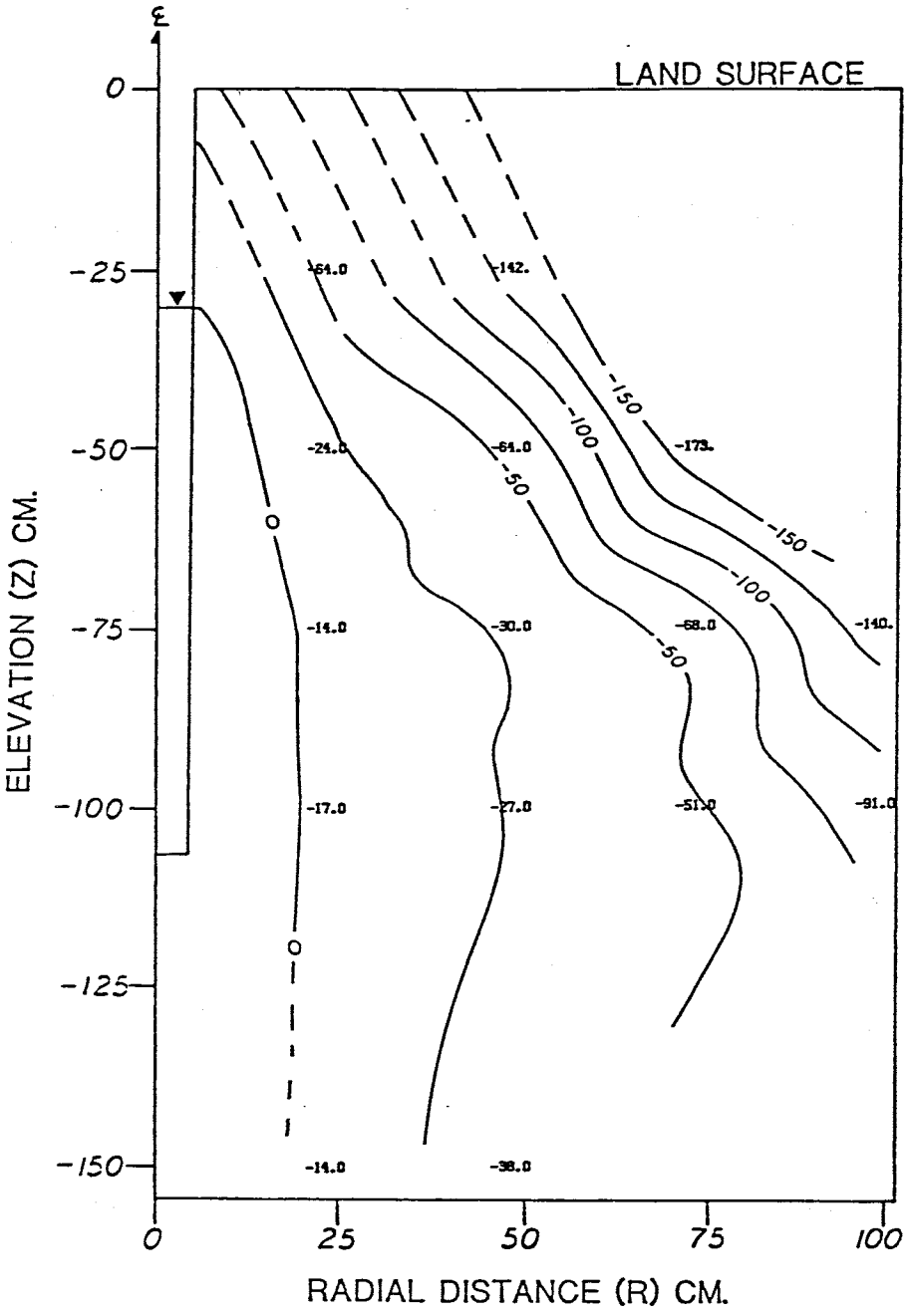

Figure 51. Pressure Head Profile at t=9022 minutes

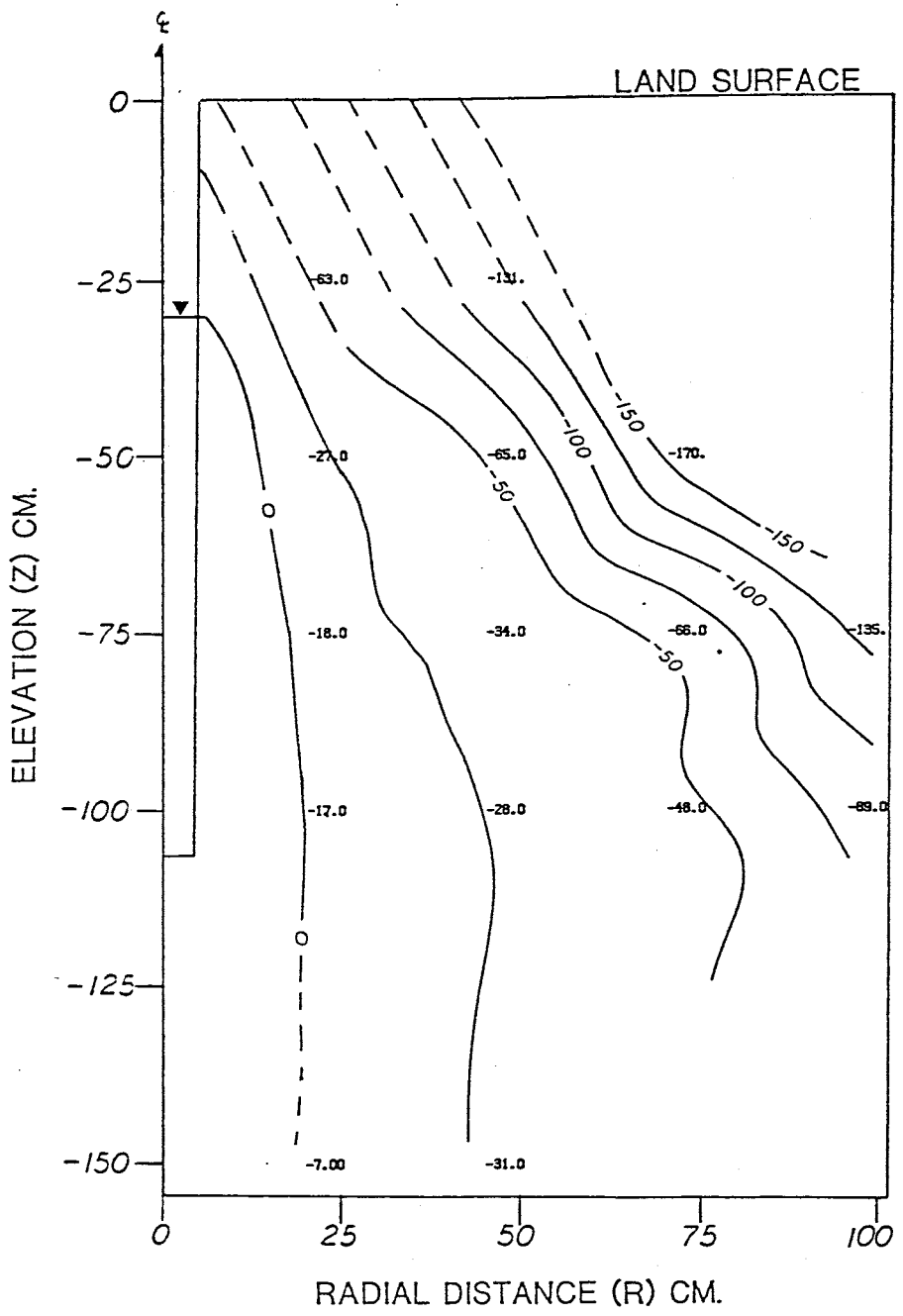

Figure 52. Pressure Head Profile at t=9827 minutes

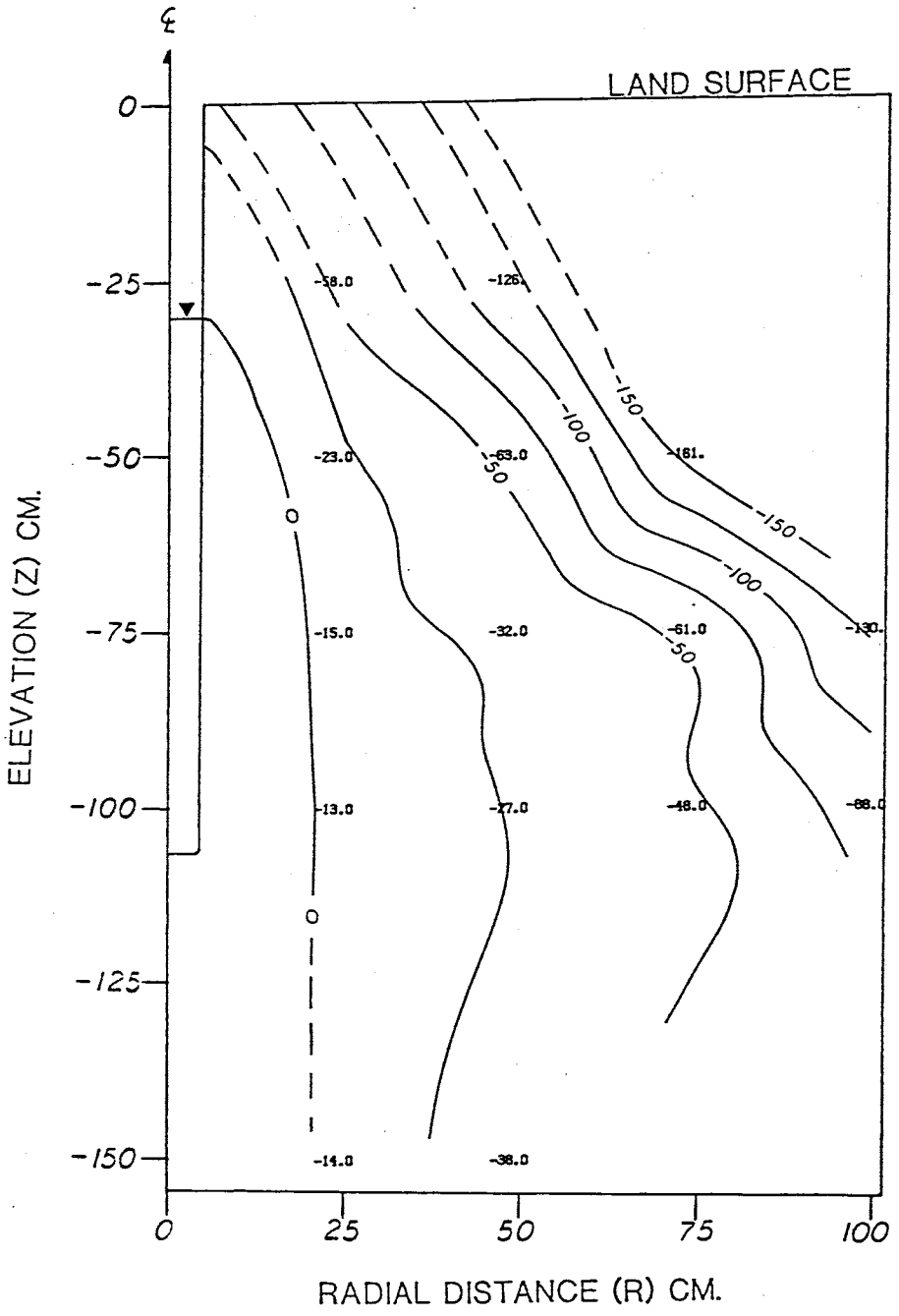

Figure 53. Pressure Head Profile at t=10,442 minutes

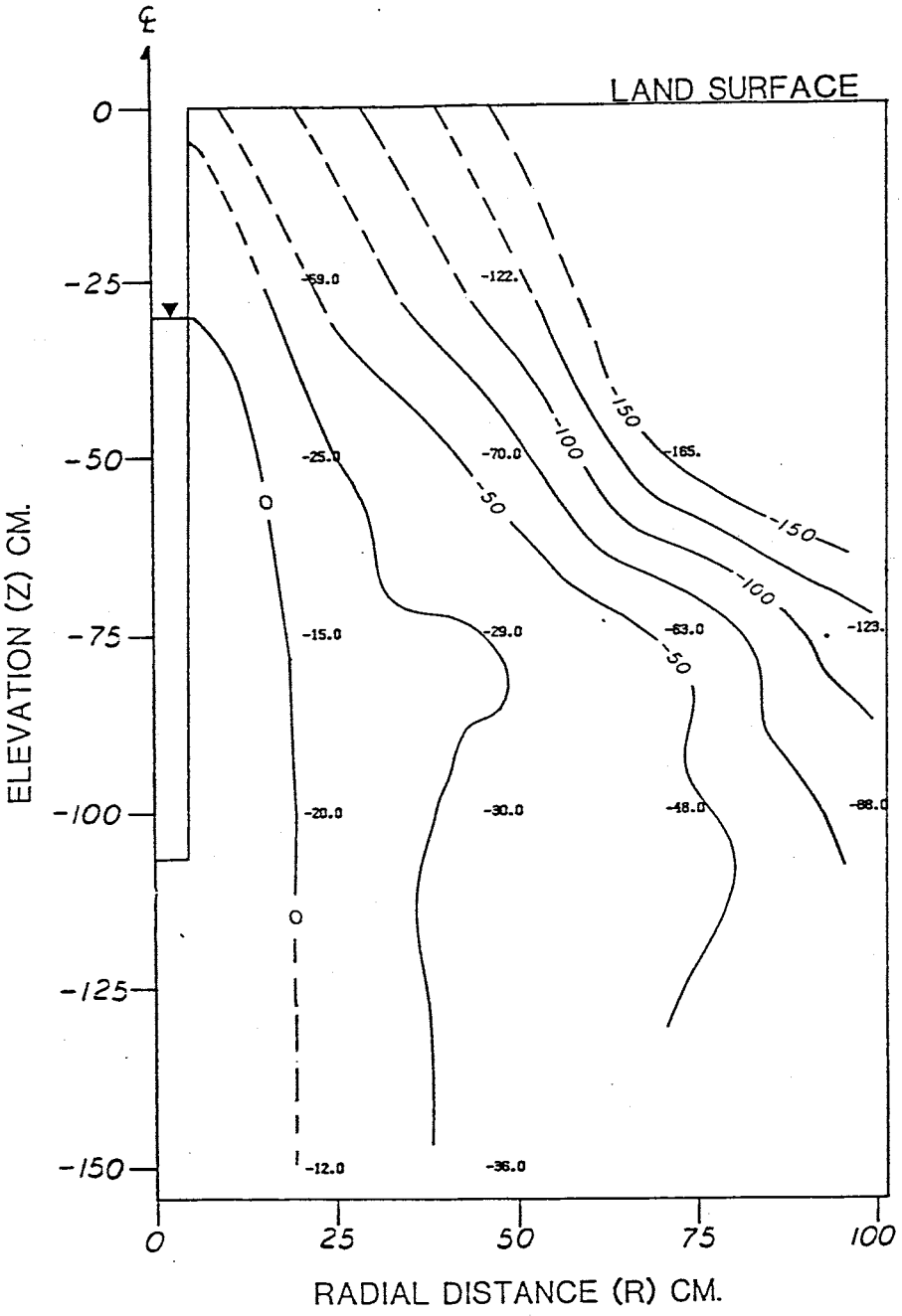

Figure 54. Pressure Head Profile at t=11,282 minutes

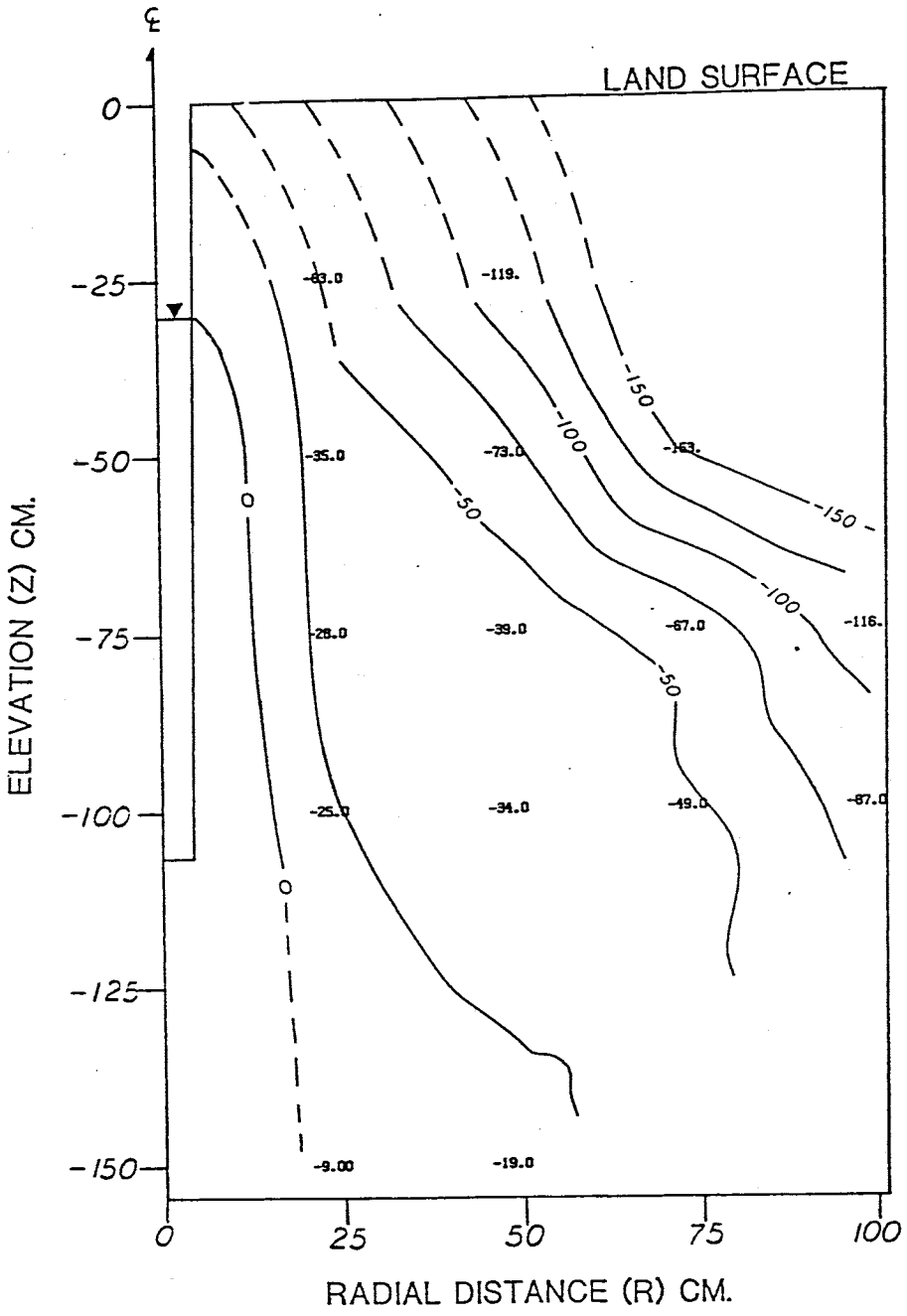

Figure 55. Pressure Head Profile at t=11,532 minutes

gradients between the borehole and the tensiometers. According to Darcy's Law, hydraulic gradients would be expected to decrease with a decrease in infiltration rate, if hydraulic conductivity remained constant. More will be said about this in the section on hydraulic gradient.

On day 7 of the test, tensiometers were emplaced at a radius of 10 cm from the borehole to accurately define conditions close to the borehole. These tensiometers were given one day to equilibrate, with the first results appearing in figure 56 (t=11,832 min). These new data considerably changed the position of the zero pressure head contour beginning at an elevation of -75 cm. A very small region of soil was saturated below an elevation of -75 cm. Above an elevation of -60 cm, the zone of saturation remained approximately the same as it had without the data from a radius of 10 cm. Between t=11,832 min and t=13,417 min (figures 56 through 58), the flow field was relatively constant.

Figure 59 shows the flow field at a steady state infiltration rate. The data from a radius of 10 cm and an elevation of -75 cm show a saturation of the soil surrounding this tensiometer. Saturation might be expected at a tensiometer this close to the borehole. However, the data from a radius of 10 cm and an elevation of -100 cm still reflected unsaturated conditions.

Figure 60 (t=15,962 min) shows another mounding of water on top of the coarser grained layer at an elevation of

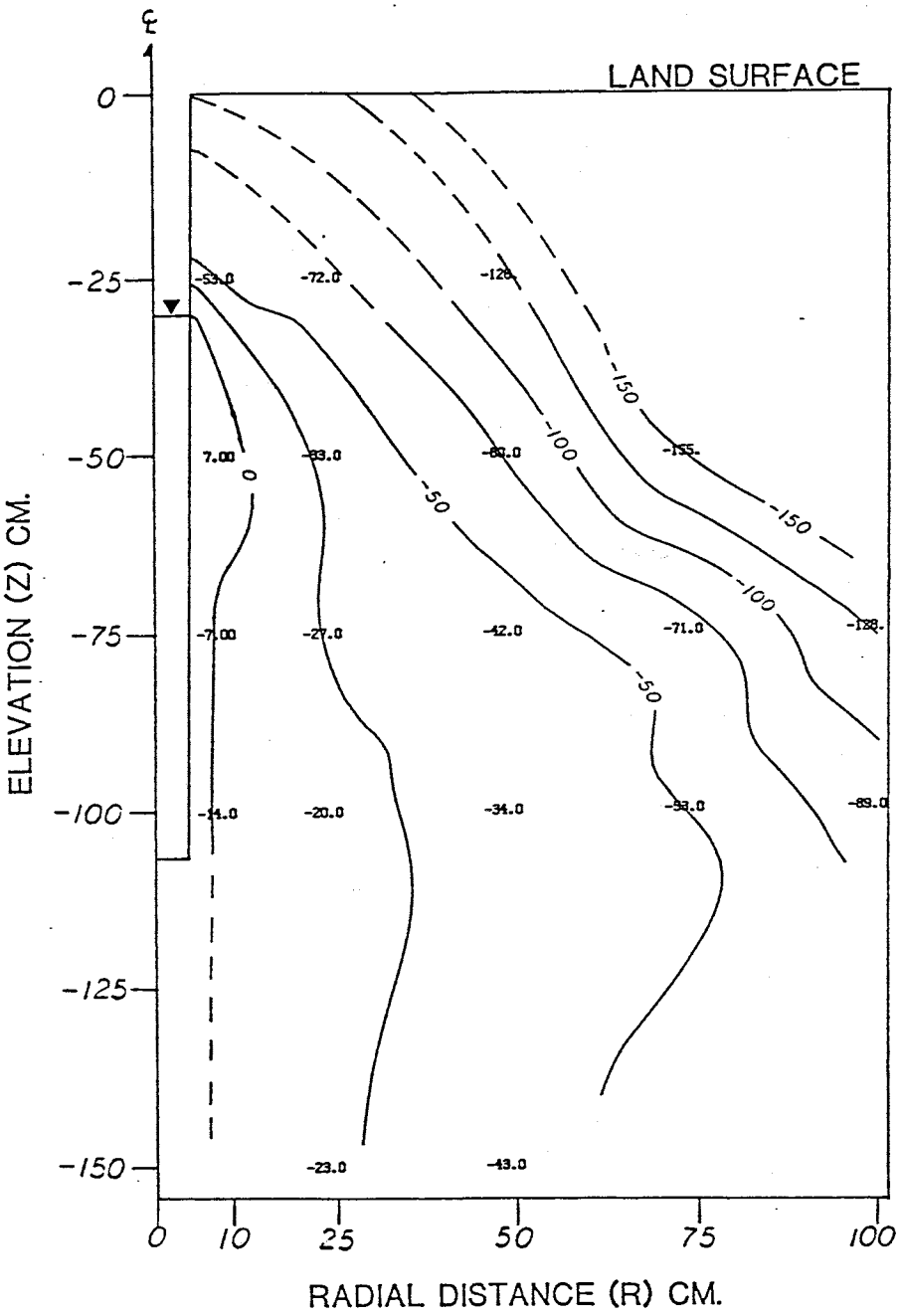

Figure 56. Pressure Head Profile at t=11,832 minutes
(Tensiometers added at R=10 cm)

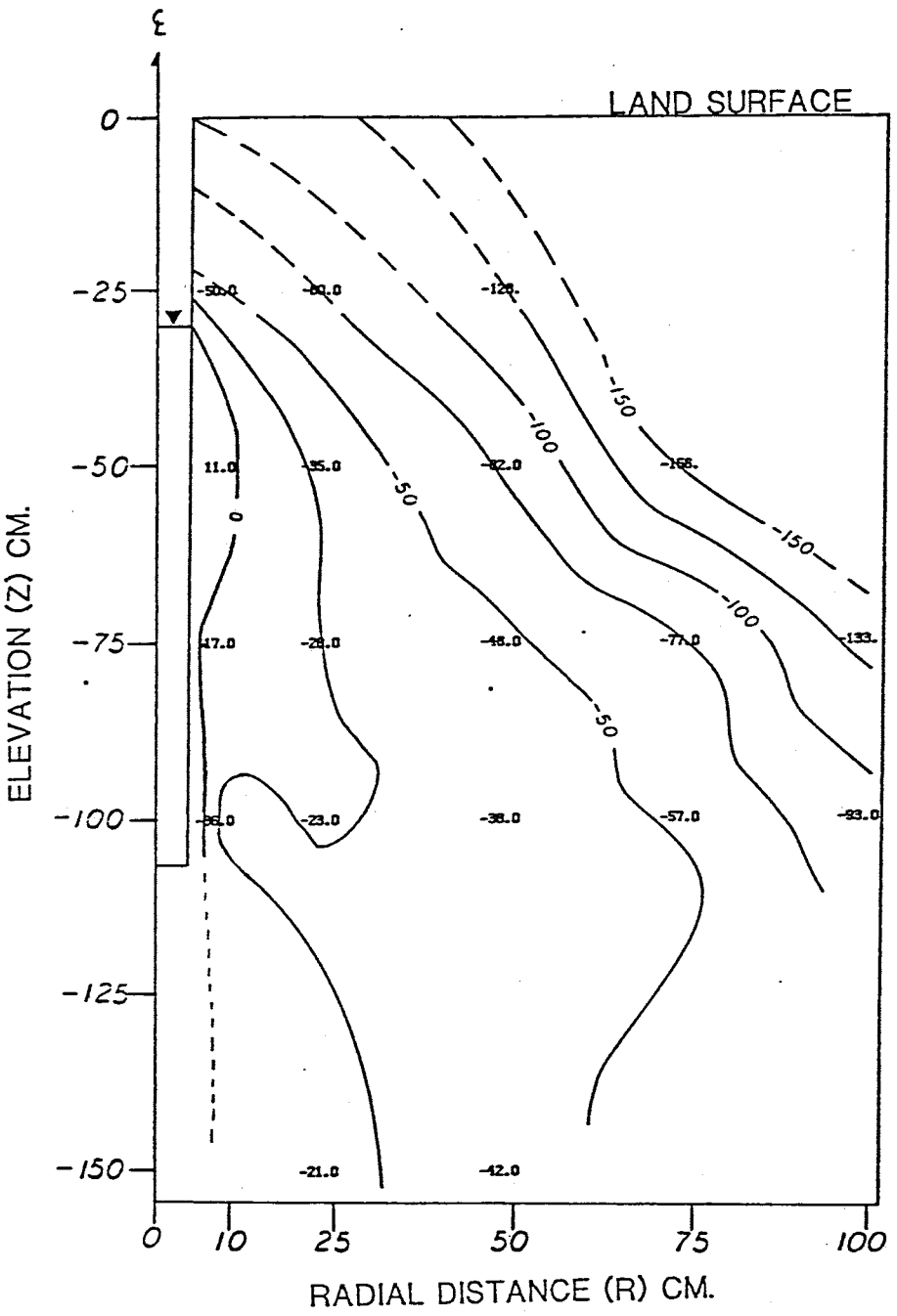

Figure 57. Pressure Head Profile at t=12,572 minutes

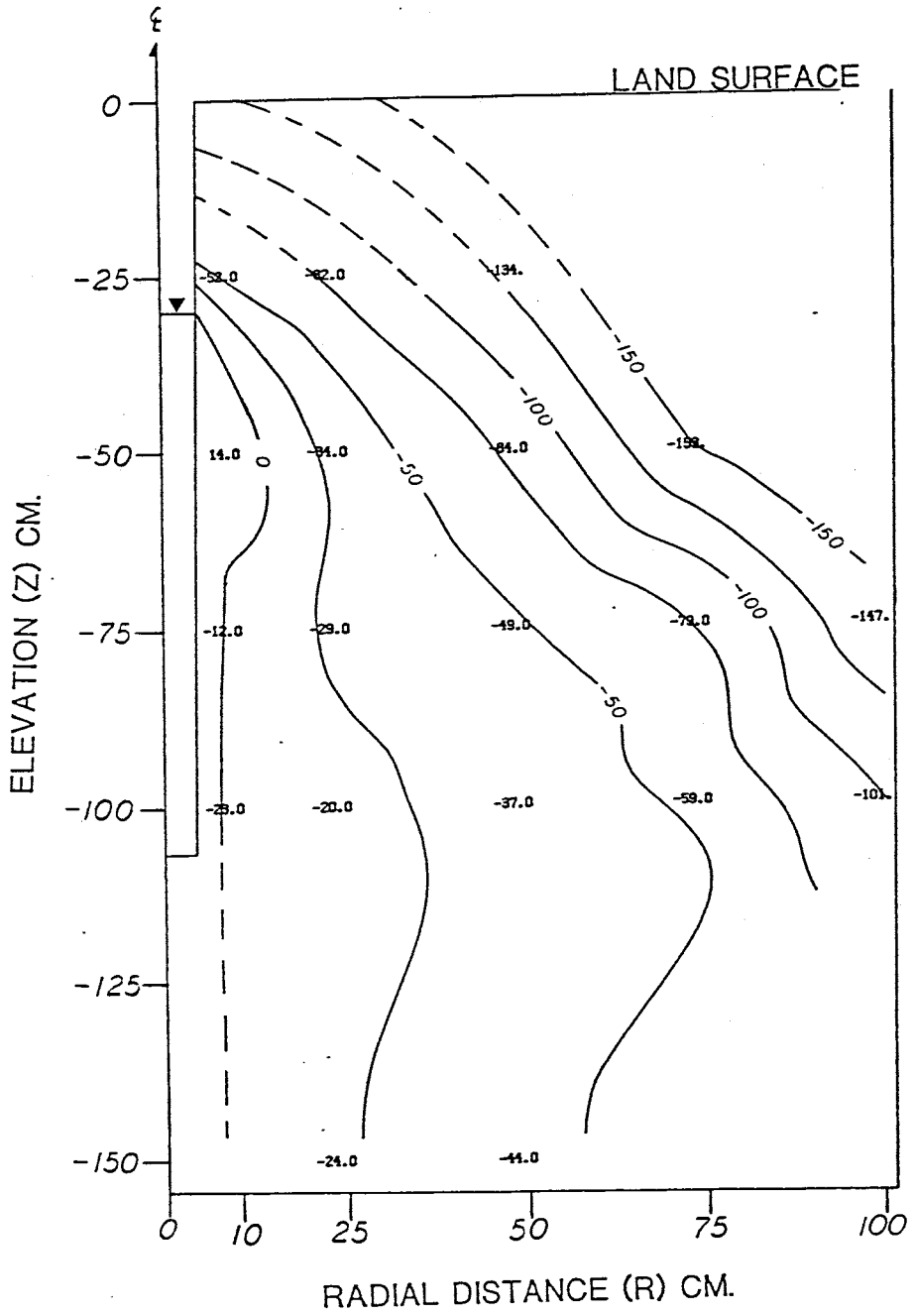

Figure 58. Pressure Head Profile at t=13,417 minutes

approximately -150 cm. The mound is dissipated after t=17,512 min (figure 61). The profiles from t=17,512 until the end of the test do not show any mounding. The tensiometer at a radius of 75 cm and an elevation of -75 cm may have had some entrapped air in its manometer line, causing the pressure head field to appear as it does in figures 65 through 67.

Pressure head data from a radius of 10 cm are presented in a different fashion in figure 68. Pressure heads at an elevation of -25 cm are fairly constant, except for the anomalous point at t=23,337 min. The pressure heads from an elevation of -50 cm increase during the period from t=11,832 to t=17,512 min, whereafter they are nearly steady, except for the peak at t=23,337 min. The sharp decrease in pressure heads at t=23,337 min are a result of a 20% decrease in the height of water in the borehole between t=22,012 min and t=23,336 min caused by a malfunction of the float valve. The decrease in height of water created a similar drying effect of the flow field at t=11,832 min.

The wetting trends exhibited by the tensiometers at elevations of -50, -75, and -100 cm between t=11,832 min and t=15,962 min may be in response to a renewed build-up of moisture on top of the coarse layer between episodes of "fingering" into the coarse layer. Moisture content profiles reveal the fingering quite well.

The drying trend of the soil at an elevation of -75 cm between t=15,962 min and t=23,337 min is correlated with a

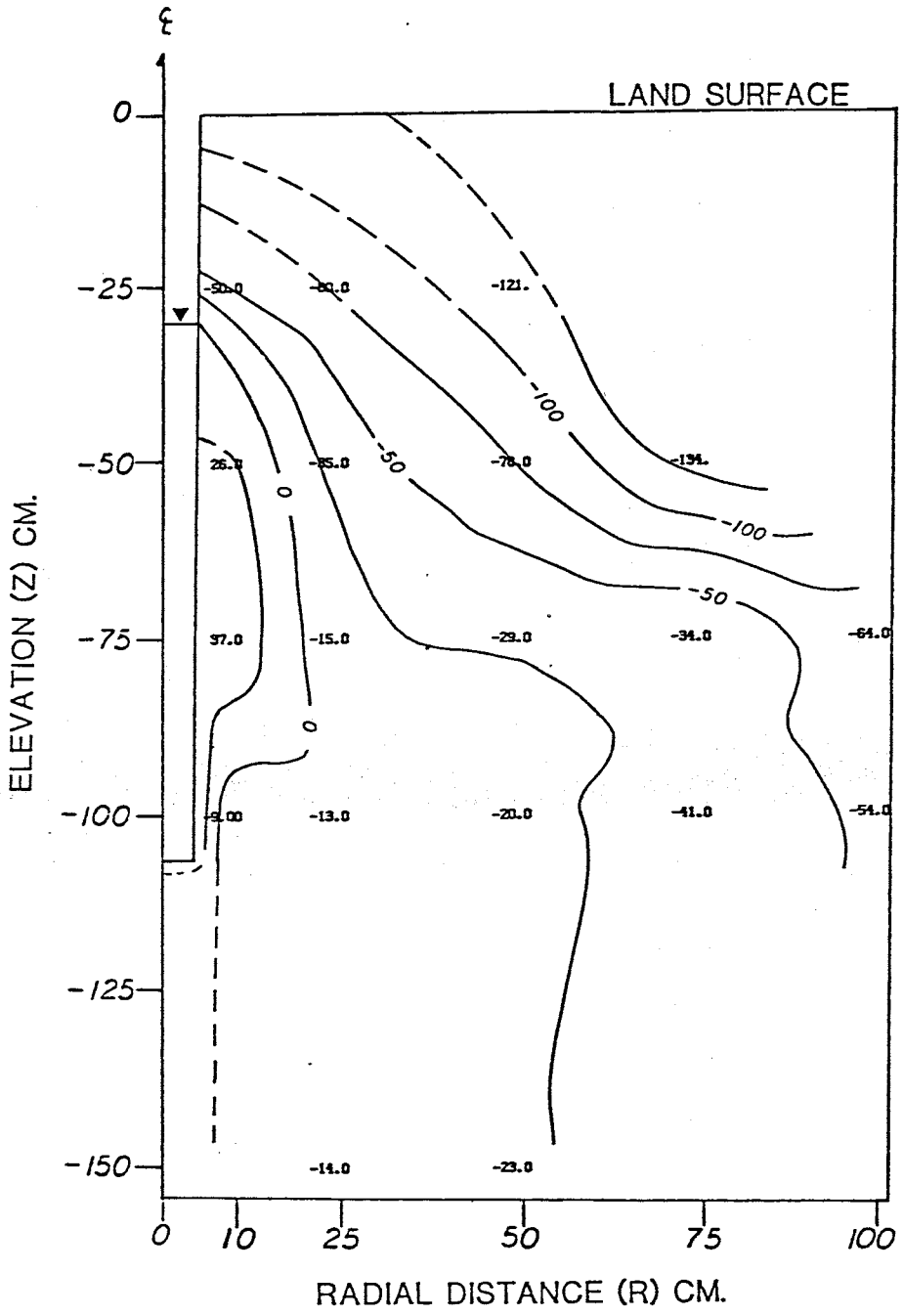

Figure 61. Pressure Head Profile at t=17,512 minutes

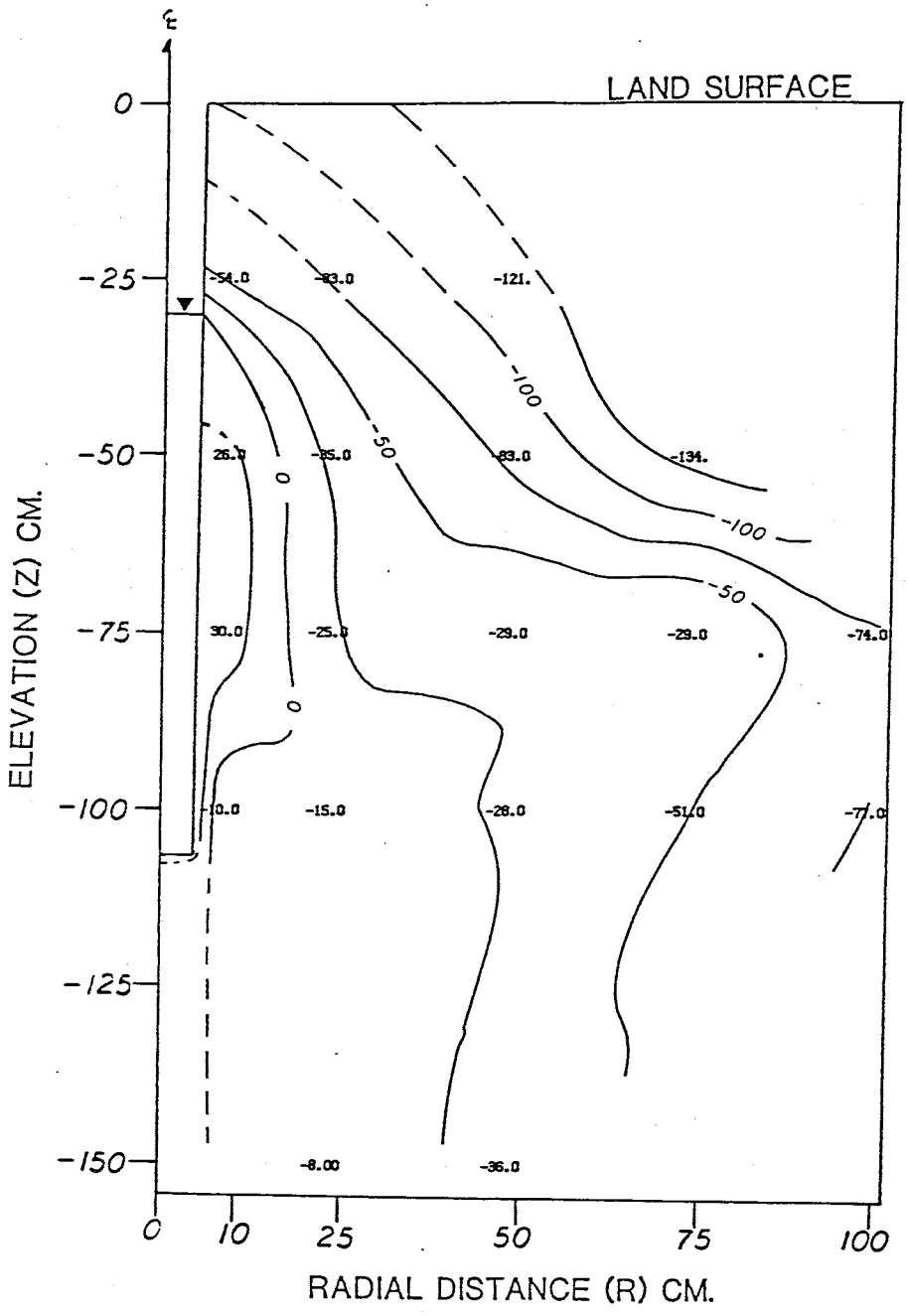

Figure 62. Pressure Head Profile at t=18,982 minutes

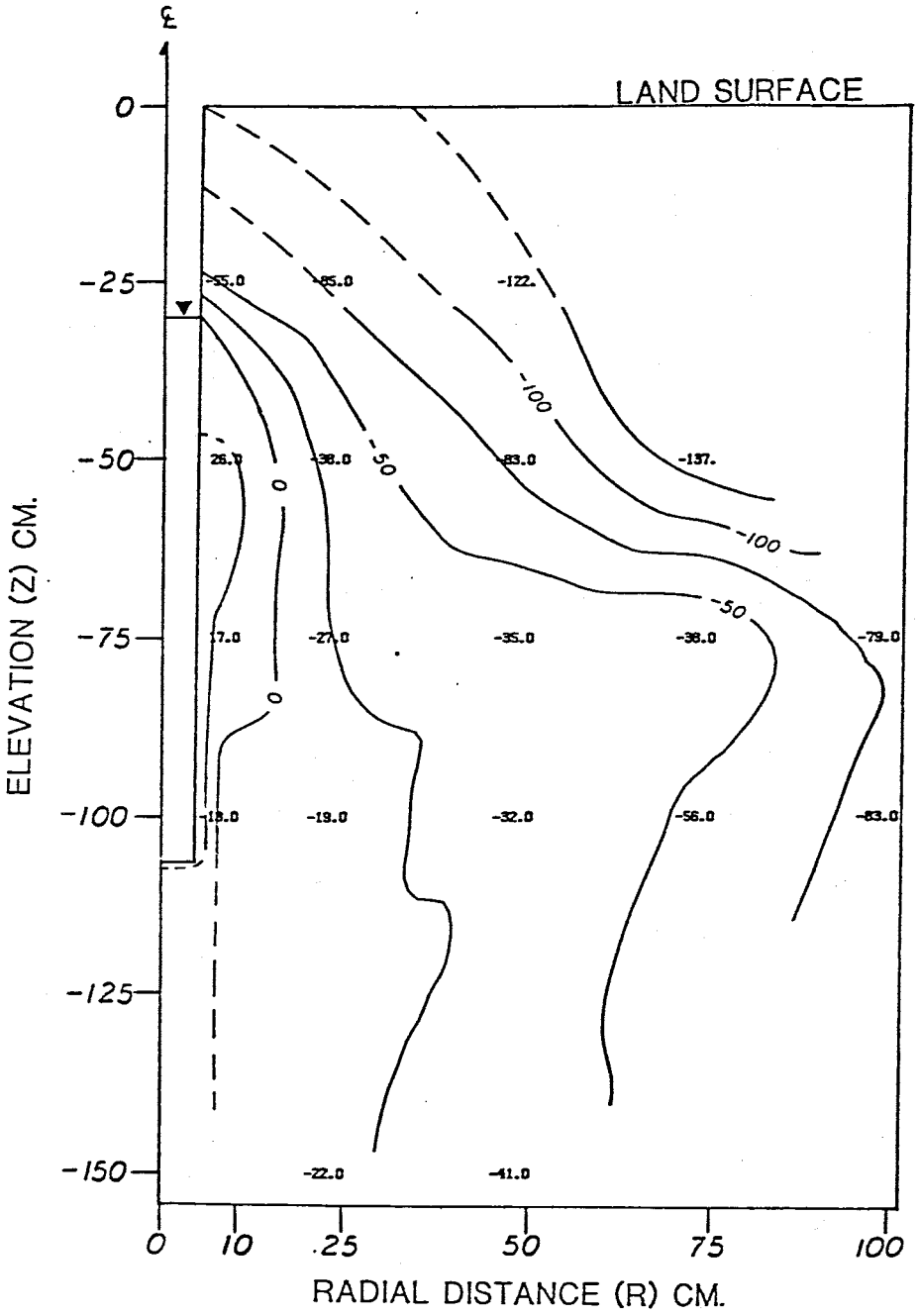

Figure 63. Pressure Head Profile at t=20,542 minutes

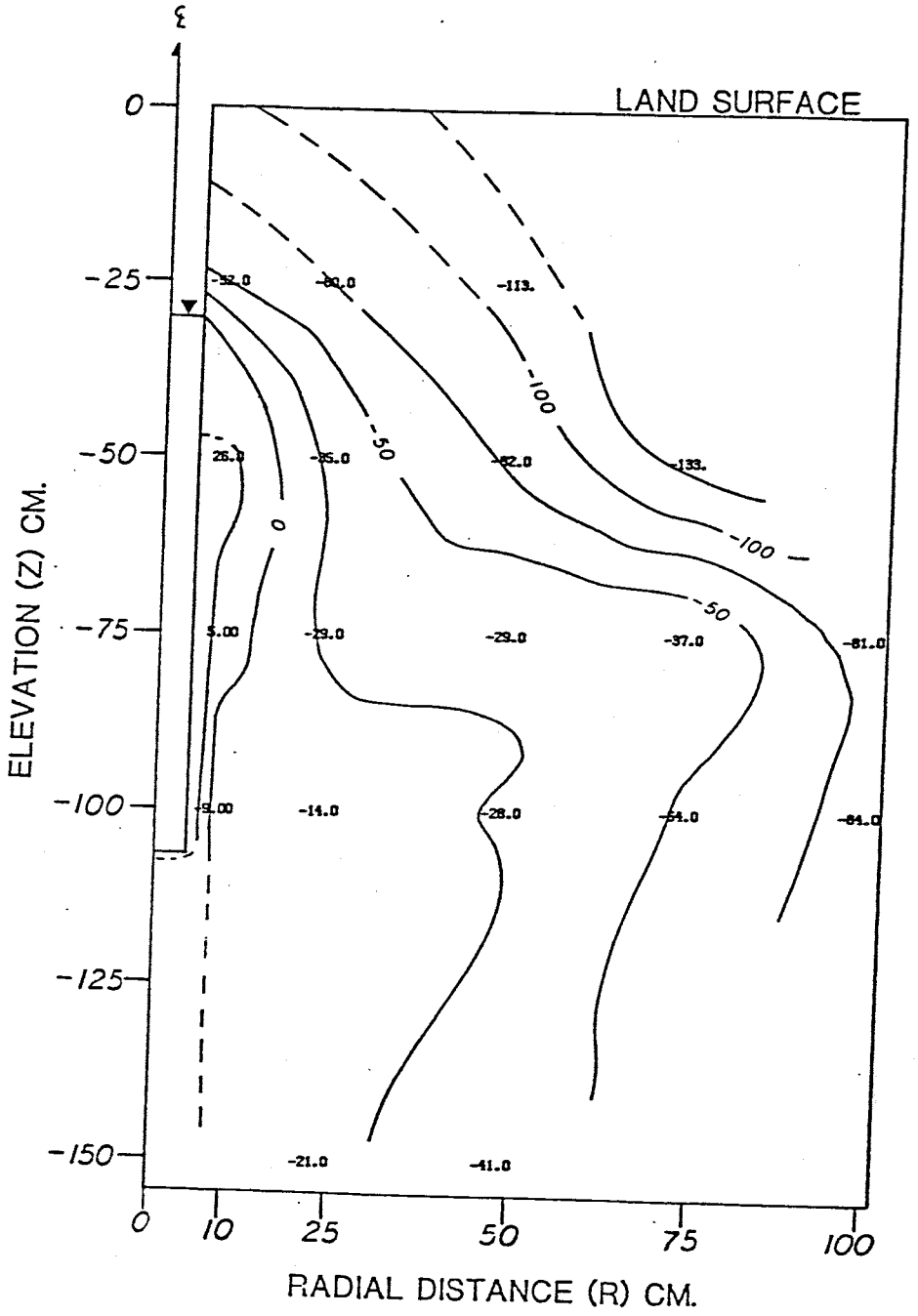

Figure 64. Pressure Head Profile at t=21,987 minutes

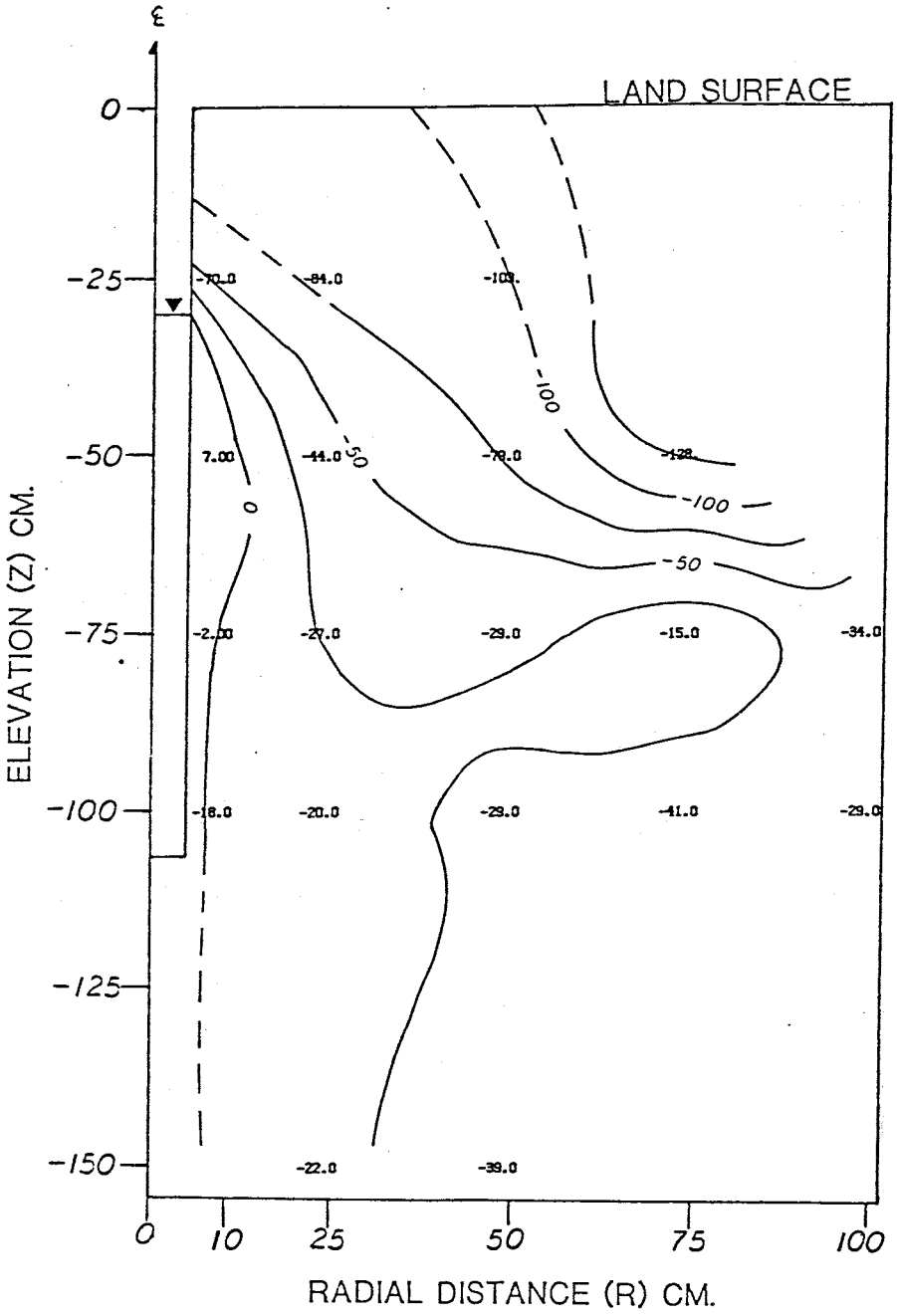

Figure 65. Pressure Head Profile at t=23,337 minutes

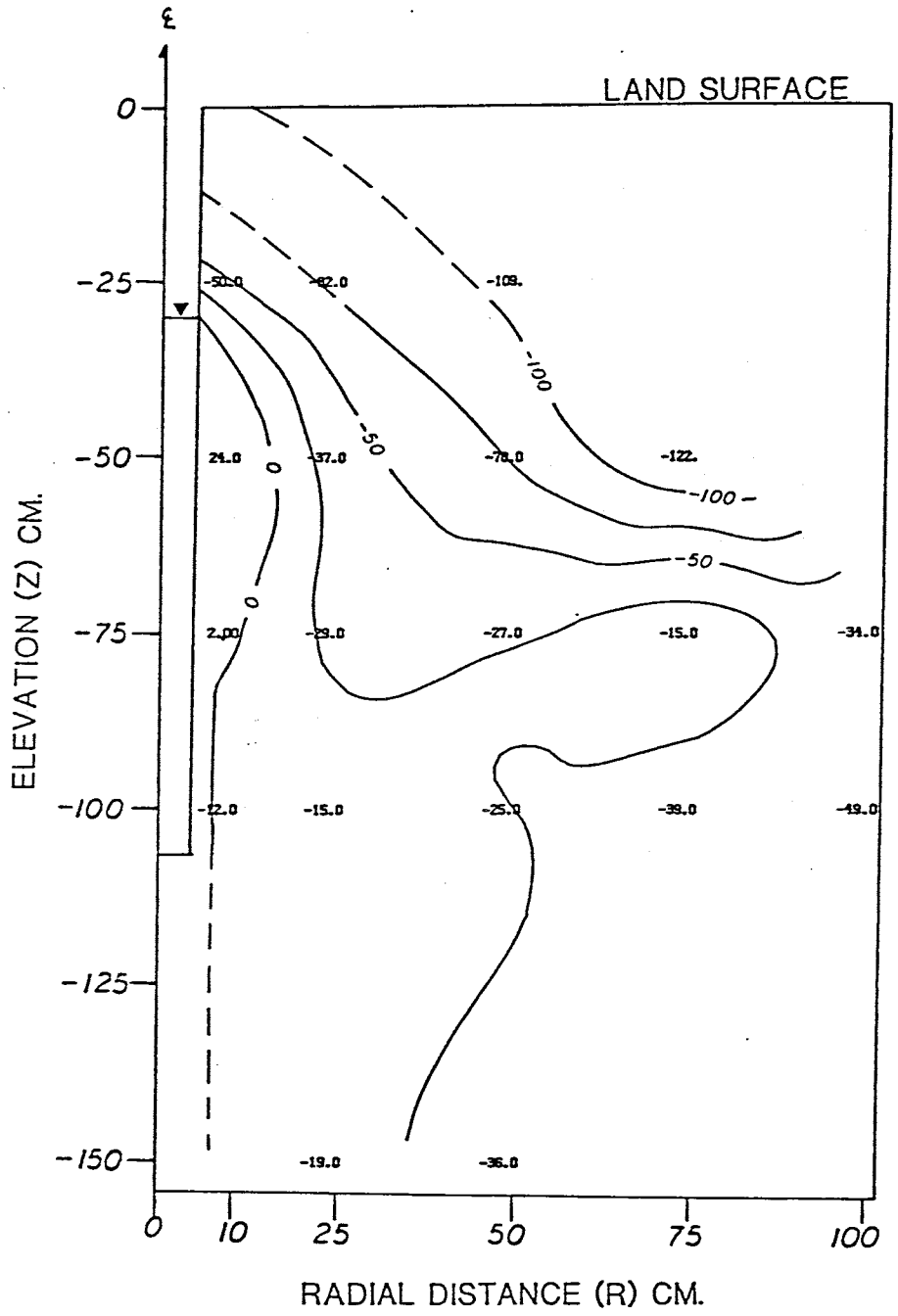

Figure 66. Pressure Head Profile at t=24,717 minutes

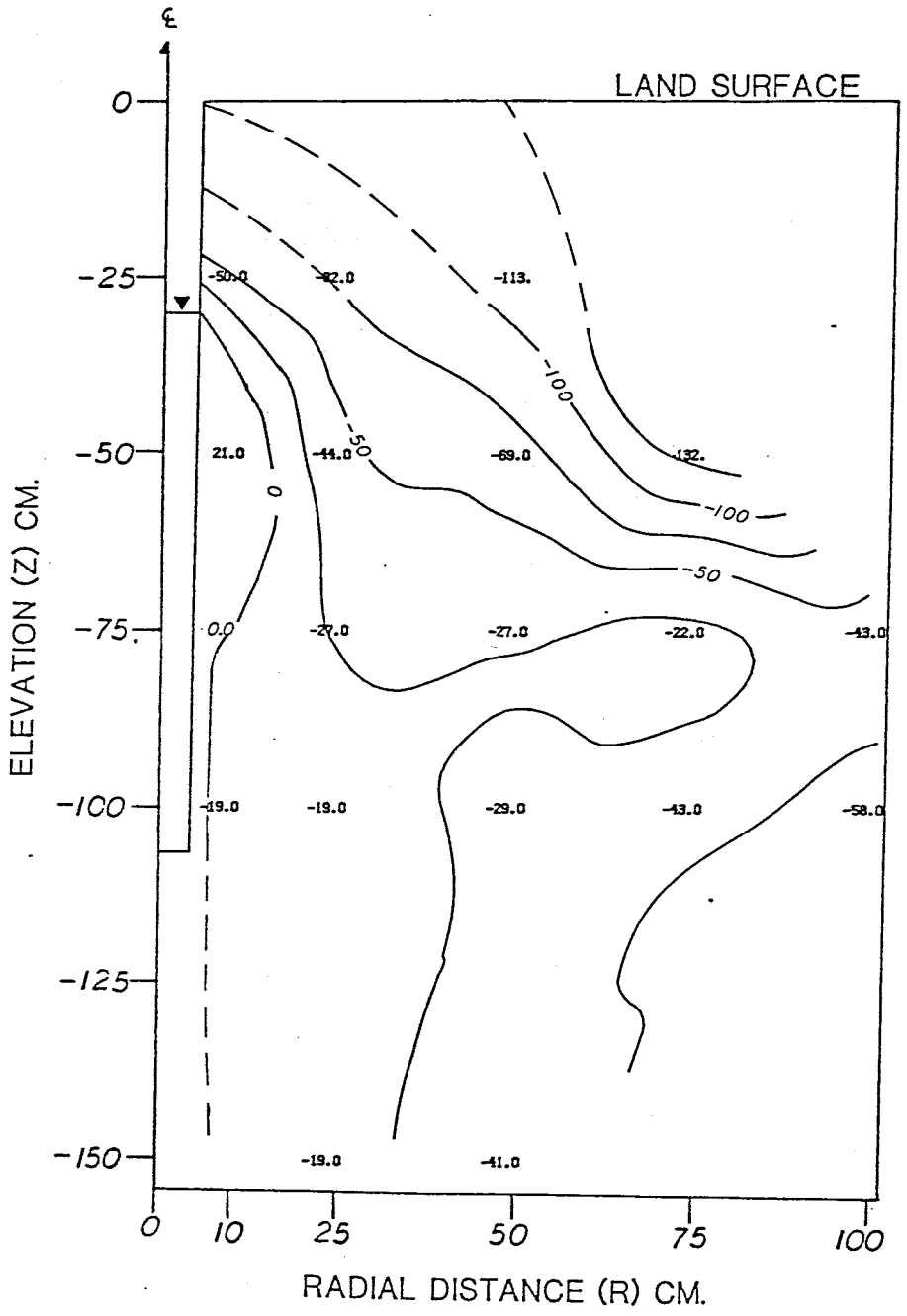

Figure 67. Pressure Head Profile at t=25,972 minutes

decrease in infiltration rate over the same time interval. Figures 68 and 69 show that other tensiometers exhibit a slight drying over this interval also. In all cases the pressure heads at elevations of -75 cm and -100 cm fluctuate more than tensiometers at elevations of -25 cm and -50 cm. This may indicate that tensiometric readings at the base of the borehole are more influenced by the buildup of water on the coarse layer than readings near the top of the borehole.

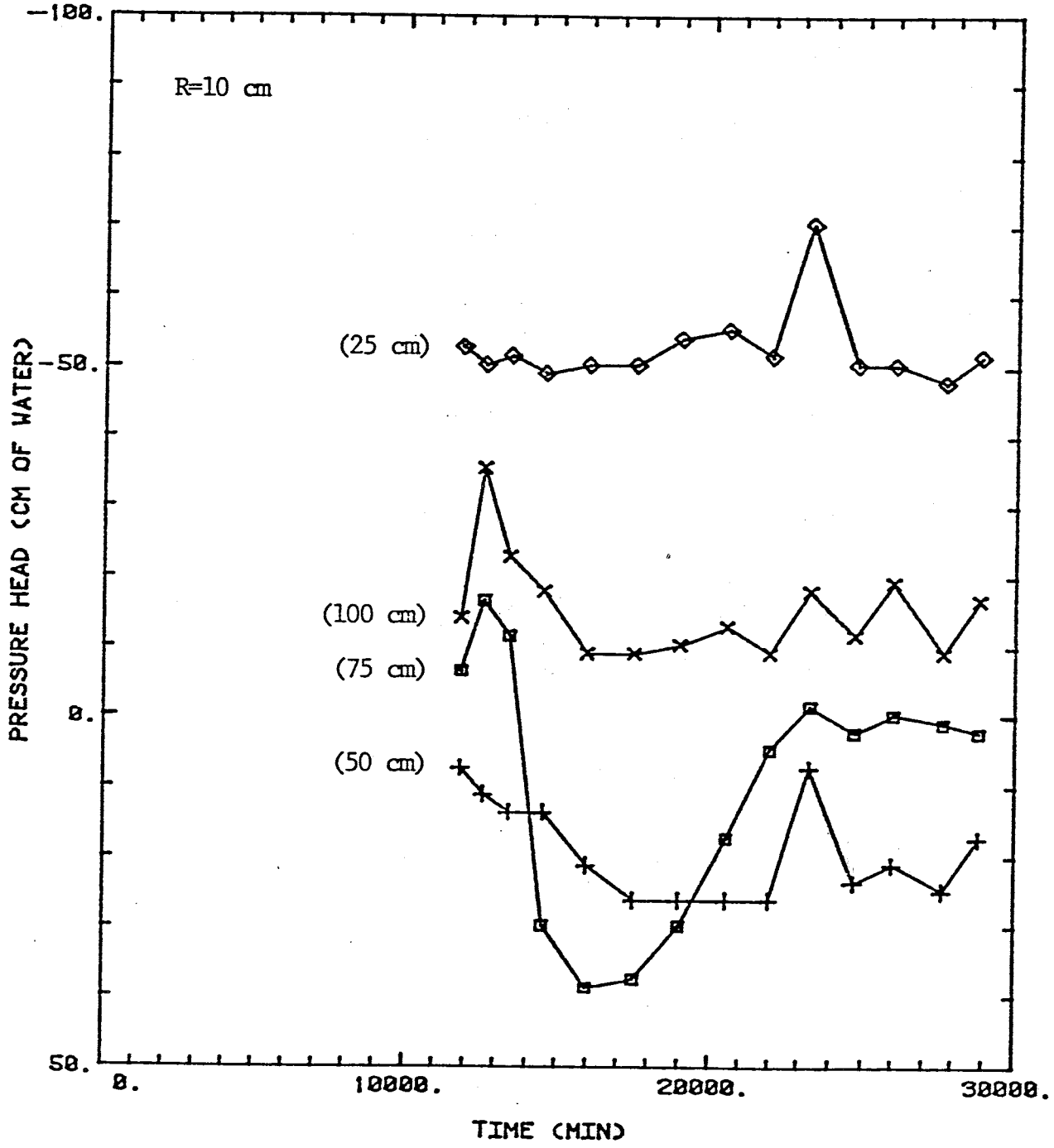

Figure 68. Pressure Head versus Time for R=10 cm

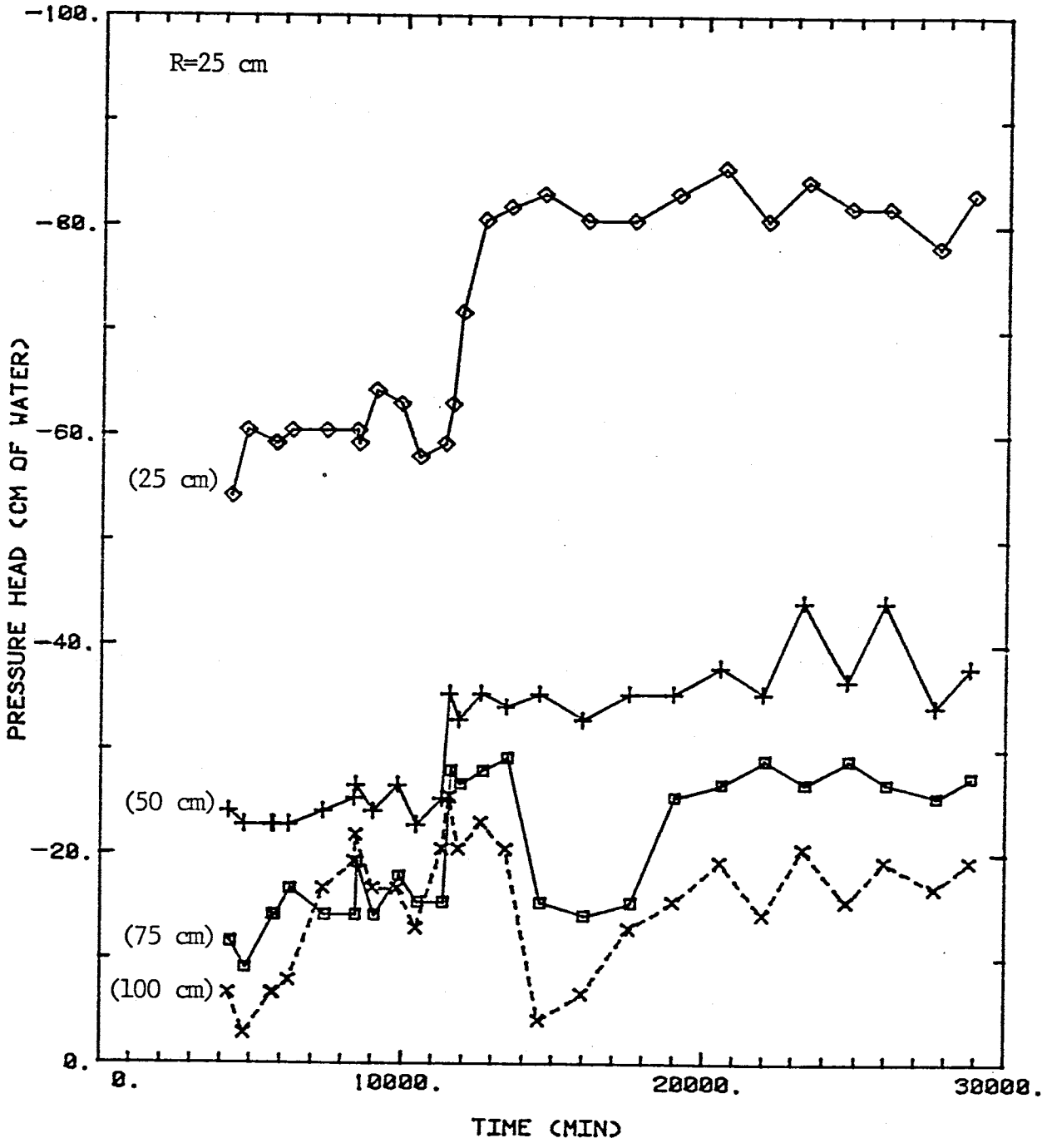

Figure 69. Pressure Head versus Time for R=25 cm

6.9 Total Head

Total head profiles were constructed using the same plotting routine as the pressure head and moisture content profiles, namely NCAR. The contours between the borehole and the first data points (either radius of 25 cm or 10 cm) were drawn in by hand. As stated in the pressure head discussion, tensiometers were not emplaced until day 2 of the test, and were not read until day 3 in order to allow the tensiometers to equilibrate.

The tensiometers were connected to mercury manometers, from which total head measurements were read directly. The formula for calibrating the manometer scale can be found in the section describing instrumentation.

The changes in pressure heads have been previously described in-depth. Only a few of the total head profiles which are considered most important will be shown here.

Figure 70 (t=4267 min) is a profile of total head from the first tensiometer data. Total hydraulic head gradients near the borehole are relatively much smaller than the gradients at farther horizontal distances, indicating the extent of the wetting front. A few flow lines have been drawn to illustrate flow directions, assuming isotropic conditions. Figure 70 shows horizontal and upward flow above an elevation of approximately -50 cm, and downward flow below approximately -50 cm.

Figure 71 is a profile at t=11,282 min. The gradients

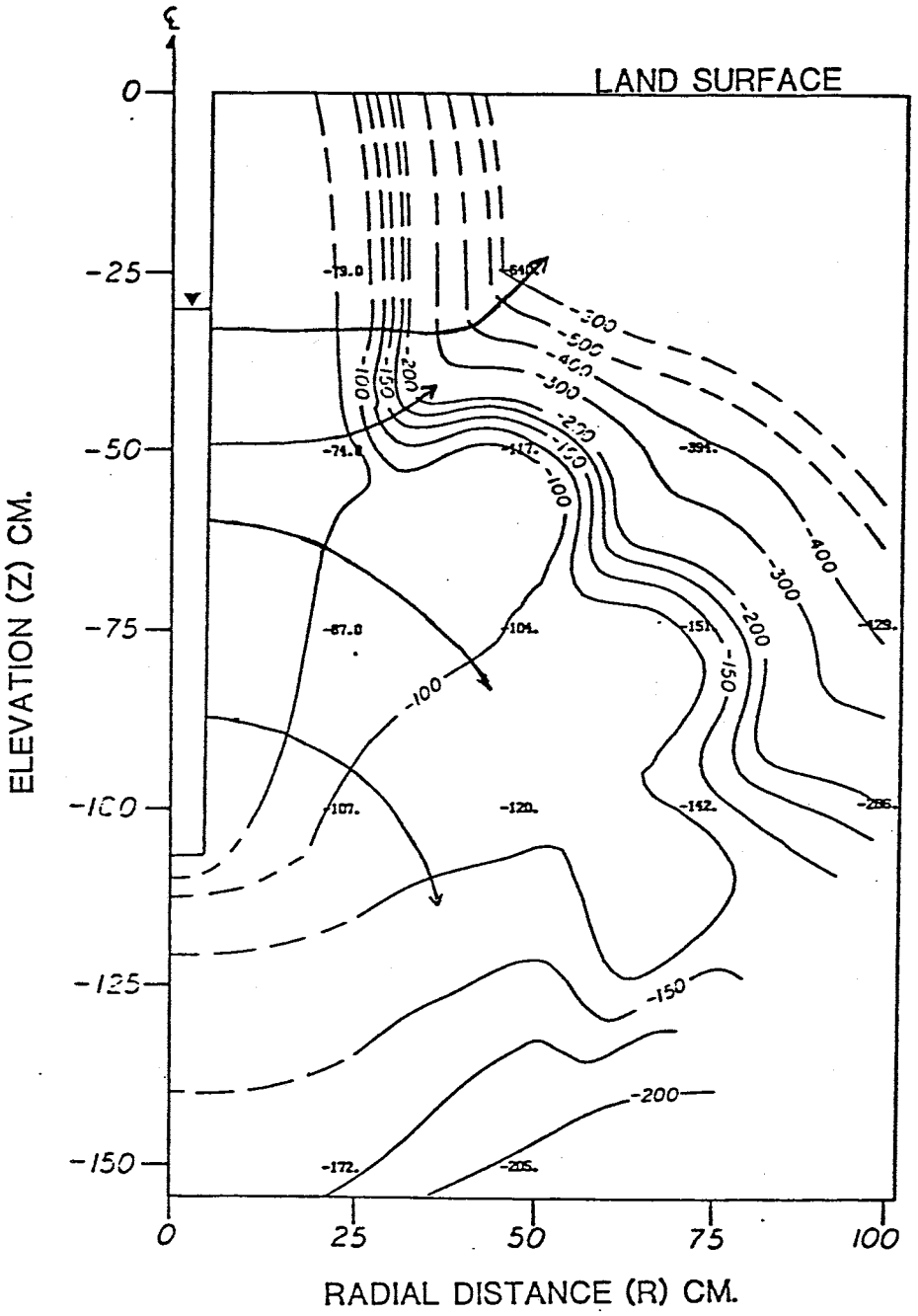

Figure 70. Total Head Profile at t=4267 minutes

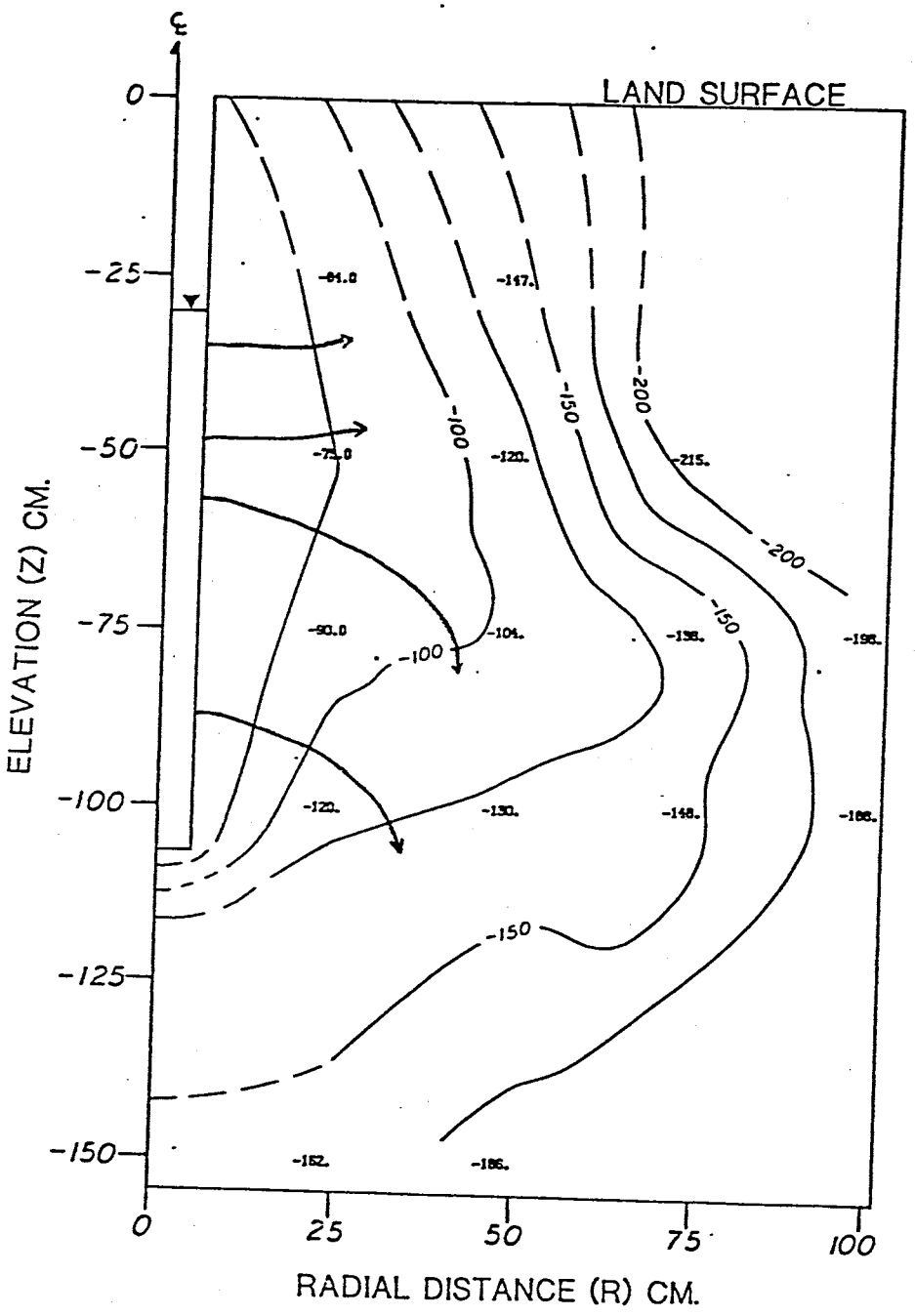

Figure 71. Total Head Profile at t=11,282 minutes

at large horizontal distances from the borehole have become much lower as the soil has become wetter. The gradients near the borehole have changed little from t=4267 min. The flow lines are essentially the same as they were at t=4267 min. This profile shows the flow field just before the float valve in the borehole malfunctioned and allowed the water level in the borehole to decrease by 10%.

Figure 72 shows the flow field at t=11,532 min, which is just after the float valve malfunctioned. The total head values have decreased (become more negative) from t=11,282 min, except at a radius of 100 cm and also at depths of -150 cm. The continued increase in total head at R=100 cm may have been caused by the continued wetting of the soil at this radius by capillary action. The increases at an elevation of -150 cm may have been caused by a slight increase in moisture content above the coarse layer as discussed in the moisture content and pressure head profiles. The decrease in total head at the other tensiometers reflects a drying of the soil in response to the decreased infiltration rate associated with the drop in height of water in the borehole. The flow lines did not change significantly between t=11,282 min and t=11,532 min, however.

Figure 73 (t=11,832 min) includes data from tensiometers installed at a radius of 10 cm from the borehole center. These tensiometers were installed to precisely define the flow field near the borehole. As

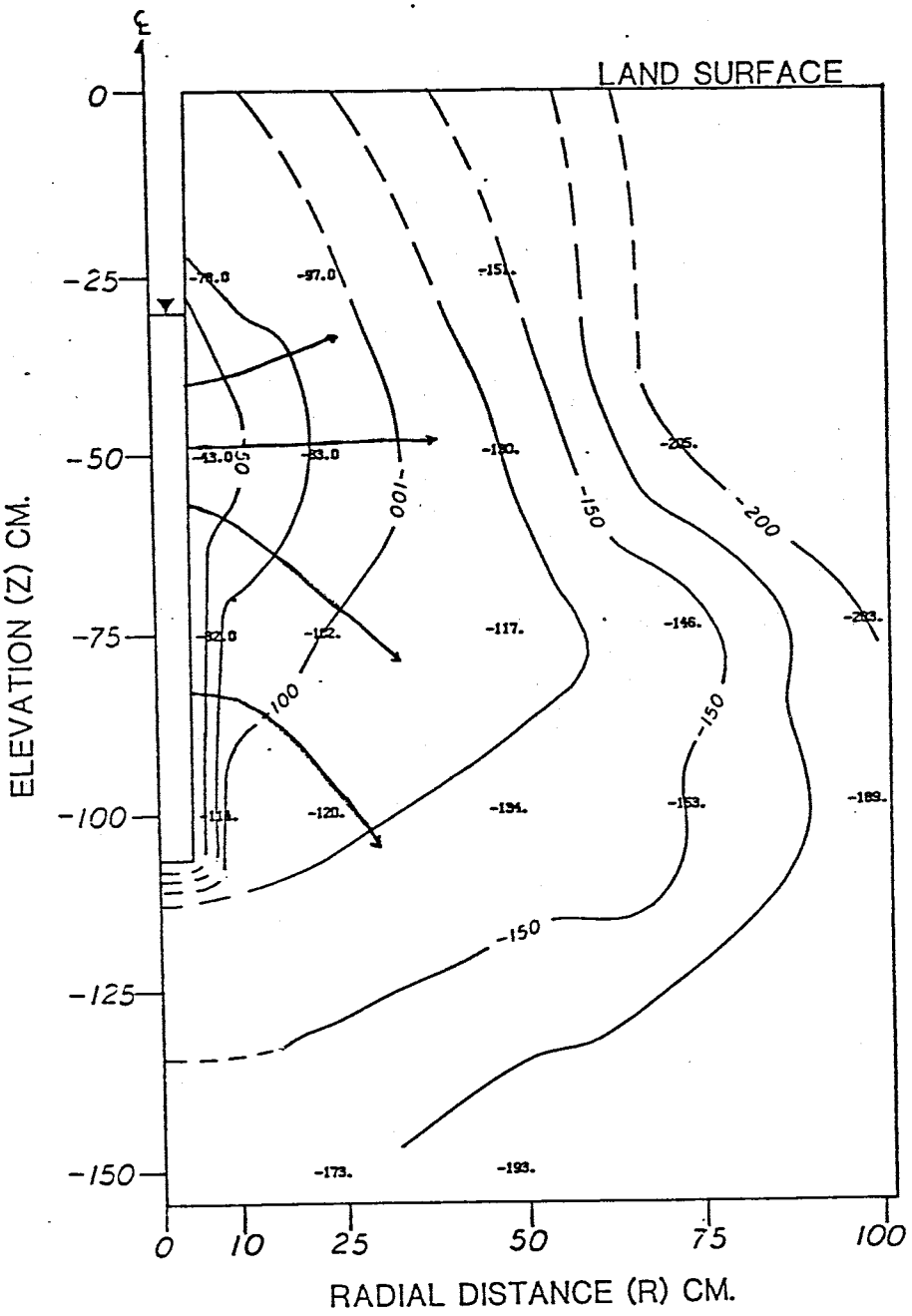

Figure 73. Total Head Profile at t=11,832 minutes
(Tensiometers added at R=10 cm)

figure 73 shows, the inclusion of data from a radius of 10 cm results in a considerable change in the inferred flow field near the borehole. The flow lines remain very much as they were before t=11,832 min, however.

The total head profile at t=14,537 min (steady state) is shown in figure 74. The flow lines in this profile are quite different than from previous profiles. Flow lines beginning at an elevation of approximately -60 cm are much more horizontal than before, while the flow line beginning at an elevation of approximately -85 cm is much more vertical. The soil surrounding the borehole (R=10 cm) at an elevation of approximately -75 cm has become much wetter than it was at t=11,832 min. The data from a radius of 10 cm and an elevation of -100 cm is actually drier at t=14,537 min than it was at t=11,832 min. This may be due to water infiltrating through the coarse layer at an elevation of -150 cm, as previously discussed.

Of particular interest is the soil at a radius of 10 cm and an elevation of -100 cm, which remains unsaturated throughout the test. This may have been caused by swelling of the soil at this elevation, as inferred from laboratory samples and fractures which were in evidence during the borehole infiltration test. Prior to the start of S9T1, the borehole screen had backfill placed between it and the borehole wall. The material used as backfill was the same soil removed when excavating to make room for the screen. Subsequent pressure head-moisture content samples revealed

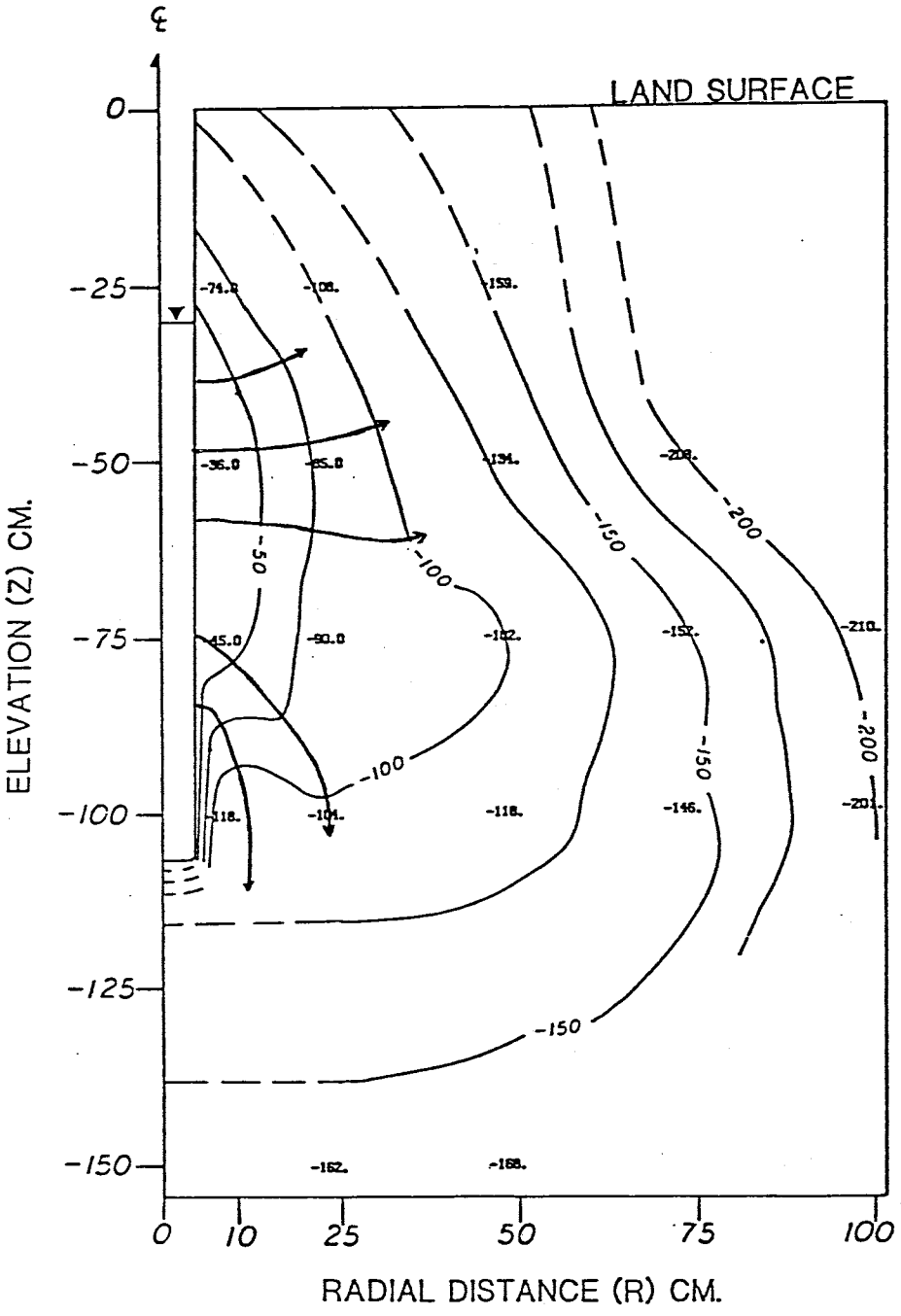

Figure 74. Total Head Profile at t=14,537 minutes

the potential of the soil to exhibit shrink-swell behavior. The most pronounced shrink-swell behavior was observed in the sample from an elevation of -100 cm. Lagerwerff, et al (1969) recognized a reduction in the saturated hydraulic conductivity (Ks) of swelling soils as they absorbed water. McNeal, et al (1966) concluded that the decrease in Ks was caused by closing of conducting pores by swelling. McNeal and Coleman (1966) found that the presence of sodium in the percolating solution caused a decrease in Ks, particularly at low salt concentrations. Hillel (1980) refers to the sodium absorption ratio (SAR). He states that a high SAR, particularly at low salt concentrations in the solution, tended to decrease Ks. The SAR is defined by equation 12:

$$SAR = \left[\frac{Na^{+}}{\left(\frac{Ca^{2+} + Mg^{2+}}{2} \right)} \right]^{1/2} \qquad (12)$$

where the concentrations are expressed in milliequivalents per liter (meq). Table 3 lists the chemical composition of the field water. Using these values, the SAR for the field water was 3.32, with a total concentration of calcium, magnesium, and sodium of 3.43 meq.

The SAR may have been high enough and the total concentrations low enough to cause a reduction of hydraulic conductivity at the bottom of the borehole. This reduction in Ks was felt mostly at the bottom of the borehole because this elevation (-100 cm) had exhibited the most pronounced shrink-swell behavior of all of the samples collected for pressure head-moisture content data. Another factor

enhancing the decrease in Ks would be the act of augering the soil. The soil was probably broken up by the augering, allowing for increased surface area for reactions with the field water and thus inducing more shrink-swell, which reduced Ks. The reduction in Ks may have been enough to prevent saturation of the soil at an elevation of -100 cm.

6.10 Hydraulic Gradient

From Darcy's Law, infiltration rate (Q) is proportional to both negative hydraulic gradient (-i) and to hydraulic conductivity (K). Also by Darcy's Law, the ratio of Q/(-i) is proportional to K. Plotting the changes in Q/(-i) or -i over time provides an insight into the processes involved during the test.

Figure 75 is a plot of (Q/-i) versus time for approximately the first 5000 minutes of S9T1. No tensiometric data were available before t=4267 min. Consequently, moisture contents recorded by the neutron probe at a radius of 45 cm from the borehole center and elevations of -76.2 cm and -107 cm were used to infer the values of i at various times by combining neutron probe readings with the soil moisture characteristic curves generated from laboratory samples at elevations of -75 cm and -100 cm. The value of pressure heads which corresponded with the field values of moisture content were recorded. The pressure head values were converted to total head values by adding the elevation (either -75 cm or -100 cm) onto the value of pressure head. The difference in total head between the borehole (-30.5 cm) and the value just found was divided by the distance between the borehole wall and the neutron probe radius of 45 cm. In other words,

$$i = dh/dl$$

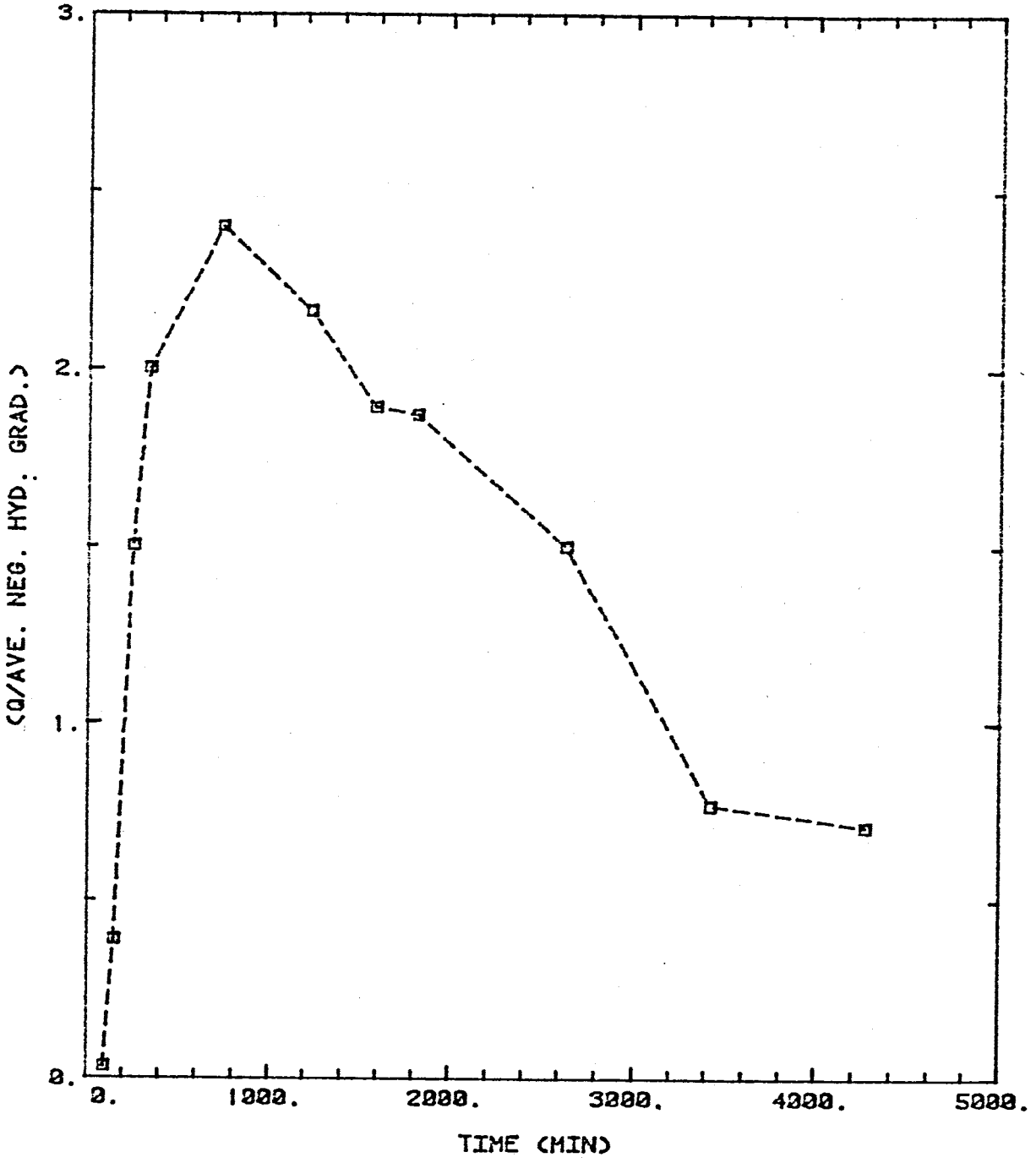

Figure 75. Q/i versus Time for the first 5000 minutes of the test (from neutron probe data)

where "dh" is the difference in total head and "dl" is the distance between the borehole wall and the neutron probe reading.

Figure 75 shows the hydraulic conductivity to increase 74 times between t=98 min and t=732 min. During this same interval, Q decreases by 55% and i decreases by 123 times. The increase in K and decrease in i are the result of the wetting front passing a radius of 45 cm. The decrease in Q is caused by the reduction in gradients as the wetting front moves away from the borehole. K decreases by 330% (3.3 times) between t=732 min and t=4267 min. Q decreases by 66% and i increases by 14% over the same interval.

Figure 76 shows the changes in K and Q versus time from tensiometric data at a radius of 25 cm from the borehole and elevations of -50, -75, and -100 cm. K varies in the same manner as Q. Between t=5692 min and t=11,282 min, K decreases by 4.6 times while Q decreases by 40% as the volume of wetted soil increases.

The sudden drop in K and Q at t=11,532 min was caused by a 10% decrease in water level in the borehole due to a float malfunction which restricted flow of water into the soil. The subsequent rise of both curves between t=11,532 and t=14,543 min is believed to be the result of returning the height of water in the borehole to its proper position. The soil profile may have drained somewhat when the water level dropped. Raising the water level again may have resulted in an increase in moisture content, and thus an

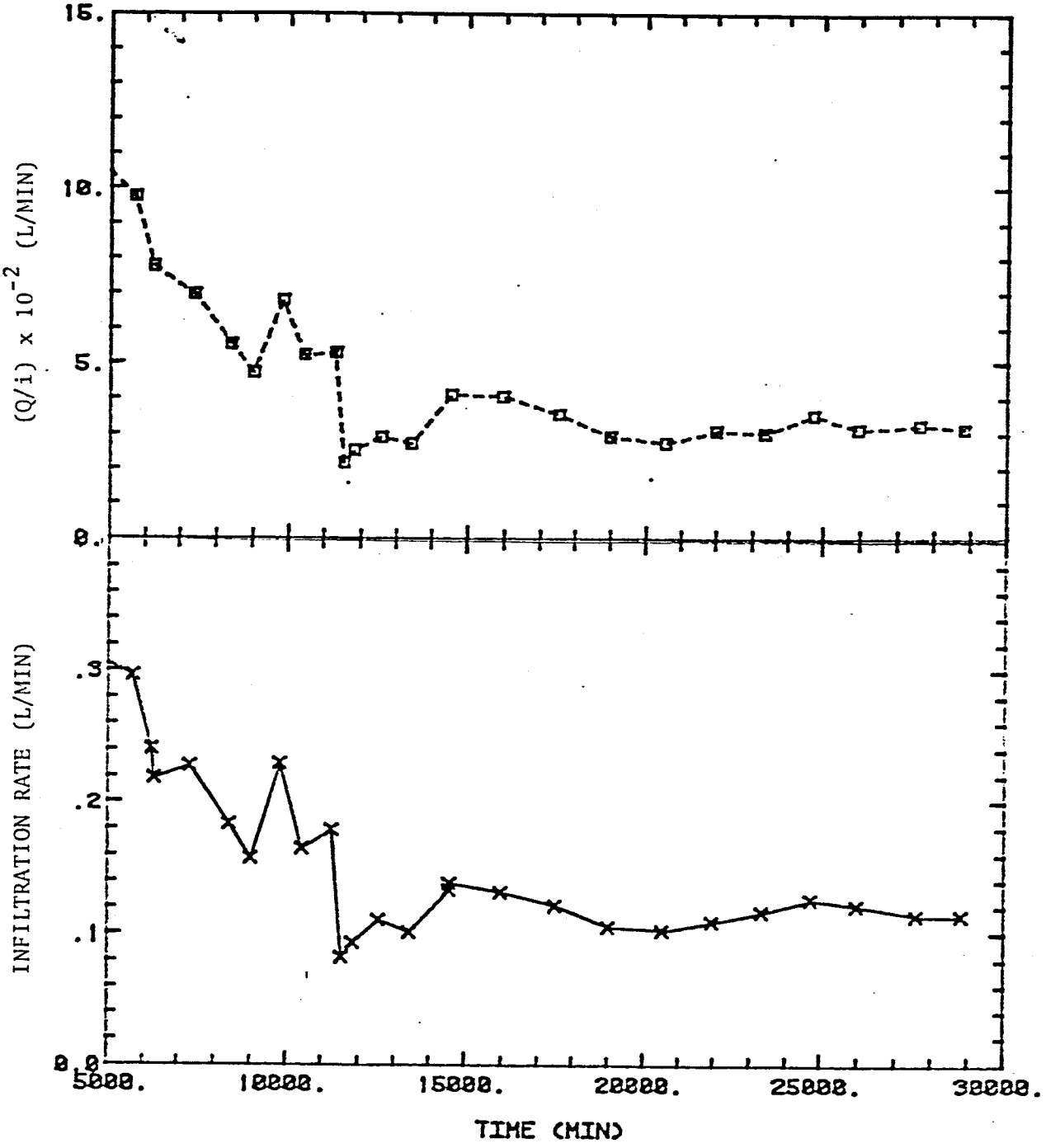

Figure 76. Q/i versus Time and Infiltration rate versus Time for t=5000 minutes to the end of the test

increased K.

At approximately t=22,000 min, the field water was replaced with tap water. As the water chemistry analysis (Table 3) shows, both waters had approximately the same chemistry, and no sudden change in infiltration rate was observed.

Figure 77 shows the changes in average negative hydraulic gradient and Q versus time after t=5000 min. These two curves appear to be mirror images of one another. When Q decreases, i increases, and vice versa. The hypothesis of an alternate wetting and drying soil between t=11,282 min and t= 14,543 min as a result of the drop in water level in the borehole and subsequent filling to the desired level is supported by figure 77. Between t=11,282 min and t=11,532 min, Q drops while i increases as a result of a float valve malfunction. Between t=11,532 min and t=14,543 min i decreases as the soil becomes wetter after returning the water level to its desired level.

After t=14,543 min, -i first increases and then becomes variable. Between t=20,542 min and t=21,987 min, i decreases by 5% due to a 10% increase in head in the borehole which was caused by a float malfunction. Between t=21,987 and t=23,337 min, i increases by 9%. This was caused by a reduction of 20% in the head in the borehole. It is interesting to note that the 20% reduction in head in the borehole was coupled with a 7% increase in Q. It is believed that the water level in the borehole was restored

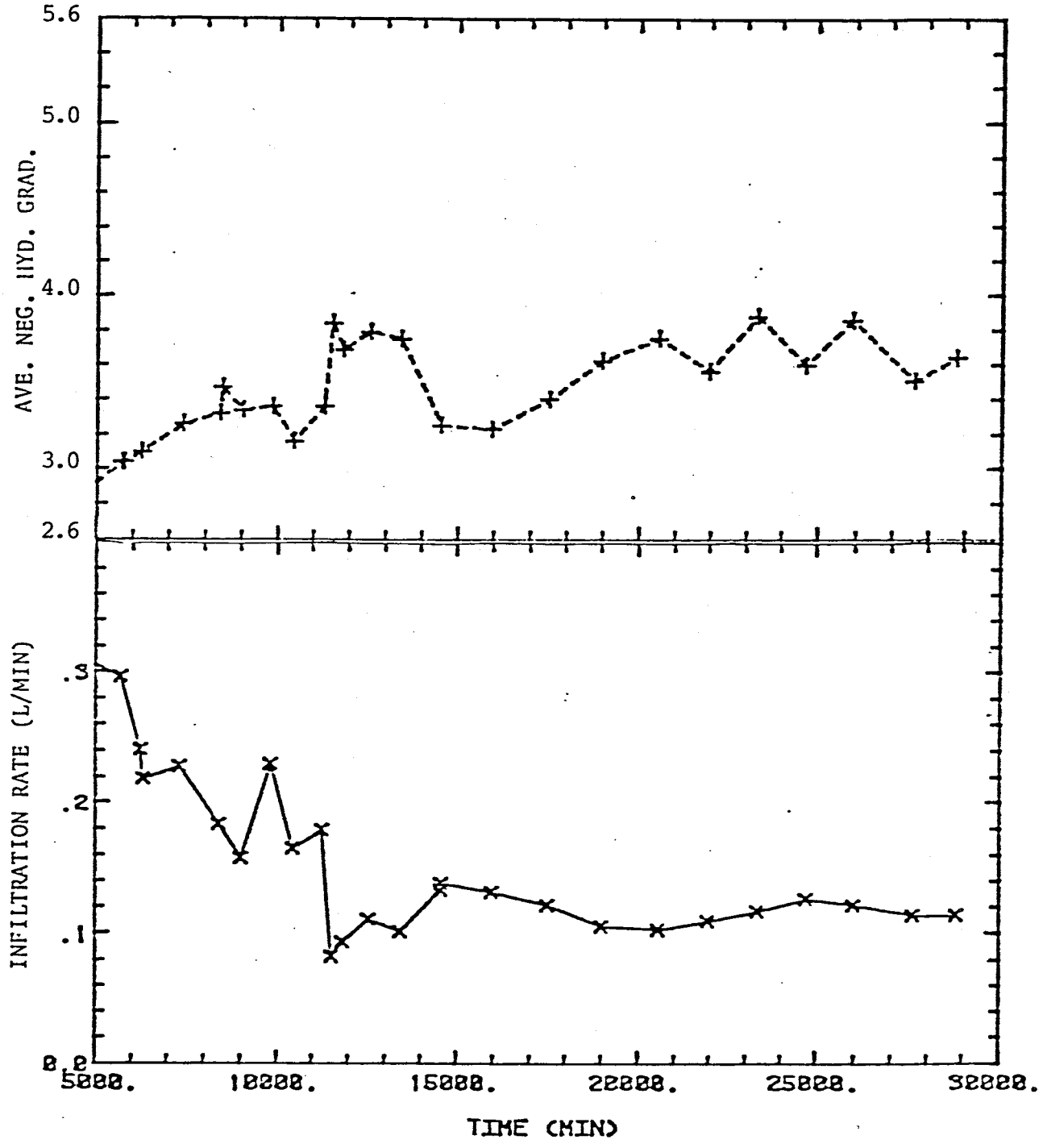

Figure 77. Average Negative Hydraulic Gradient versus Time and Infiltration rate versus Time for t=5000 minutes to the end of the test

to its original position before recording the changes in Q. The excess water needed to return the water level in the borehole to its original position compensated for the float valve malfunction.

After t=25,972 min, Q and i vary proportionally. Between t= 25,972 min and t=27,618 min, i decreases by 9.1% while Q decreases by 6.2%. Between t=27,618 min and t=28,802 min, i increases by 3.7% while Q increases by 1.8%. These changes are according to Darcy's Law. Why Q and i should vary proportionally after t=25,972 min while being inversely proportional prior to t=25,972 min may be explained by entrapped air. Stephens, et al (1983) reported Q and i varying inversely due to the influence of entrapped air. Figure 23 indicates that the temperature of the infiltrating water probably fell below the temperature of the soil water during the early-morning hours of each day. As discussed by Stephens, et al, infiltrating water temperature less than soil water temperature favors the formation of entrapped air. This in turn results in a decrease in Q and an increase in i.

Some conclusions can be drawn from figures 75 through 77. One of the most important is that while Q varies with K according to Darcy's Law, at late times, after the wetting front has passed, Q is generally inversely proportional to i, which is counter to Darcy's Law. Stephens, et al (1983) reported Q varying inversely with i as a result of entrapped air which expands with increasing temperature, resulting in

decreased infiltration rate and increased gradient.

6.11 Saturated Hydraulic Conductivity

Glover (1953) developed an equation subsequently recommended by the USBR (1974) for estimating saturated hydraulic conductivity (Ks) from borehole infiltration tests. The Glover method utilizes the value of steady infiltration rate and the distance from the borehole to the water table or impeding layer to estimate Ks. This equation assumes the existence of a free-surface within which all flow takes place. Philip (1985), Rabold (1984), Stephens, et al (1983), and Stephens and Neuman (1982b) have shown that flow takes place both inside and outside the free surface assumed by Glover. Stephens, et al (1983) developed empirical equations for finding Ks based on the assumption of both saturated and unsaturated flow. These equations are presented in Appendix 1.

Results of vertically oriented shelby-tube permeameter samples (figure 14) showed saturated hydraulic conductivity to vary between 7.1 x 10-4 cm/sec to 1.3 x 10-3 cm/sec near the base of the borehole. Stephens and Neuman (1982b) showed that flow rate out of the borehole increases approximately linearly with depth along the borehole. In light of this, one might expect the value of Ks obtained from the borehole infiltration test to be on the order of 1.3 x 10-3 cm/sec. A weighted arithmetic average of the Ks results from the shelby- tubes is approximately 5 x 10-4 cm/sec.

Table 5 shows the resulting values of Ks from the borehole infiltration test when using various equations. Stephens I and Stephens II parameters were found by using data from laboratory pressure head-moisture content curves obtained from an elevation of -100 cm. Mualem's parameters were obtained by using SOHYP of van Genuchten (1978) on the same laboratory sample. The bubbling pressure used in Brooks-Corey was also taken from the same laboratory sample. Burdine's equation could not be used because his equations in SOHYP resulted in a residual moisture content of zero for the same laboratory sample.

An argument might be made for using data from other laboratory samples taken at elevations of -75, -50, and -25 cm. However, these samples were found to have similar pressure head-moisture content curves to the data from -100 cm (figures 6 through 9).

The values of Ks from the borehole infiltration test are 2 to 5 times lower than the shelby-tube estimates of Ks. Soil heterogenity may have had more influence on the results of the infiltration test than on the shelby-tube permeameter results. The borehole infiltration test results indicate water mounded at the interface of fine and coarse layers, suggesting soil heterogeneity had a significant effect on the borehole infiltration test, particularly heterogeneity at an elevation of approximately -180 cm (Table 1). The shelby-tube permeameter samples extended only to an elevation of about -160 cm, and so did not include soil from

Table 5. Estimated Values of Saturated Hydraulic Conductivity

	Ks (cm/sec)
Glover	1.3×10^{-4}
Empirical Solutions:	
Brooks-Corey	1.0×10^{-4}
Mualem	1.2×10^{-4}
Stephens I	1.5×10^{-4}
Stephens II	2.2×10^{-4}

Parameters:
H = 76.2 cm
r = 5.08 cm
Qs = 0.12 lpm

Brooks-Corey: ψ_b = 20 cm
Mualem: α_v = 0.05005; N = 1.10087
Stephens I: α = 198 m^{-1}
Stephens II: α_3 = 2.0 cm^{-1}

the coarser layer. The shelby-tube permeameter results may also have been affected by wall effects, which exist where the soil sample does not perfectly conform to the contours of the shelby tube and allow water to percolate more quickly through the permeameter than would otherwise have occurred if the soil fit perfectly inside the shelby tube.

It is interesting to note that the new equations developed by Stephens, et al (1983) do not result in much of a change in calculated Ks from Glover. This is surprising, since the soil in S9T1 was a loam, a fairly fine-grained soil. One might expect infiltration rate into a fine-grained soil to be influenced by unsaturated flow phenomenon more than a coarse grained soil since the saturated bulb would be smaller in a fine-grained soil than in a coarser-grained soil (Philip, 1985), (Stephens and Neuman, 1982b), causing a large unsaturated flow field.

The data from S9T1 suggest that for this test, unsaturated flow could be neglected without any significant change in the calculated value of Ks. The solutions designated as Stephens I and Stephens II yield saturated hydraulic conductivities which are the closest to estimates of Ks from shelby tube permeameter data (Table 5).

7. ESTIMATING STEADY INFILTRATION RATE FROM EARLY TIME DATA

Infiltration rate data between the time when the water level in the borehole reached the desired level of 76.2 cm (t=66 min) and the time when Vmax was reached (t=265 min) were used to estimate Qs by linear regression. Vmax was used as an endpoint because steady infiltration had not been reached, and because Vmax is fairly easy to compute. Using these data, an intercept of 0.057 lpm was found, which underestimated the field measured value of steady infiltration rate of 0.12 lpm by 52%.

A better intercept was found by substituting the value of residual saturation from SOHYP for the residual saturation at 15 bars of pressure. A value of about 0.043 for residual saturation was generated by the computer model of van Genuchten (1978), which changes the value of specific yield (Ys) from 0.22 to 0.43. The increase in specific yield changes the value of Vmin and Vmax to 299 liters and 614 liters, respectively. These volumes occur at times of 242 min and 765 min into the test. Executing a linear regression analysis on the data between t=66 min and t=765 min results in an intercept of 0.126 lpm, which overestimates the value of steady infiltration rate by 6%. The equation derived by this linear regression is:

$$Qs = 9.03 * (t^{-1/2}) + 0.126 \qquad R^2 = 0.849 \qquad (13)$$

where Qs = steady infiltration rate (L^3/T).

The data included in the linear regression equation and the resulting linear regression curve fit are shown on figure 78. Before this method can be used confidently, more study needs to be carried out to determine what data to include in the linear regression curve fit on Q vs. inverse square root of time. It does have the potential for saving much time and should not be abandoned without more study.

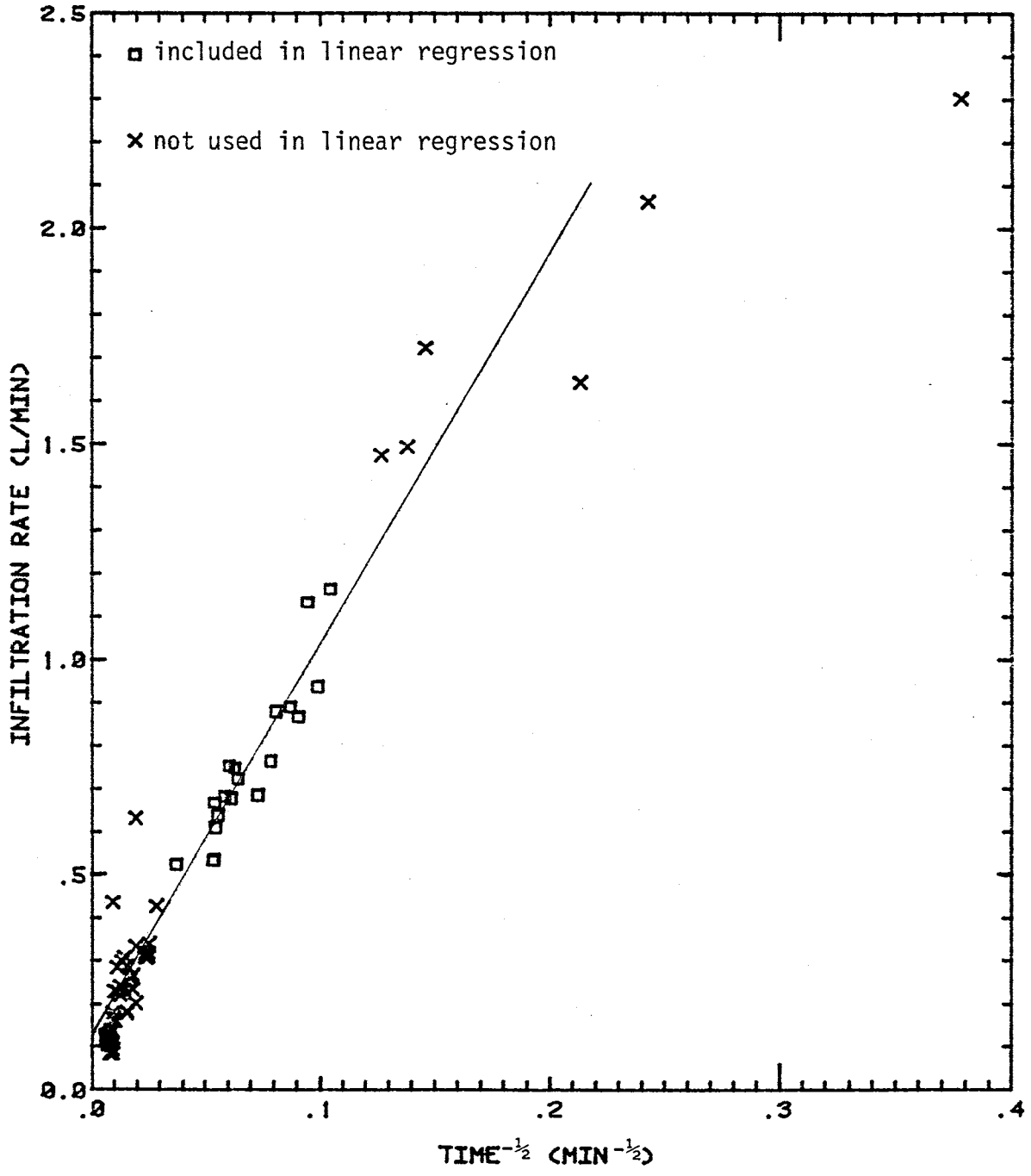

Figure 78. Infiltration rate versus Inverse Square Root of Time

8. FLOW NET METHOD FOR DETERMINING RELATIVE HYDRAULIC CONDUCTIVITY (Kr)

Stephens (1985) developed a field method to evaluate hydraulic conductivity using a flow net approach. Basically, the process involves combining stream tube geometry and hydraulic gradients and then using Darcy's Law to determine either hydraulic conductivity along the stream tube (if the saturated hydraulic conductivity is known) or Kr if Ks is not known. The following formula is the basis for determining K or Kr along the stream tube:

$$(Ksl, Krl), Jl, Al = (Ki, Kri), Ji, Ai \qquad (14)$$

where Ks = saturated hydraulic conductivity, Kr = K/Ks, J = average hydraulic gradient, A = cross-sectional area of the stream tube. The subscript 1 refers to the first segment of the stream tube; i refers to any stream tube segment downgradient from segment 1.

The following is the methodology for finding Ki or Kri along the stream tube:

1) Draw a stream tube along a total head profile and locate points on each total head contour halfway between the two sides of the stream tube.

2) Draw a straight line through each point which most closely follows the total head contour through the point, as pictured in figure 79.

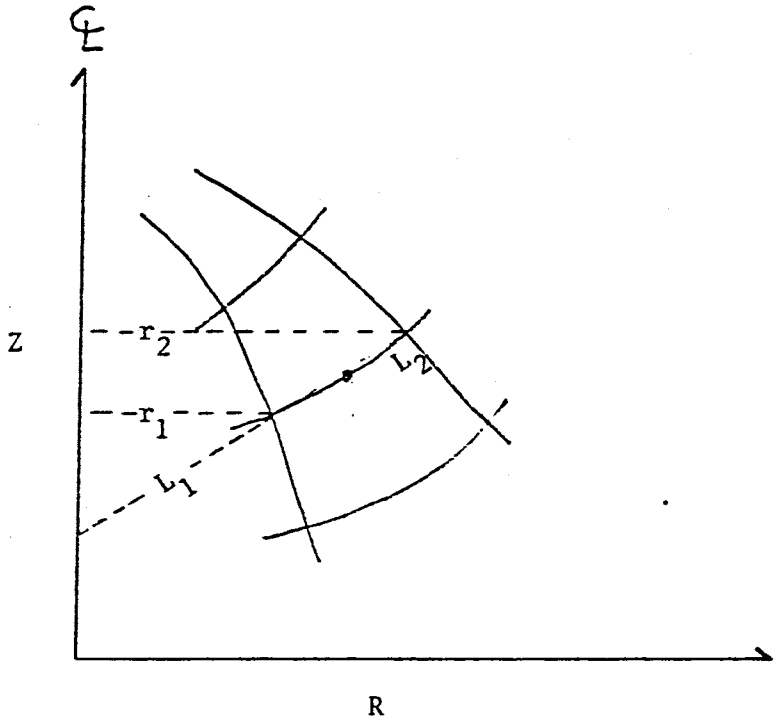

Figure 79. Flow Net Parameters

3) Measure the distance from each side of the stream tube to the center line of the borehole (L1 and L2 in figure 79).

4) Measure the horizontal distance from each side of the stream tube to the center line of the borehole (r1 and r2 in figure 79).

5) Find the area of each segment by:

$$\text{Area} = \pi (r2 * L2 - r1 * L1) \qquad (15)$$

6) Find J1, by:

$$J1 = dH/dL \qquad (16)$$

where dH = the total head difference between the borehole and point number 1. dL = the distance along the stream tube from the borehole wall to point 1.

7) Find Ji for all other segments in the same manner as 6), only with dH = the total head difference between the preceeding point and the point of interest, and dL = the distance along the stream tube between the preceeding point and the point of interest.

8) Find the pressure head at each point by:

$$U = H - z \qquad (17)$$

where U = pressure head, H = total head, z = elevation

9) Use equation (14) to find Kr of K at each point, assuming Kr1 = 1 or Ks1 = K sat.

Notice that in figure 80 point 1 was not located on the -40 cm total head contour, but rather was placed on the -60

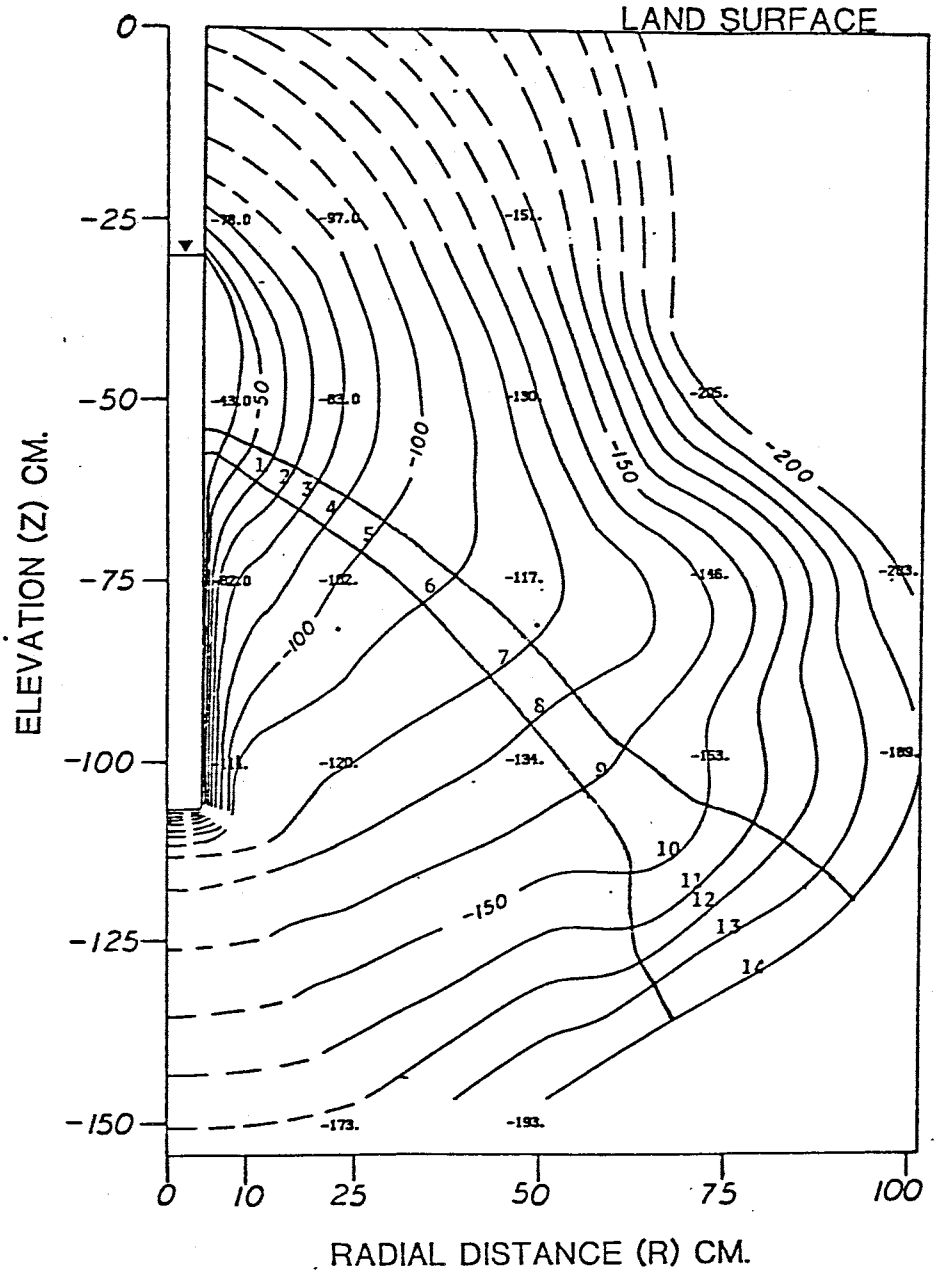

Figure 80. Stream Tube and Data Points for Flow Net

cm contour. Total head contours of -40 and -50 cm represent saturated conditions and yield Kr of 1.0 each.

Figure 81 shows the computed values of Kr at each point beyond the -50 cm total head contour. Kr decreases between points 1 and 4, then increases between points 4 and 7. The increase in point 7 corresponds very well to the decreased Ks obtained from shelby tube permeamter samples at an elevation of about -60 to -70 cm compared to that immediately above (figure 14). Kr then falls off fairly steadily between points 7 and 14.

The flow net method provides a relatively good fit to the observed variations in Ks obtained from shelby-tube permeameter samples. More study might show this method to be quite reliable for studying variations in the soil profile, which would be helpful when laboratory samples are not available.

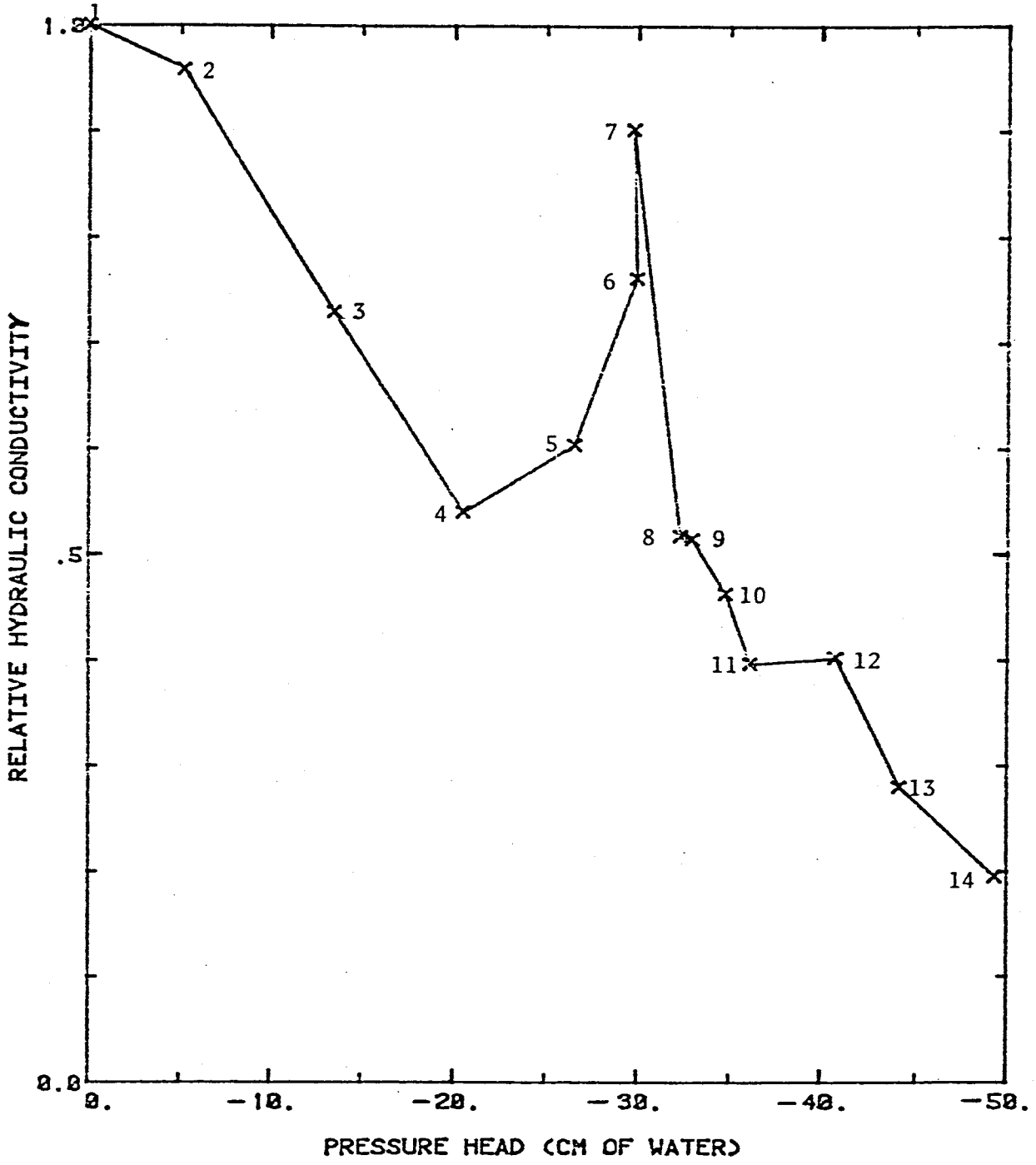

Figure 81. Relative Hydraulic Conductivity from Flow Net analysis

9. COMPARISONS TO BOREHOLE INFILTRATION TESTS CONDUCTED IN FINE SANDS

Borehole infiltration test S9T1 was specifically designed to facilitate comparisons to borehole tests conducted by Lambert (1983), which was carried out in fine sands at the Sevilleta National Wildlife Refuge north of Socorro, New Mexico. The radius of the borehole casing, the casing material, the height of water in the borehole, and the length of borehole in contact with the soil were identical to borehole tests S5T3 through S5T8 conducted by Lambert (1983) Table 6 lists some important characteristics of borehole tests S5T4-S5T8 (Sevilleta Sands) and S9T1 (loam). Test S5T3 was not included in the comparison of water volume requirements because it was not flooded with carbon dioxide before initiating infiltration of water into the borehole. As Lambert (1983) showed, not flooding the soil with carbon dioxide caused more water to be needed in order to reach steady infiltration rates.

As Table 6 indicates, the value of steady infiltration rate for S9T1 was approximately 67 times lower than the steady infiltration rates for tests S5T3-S5T8. However, S9T1 needed only approximately 1.4 times more water to reach steady infiltration rate (Cum. Q) than the average volume of water needed to reach steady infiltration rates in tests S5T4-S5T8.

Table 6. Comparisons of S5T4 - S5T8 to S9T1

Test:	S5T4	S5T5	S5T6	S5T7	S5T8	S9T1
Q_s (L/MIN)	5.05	6.79	7.01	6.79	8.94	0.1193
t_s (MIN)	312	349	305	375	735	14,543
Cum. Q_s (Liters)	1896	2496	2252	2685	4582	3827

Q_s = Steady-State infiltration rate
t_s = time to reach steady-state infiltration rate
Cum. Q_s = Cumulative infiltration at steady-state

K_s (Sevilleta) = 1×10^{-2} cm/sec

K_s (S9T1) = 1.5×10^{-4} cm/sec

While the water volume requirements may have been similar for the Sevilleta Sands and the loam (S9T1), the time needed to reach steady infiltration rate was quite different for the two soil types. An average of 415 minutes were needed to reach steady infiltration rates in the Sevilleta Sand, while 14,543 minutes were needed to reach steady infiltration rates in the loam. Saturated hydraulic conductivities for the two soil types differed by approximately 2 orders of magnitude.

From the preceeding discussion, it can be inferred that a large change in saturated hydraulic conductivity between soil types results in a much longer time needed to reach a steady value of infiltration rate. Also, the value of steady infiltration rate is much lower, given the same borehole conditions such as height of water in the borehole and radius of the borehole. However, the volume of water needed to reach a value of steady infiltration rate does not increase in proportion to the decrease of saturated hydraulic conductivity. In fact, a reduction of 67 times in Ks caused the time needed to reach steady state to increase by 35 times while the volume of water needed to reach steady state increased by only 1.4 times.

Infiltration rates versus time, pressure head profiles at steady state, and total head profiles at steady state will be examined more in-depth in the next sections.

9.1 Infiltration Rate

Dimensionless infiltration rate (Q_D) for S5T7 will be compared to dimensionless infiltration rate for S9T1. Dimensionless infiltration rate was calculated similar to the method described by Stephens (1979), namely:

$$Q_D = Q / (H * Ks * r) \qquad (18)$$

Dimensionless time was found by dividing time by time at steady state infiltration rate. Values for Q and Ks are presented in Table 6. The values of H and r were 76.2 cm and 5.08 cm, respectively, for both tests.

Dimensionless infiltration rate (Q_D) versus dimensionless time (t_D) is shown on figure 82. It is interesting to note that Q_D for S9T1 is almost always greater than Q_D for S5T7 at any dimensionles time. At small t_D, Q_D is much greater in S9T1 than in S5T7 (Recall equation 18). The radius of the borehole and height of water was the same for both tests, implying that Q/Ks for S9T1 is greater than Q/Ks for S5T7. Ks for S9T1 is approximately 67 times lower than Ks for S5T7. Consequently, Q for S5T7 must be less than 67 times greater than Q for S9T1. In fact, at early time, Q for S5T7 is only 6.5 times greater than Q for S9T1.

Hydraulic gradient difference between S9T1 and S5T7 can explain the higher values of Q_D for S9T1. According to

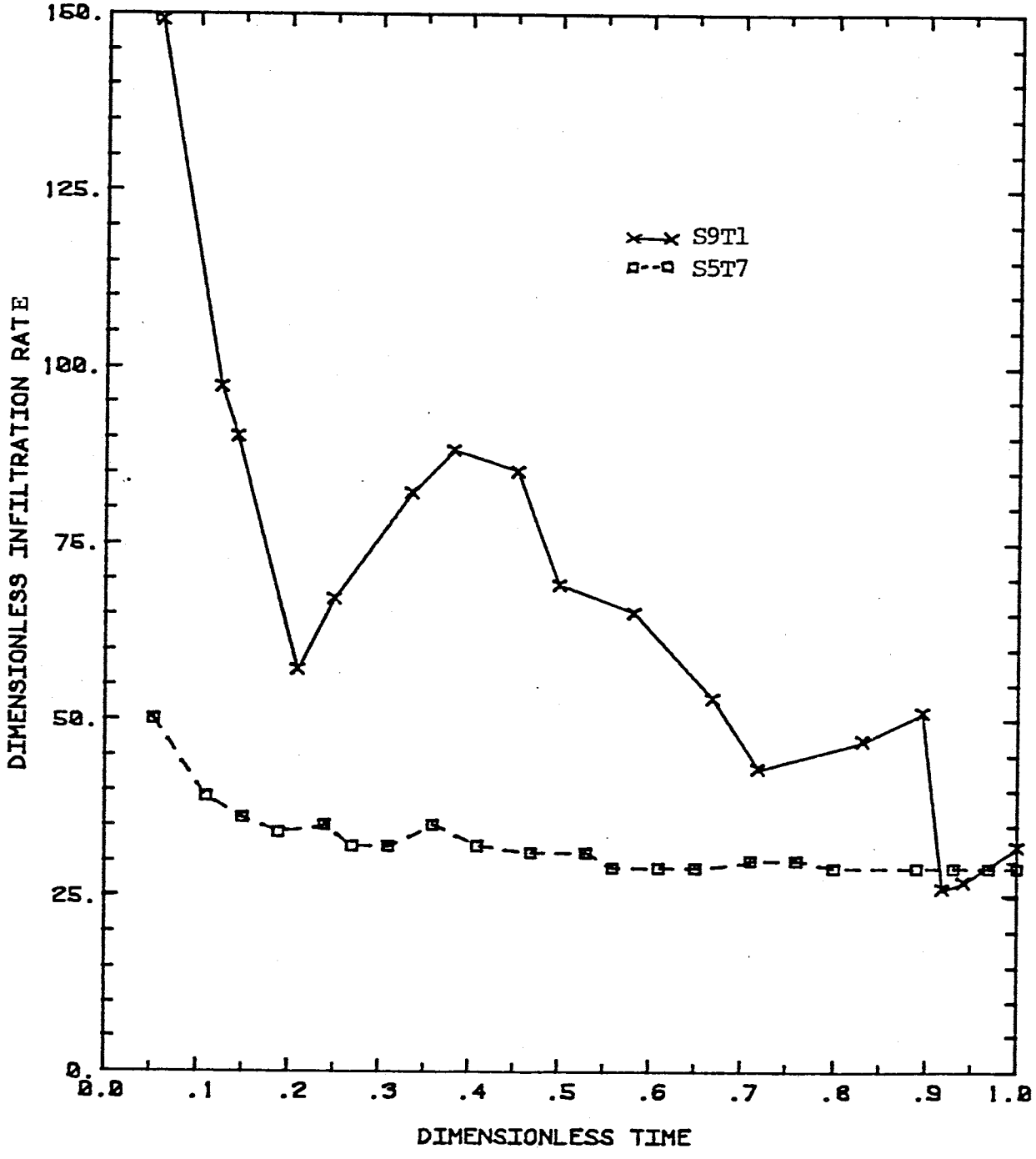

Figure 82. Dimensionless Infiltration rate versus Dimensionless time for S5T7 and S9T1

Darcy's Law, infiltration rate is proportional to hydraulic gradient. The hydraulic gradients near the borehole were much greater in S9T1 than in S5T7, which resulted in the high value of dimensionless infiltration rate.

From the preceeding discussion, one can conclude that early time infiltration rates in different soils may not be influenced simply by hydraulic conductivity. While Ks for S5T7 was 67 times greater than Ks for S9T1, Q for S5T7 was generally less than 67 times greater than Q for S9T1. In other words, a large decrease in Ks does not imply a correspondingly large decrease in Q.

9.2 Pressure Head Comparisons

Figures 83 and 84 are profiles of pressure head at steady-state for S5T6 and S9T1, respectively. These two figures are especially interesting as far as the zone of saturation is concerned. Philip (1985) and Stephens and Neuman (1982b) observed that the zone of saturation in a coarser-grained soil should extend farther from the borehole than in a finer-grained soil. At first glance, one might suppose that these two tests do not follow predicted behavior. However, Lambert (1983) states that the zone of saturation for tests S5T3 through S5T8 could extend to -20 cm of pressure head. As shown on figures 6-9 of this report, the zone of saturation for S9T1 may extend to about -10 cm. The -20 cm pressure head contour for S5T6 (figure 83) lies farther from the borehole than the -10 cm pressure head contour for S9T1 (figure 84), which confirms previous observations.

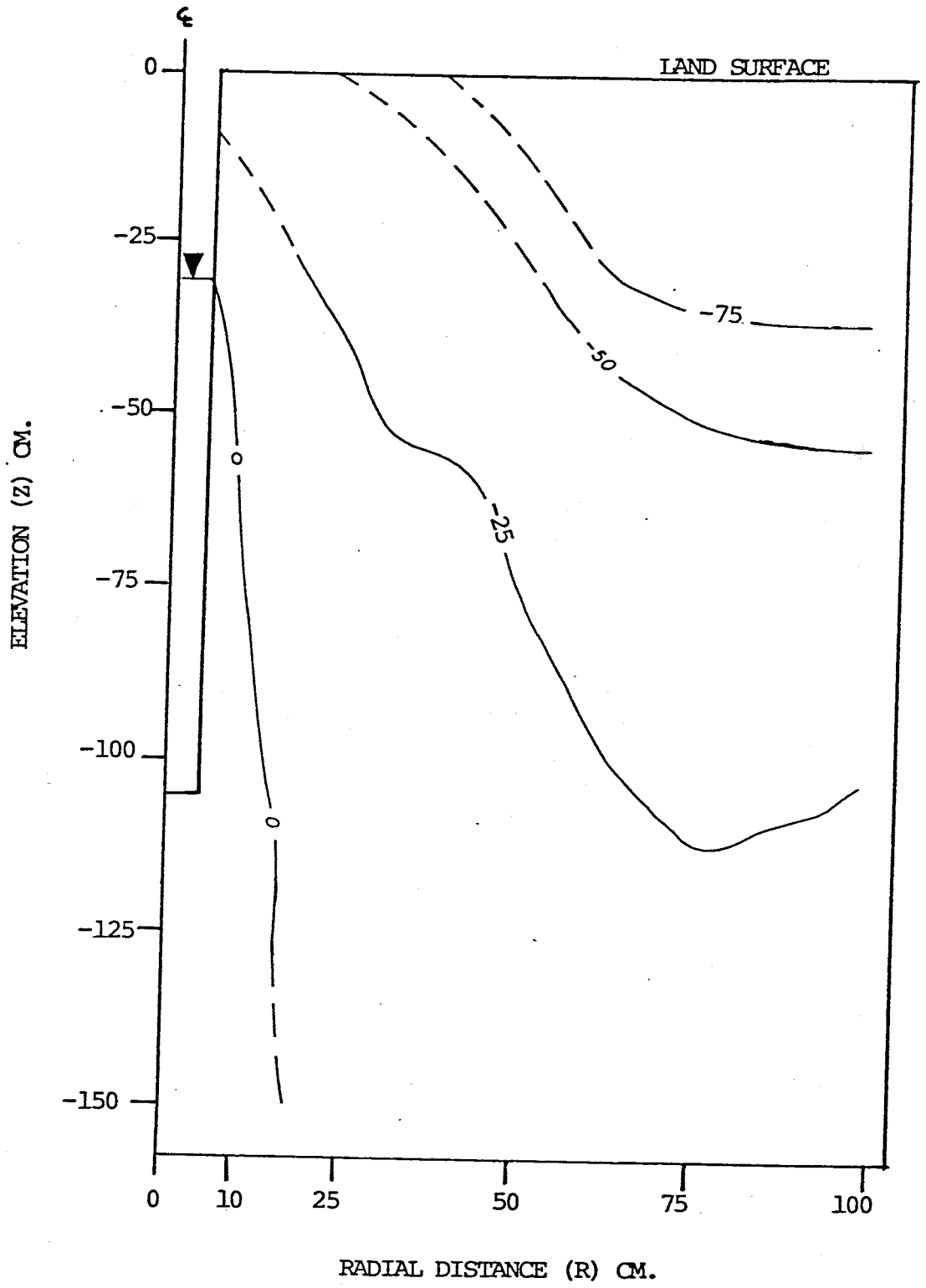

Figure 83. Pressure Head at Steady State for S5T6

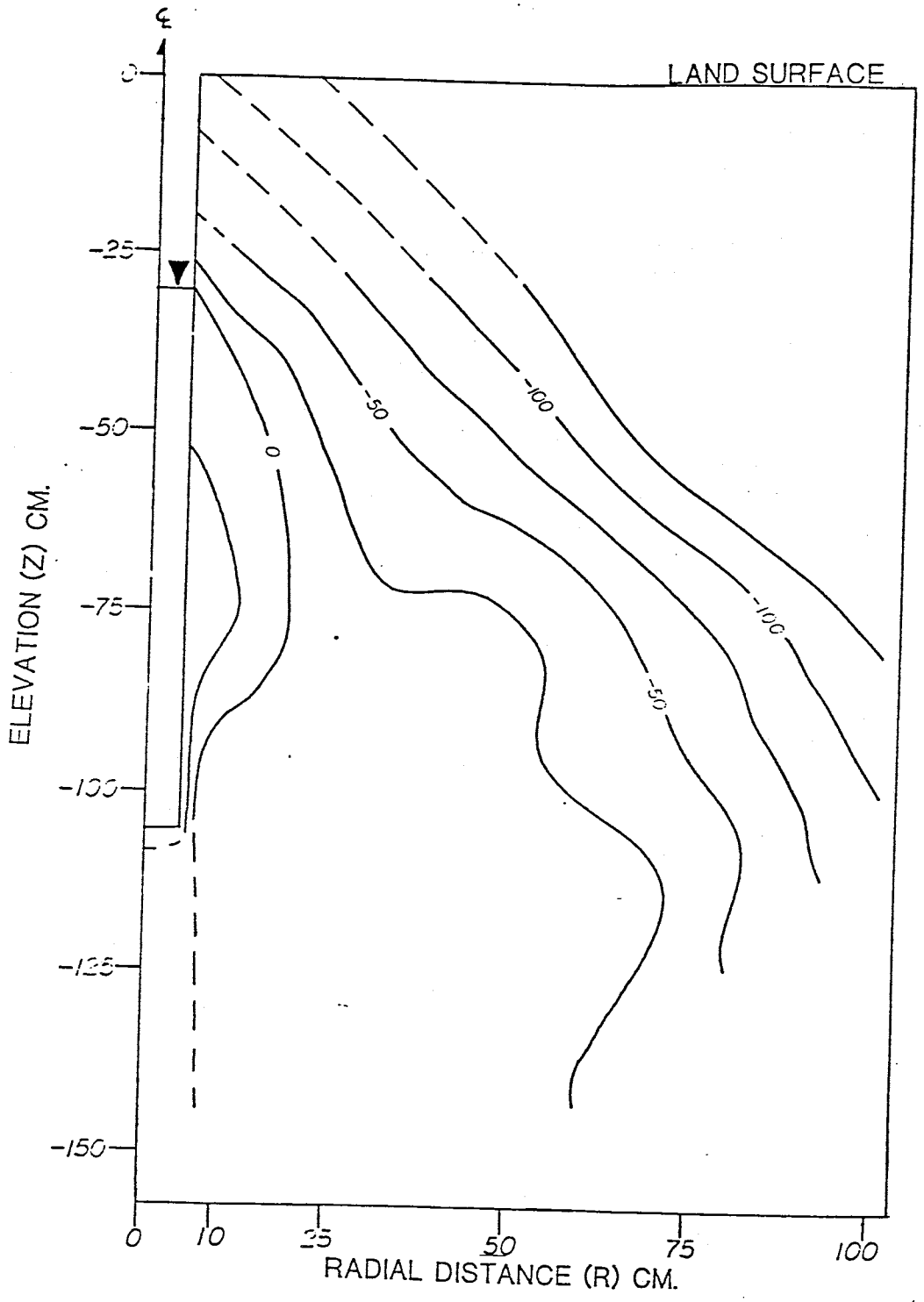

Figure 84. Pressure Head at Steady State for S9T1

9.3 Total Head Comparisons

The steady state (t=295 min.) total head profile for S5T6 is shown on figure 85, while the total head profile at steady-state (t=14,543 min) for S9T1 is shown on figure 86. Notice that the -50 cm contour for S5T6 lies closer to the borehole than the -50 cm contour in S9T1, except near the bottom of the borehole. Since hydraulic gradient is defined as dH/ dL, the hydraulic gradient near the borehole is greater for S5T6 than for S9T1. Steady infiltration rate for S5T6 is 59 times greater than steady infiltration rate for S9T1, while saturated hydraulic conductivity (Ks) using Glover's equation (USBR, 1974) is 55 times greater in S5T6 than in S9T1. If Glover's equation is assumed to give the true values of ks, then according to Darcy's Law, hydraulic gradient for S5T6 should be greater than hydraulic gradient for S9T1. In fact, this is what is seen.

Above elevations of approximately -65 cm, flow out of the borehole is more vertical downward in S5T6 than in S9T1. Capillary action in the finer-grained soil of S9T1 may be causing the more horizontal flow. Soil anisotropy and heterogeneity may also be influencing the flow out the borehole at these elevations. An order of magnitude reduction in saturated hydraulic conductivity was observed between elevations of approximately -50 cm and -58 cm by shelby-tube permeameter experiments for S9T1. Outflow from the borehole may have flowed horizontally along the top of

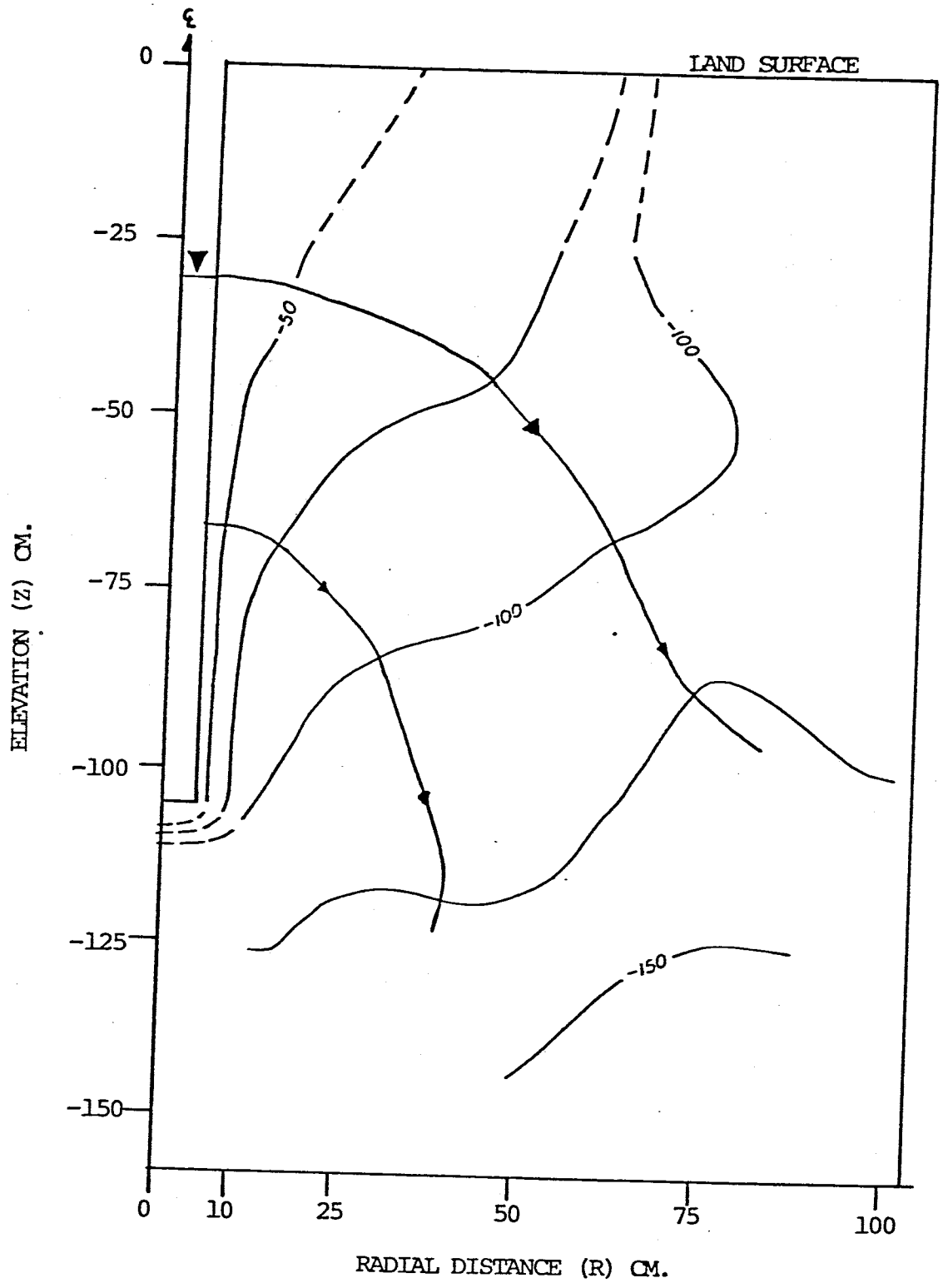

Figure 85. Total Head at Steady State for S5T6

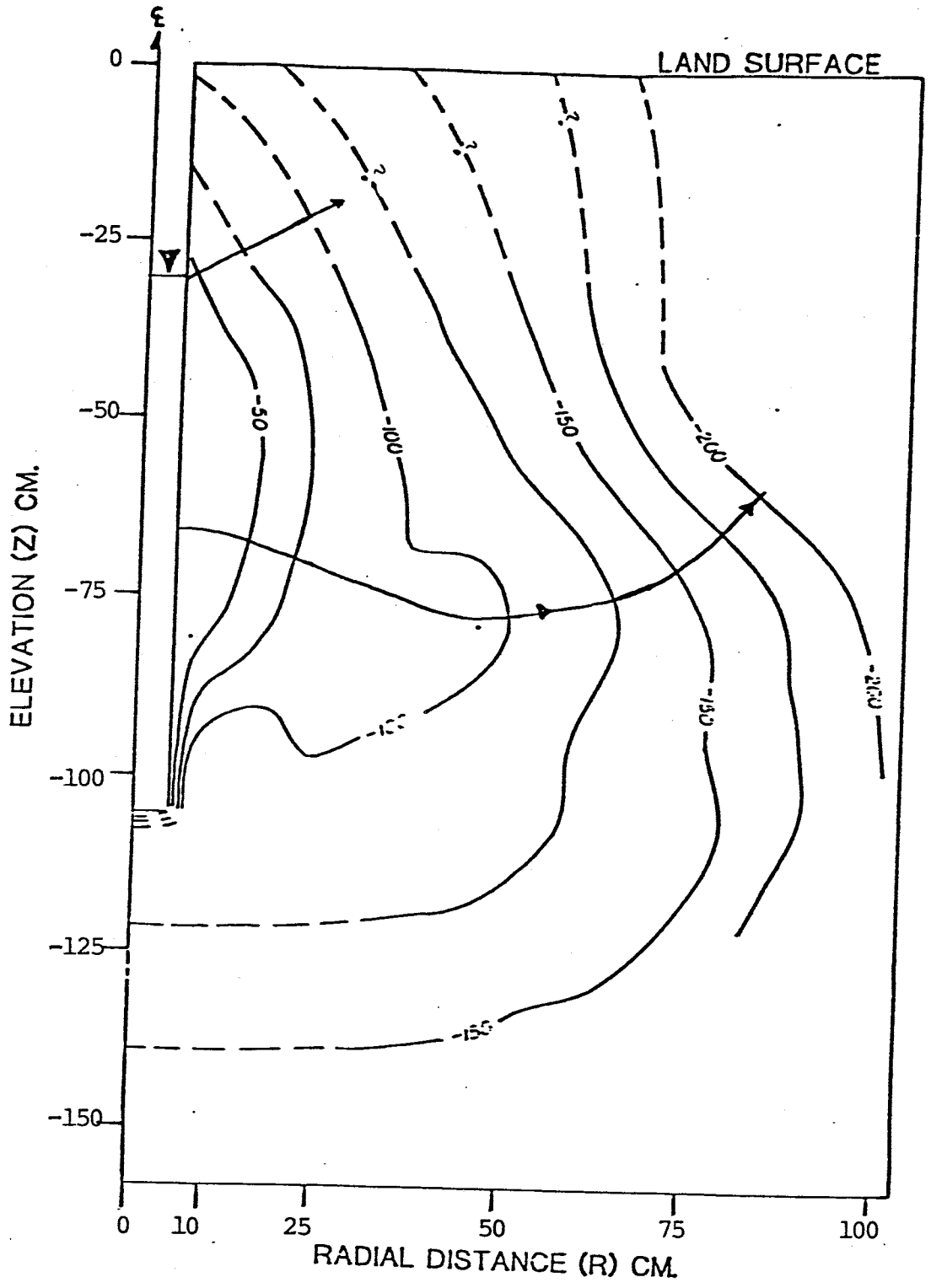

Figure 86. Total Head at Steady State for S9T1

the layer having the lower value of Ks.

Near the base of the borehole, flow in S5T6 is more horizontal than in S9T1. It is thought that the bottom portion of the borehole screen in S9T1 became clogged with precipitates, resulting in the more vertical flow near the base of the borehole, as well as the increased gradients.

10. CONCLUSIONS

We have obtained an estimate of the time and water volume needed to reach steady infiltration rate in a relatively fine-grained soil under condition I of the United States Bureau of Reclamation. The time to reach steady infiltration rate approached 15,000 minutes and the water volume approximated 3850 liters. USBR guidelines suggest terminating the test after the water volume had reached about 320 liters, when only about 1000 minutes had elapsed.

The empirically derived equations designated as Stephens I and Stephens II, which attempt to account for unsaturated flow, yielded approximately the same value of saturated hydraulic conductivity as the Glover equation, which does not account for unsaturated flow.

Comparisons to tests performed in fine sands indicate the time needed to reach steady infiltration rate in the loamy soil was about 35 times greater than for the fine sands. Water volumes needed to reach steady infiltration rate were 1.4 times higher in the loamy soil than the fine sands. Saturated hydraulic conductivities differed by about 65 times.

Comparisons with previous borehole infiltration tests conducted in fine sands indicate water volume requirements are not strongly dependent upon saturated hydraulic conductivity. This questions the reliability of the USBR

equations which discontinue infiltration once a certain volume of water has infiltrated. The USBR equations may overestimate saturated hydraulic conductivity.

Other conclusions not included in the objectives can be drawn from S9T1. They are outlined in the following sections:

Estimating steady infiltration rate from early time data yielded an excellent fit to the observed value of steady infiltration rate, if data from t=66 min to t=765 min are used in a linear regression analysis. The estimated value of steady infiltration rate was only 6% higher than the observed value of steady infiltration rate.

The flow net method for estimating relative hydraulic conductivity near the borehole defined soil stratigraphy quite well. Variations in saturated hydraulic conductivity with depth as defined by shelby-tube permeameter samples were also supported by the flow net method.

Soil heterogeneity can affect flow out of the borehole and thus the value of saturated hydraulic conductivity estimated from borehole infiltration tests. Any conclusions regarding saturated hydraulic conductivity should not be made without analyses of soil stratigraphy surrounding the borehole.

11. FUTURE RESEARCH

Borehole test S9T1 was the first step in estimating the changes in volume of water and the time needed to reach steady infiltration rate (Qs) in different soil types. More tests should be conducted in different soil types to accurately define the differences in water requirements and time needed to reach Qs.

More field evaluation of equations which account for unsaturated flow should be carried out.

Variations in the number of pore volumes of carbon dioxide injected into the soil prior to beginning water infiltration should be conducted in soils similar to the soil in S9T1 in order to define the minimum number of pore volumes needed to most effectively reduce entrapped air. It is difficult to evaluate the effectiveness of the carbon dioxide flood in S9T1 due to the lack of other tests in similar soil types.

The flow net method for evaluating relative hydraulic conductivity changes along stream tubes could be used in different soils and in different soil stratigraphies.

The ratio of head in the borehole to radius of the borehole (HD) could be reduced, which would reduce the time needed to reach steady infiltration rate. Reynolds and Elrick (1983) have developed equations which can be used when HD is between five and ten. These equations could be

verified in the field as well.

A means for confidently estimating steady infiltration rate from early time data could be found. The method used in S9T1 worked quite well, if one had a prior knowledge of steady infiltration rate. A consistent method for estimating Qs would be extremely helpful since it would reduce both the volume of water needed as well as the time needed to conduct a borehole infiltration test.

ACKNOWLEDGEMENTS

My sincere thanks to Dr. Daniel B. Stephens for his guidance in this project. I would also like to thank Mr. Christopher Mikell and Mr. Thomas Duval for their field assistance during the test; Mr. Gary Johnson for his assistance in the laboratory; Mr. Richard Rabold for his help during the initial phases of the project; and Mr. Robert Knowlten for his technical input. Thanks to Ms. Nancy O. Jannick for her moral support. Special thanks to Ms. Barbara Kickham for her laboratory and overall help. You made the final stages of the project go much smoother than they would have without your help. I wish to thank Mr. Steven Conrad for helping me time after time.

Thanks most especially to my wife, Mrs. Deborah L. Moyer, for waiting for me. I will spend the rest of my life making it up to you.

REFERENCES

Black, C.A., editor, 1965. Methods of Soil Analysis. American Society of Agronomy, No. 9, Part 1, pp. 545-567.

Bouwer, H., 1978. Groundwater Hydrology. McGraw-Hill Inc., New York, pp. 1-480.

Boyle, J.T., 1984. Soil Hydraulic Properties and Soil Water Movement of the M-Mountain Waste Storage Site. Independent Study, New Mexico Institute of Mining and Technology.

Christiansen, J.E., 1944. Effect of Entrapped Air Upon the Permeability of Soils. Soil Sci., V. 58, pp. 355-365.

Hillel, Daniel, 1980. Fundamentals of Soil Physics. Academic Press, Inc., pp. 1-413.

Lagerwerff, J.V., Nakayama, F.S., and Frere, M.H., 1969. Hydraulic Conductivity Related to Porosity and Swelling of Soil. S.S.S.A.P., V. 33, pp. 3-11.

Lambert, K.A., 1983. The Effects of Carbon Dioxide Flooding on Constant Head Borehole Infiltration Tests. Independent Study, New Mexico Institute of Mining and Technology.

Larson, M.B., 1984. A Comparison of Empirical/ Theoretical, Laboratory, and Field Techniques in Evaluating Unsaturated Hydraulic Properties of Mill Tailings. Independent Study, New Mexico Institute of Mining and Technology.

McNeal, B.L., and Coleman, N.T., 1966. Effect of Solution Composition on Soil Hydraulic Conductivity. S.S.S.A.P., V. 30, pp. 308-312.

McNeal, B.L., Norvell, W.A., and Coleman, N.T., 1966. Effect of Solution Composition on the Swelling of Extracted Soil Clays. S.S.S.A.P., V. 30, pp. 313-317.

REFERENCES (cont.)

Mualem, Y., 1976. A New Model for Predicting the Hydraulic Conductivity of Unsaturated Porous Media. W.R.R., V. 12, No. 3, pp. 513-522.

Philip, J.R., 1985. Approximate Analysis of the Borehole Permeameter in Unsaturated Soil. W.R.R., V. 21, No. 7, pp. 1025-1033.

Rabold, R.R., 1984. The Results of a Borehole Infiltration Test with a Shallow Water Table. Independent Study, New Mexico Institute of Mining and Technology.

Reynolds, W.D., and Elrick, D.E., 1983. A Reexamination of the Constant Head Well Permeameter Method for Measuring Saturated Hydraulic Conductivity Above the Water Table. Soil Sci., V. 136, No. 4, pp. 250-269.

Stephens, D.B., and Neuman, S.P., 1982a. Vadose Zone Permeability Tests: Summary. Journal of Hydraulics Division, ASCE, V. 108, No. HY5, Proc. Paper 17058, pp. 623-639.

Stephens, D.B., and Neuman, S.P., 1982b. Vadose Zone Permeability Tests: Steady State Results. Journal of Hydraulics Division, ASCE, V. 108, No. HY5, Proc. Pager 17059, pp. 640-659.

Stephens, D.B., and Neuman, S.P., 1982c. Vadose Zone Permeability Tests: Unsteady Flow. Journal of Hydraulics Division, ASCE, V. 108, No. HY5, Proc. Paper 17060, pp. 660-677.

Stephens, D.B., Neuman, S.P., Tyler, S., Lambert, K., Watson, D., Rabold, R., Knowlten, R., Byers, E., and Yates, S., 1983. Insitu Determination of Hydraulic Conductivity in the Vadose Zone Using Borehole Infiltration Tests. Technical Completion Report, Project B-073-NMEX, Water Resources Research Institute, Las Cruces, N.M., pp. 1-165.

REFERENCES (cont.)

Stephens, D.B., 1985. A Field Method to Determing Unsaturated Hydraulic conductivity Using Flow Nets. W.R.R., V. 21, No. 1, pp. 45-50.

Tyler, S.W., 1982. Field Results of Borehole Infiltration Tests. Independent Study, New Mexico Institute of Mining and Technology.

United States Bureau of Reclamation, 1974. Earth Manual. second edition, U.S. Government Printing Office, Washington, D.C., pp. 1-310.

van Genuchten, R., 1978. Calculating the Unsaturated Hydraulic Conductivity with a new Closed-Form Analytical Model. Publication of the Water Resources Program, Department of Civil Engineering, Princeton University, N.J., 08540, pp. 1-43.

Watson, D.B., 1983. The Effect of Head on Constant Head Borehole Infiltration Tests and Other Related Flow Phenomenon. Independent Study, New Mexico Institute of Mining and Technology.

Zanger, C.N., 1953. Theroy and Problems of Water Percolation. Engineering Monograph No. 8, U.S. Bureau of Reclamation, Denver, Col.

APPENDICES

NOMENCLATURE

a = rise of mercury

c = height of mercury level

elevation = relative to land surface datum. Negative downwards

H = height of water in the borehole (L)

H_D = ratio of H over r, dimensionless

i = hydraulic gradient or average negative hydraulic gradient, dimensionless

K = hydraulic conductivity (L/T)

K_r = relative hydraulic conductivity (L/T)

K_s = saturated hydraulic conductivity (L/T)

n = porosity, dimensionless

N = parameter from SOHYP

N.P. = neutron probe reading (% volume)

pb = dry bulk density (M/L^3)

pHg = density of mercury (M/L^3)

ps = particle density (M/L^3)

PH = pressure head (L)

Q = infiltration rate (L^3/T)

Q_c = infiltration rate corrected for temperature variations (L^3/T)

Q_D = dimensionless infiltration rate

Qs = infiltration rate at steady state (L^3/T)

r = radius of the borehole (L)

R= radial distance from the borehole center (L)

NOMENCLATURE (cont.)

t_D = dimensionless time

ts = time at steady infiltration rate (T)

TH = total hydraulic head (L)

Tu = distance from water level in borehole to water table or impeding layer (L)

w = gravimetric moisture content

z = elevation (L)

Δw = decline in water level in manometer

α = parameter from SOHYP

θ= volumetric moisture content

θ_r = residual moisture content

Saturated Hydraulic Conductivity Equations (page 1 of 2)

I) Glover:

$$K_s = \frac{0.159\ Q}{H^2}\ [\sinh^{-1}(H_D) - 1]$$

where K_s = saturated hydraulic conductivity (L/T)
Q = flow rate out of the borehole (L^3/T)
H = height of water in the borehole (L)
H_D = H/r (unitless)
r = radius of the borehole (L)

II) Brooks-Corey:

$$\log_{10}Cu = 0.484\ \log_{10}H_D + 0.027\ \Psi_b^{0.5} - 0.466\ \log_{10}H + 0.018\ H_D^{1.5} + 0.846$$

where $Cu = \frac{Q}{rHK_s}$

Q = flow rate out of the borehole (cm^3/T)
r = radius of the borehole (cm)
H = height of water in the borehole (cm)
K_s = saturated hydraulic conductivity (cm/T)
H_D = H/r (unitless)
Ψ_b = bubbling pressure (cm). $\Psi_b < 0$

III) Maulem:

$$\log_{10}Cu = 0.653\ \log_{10}H_D - 0.257\ \log_{10}\alpha_v - 0.633\ \log_{10}H + 0.021\ H_D - 0.313\ N^{-0.5} + 0.453$$

where $Cu = \frac{Q}{rHK_s}$

Q = flow rate out of the borehole (m^3/T)
r = radius of the borehole (m)
H = height of water in the borehole (m)
K_s = saturated hydraulic conductivity (m/T)
H_D = H/r (unitless)
α_v = parameter from SOHYP (van Genuchten, 1978) (cm^{-1})
N = parameter from SOHYP (van Genuchten, 1978)

Saturated Hydraulic Conductivity Equations (page 2 of 2)

IV) Stephens I:

$$\log_{10}Cu = 0.486 \log_{10}H_D + 0.398\,\alpha^{-1} - 0.489 \log_{10}H + 0.019\,H_D^{0.5} + 0.828$$

where $Cu = \frac{Q}{rHK_s}$

Q = flow rate out of the borehole (m^3/T)
r = radius of the borehole (m)
H = height of water in the borehole (m)
K_s = saturated hydraulic conductivity (m/T)
H_D = H/r (unitless)
α = slope of natural logarithm of relative hydraulic conductivity, K_r, versus pressure head, Ψ, from $K_r(\Psi=0)=1.0$ to $K_r(\Psi)=0.5$ ($\Psi<0$). Units = m^{-1}.

V) Stephens II:

$$\log_{10}Cu = 0.502 \log_{10}H_D - 0.104 \log_{10}\alpha_3 - 0.467 \log_{10}H + 0.0175\,H_D^{0.5} + 0.0028\,\alpha_3^{-1} + 0.794$$

where $Cu = \frac{Q}{rHK_s}$

Q = flow rate out of the borehole (cm^3/T)
r = radius of the borehole (cm)
H = height of water in the borehole (cm)
K_s = saturated hydraulic conductivity (cm/T)
H_D = H/r (unitless)
$\alpha_3 = \frac{-\ln(0.1)}{-\Psi(K_r=0.1)}$ $\Psi<0$. Units = cm^{-1}